

Factors controlling ^{234}Th scavenging and the application of
 ^{234}Th as particle tracer

Dissertation

ZUR

Erlangung des akademischen Grades

Doctor rerum naturalium (Dr. rer. nat.)

Mathematisch-Naturwissenschaftlichen Fakultät
der Universität Rostock



vorgelegt von

Anne Schuster, geboren am 10.06.1986 in Finsterwalde

wohnhaft in Rostock

Rostock, 31.08.2016

Gutachter:

Prof. Dr. Gerhard Graf

Universität Rostock

Prof. Dr. Detlef Schulz-Bull

Institut für Ostseeforschung Warnemünde

Eingereicht am 01.09.2016

Verteidigung am 28.04.2017

CONTENT

ABSTRACT.....	IX
ZUSAMMENFASSUNG	XI
1 INTRODUCTION.....	1
2 ²³⁴TH METHOD.....	6
2.1 Laboratory analyses and measurement via β -counting.....	6
2.2 Spiking with ²³⁴ Th	8
2.3 Determination of ²³⁴ Th activity.....	8
3 ADSORPTION OF ²³⁴TH ONTO PARTICLES WITH VARIABLE SURFACE QUALITIES AND SURFACE AREAS	10
3.1 Method and material	10
3.1.1 Particle types and preparation	10
3.1.2 Experimental design	12
3.1.3 Particle analyses	13
3.1.3.1 Total particulate matter and particulate carbon.....	13
3.1.3.2 Elemental analyses of fine sediment <100 μ m	13
3.1.3.3 Particle surface.....	15
3.1.4 The distribution coefficients K_d and K_A	16
3.1.5 Statistics	17
3.2 Results	17
3.2.1 Recovery and ²³⁴ Th adsorption onto the container walls.....	17
3.2.2 ²³⁴ Th adsorption on different particles.....	19
3.3 Discussion	21
3.3.1 Variation in ²³⁴ Th loss between the particle types.....	21
3.3.2 Affinity of ²³⁴ Th to different organic coated particles.....	23
3.3.3 The particle concentration effect	24
3.3.4 ²³⁴ Th adsorption onto different particles and the influence of surface area.....	25
3.3.5 Importance for natural Environment.....	27
4 THE INFLUENCE OF COLLOIDS ON ²³⁴TH SCAVENGING WITH RESPECT TO VARYING FUNCTIONAL GROUPS IN THE POLYSACCHARIDE FRACTION	1
4.1 Method and material	29
4.1.1 Colloidal substances and experimental conditions	29
4.1.2 Experimental design	31
4.1.2.1 Experiment A - ²³⁴ Th adsorption onto different PS (single-sorbent)	31
4.1.2.2 Experiment B - ²³⁴ Th adsorption onto fine sediment in presence of Fucoïdan (binary-sorbent).....	31
4.1.2.3 Experiment C - ²³⁴ Th adsorption onto fine sediment in presence of natural COM (binary-sorbent).....	32
4.1.2.4 Control run- ²³⁴ Th loss onto container walls	32
4.1.3 Determination of the polysaccharide concentration.....	33
4.1.4 ²³⁴ Th fractions and distribution coefficient.....	34
4.1.5 Statistics	34

4.2	Results	35
4.2.1	Concentration of polysaccharides	35
4.2.2	²³⁴ Th lost onto container walls	36
4.2.3	²³⁴ Th adsorption onto different polysaccharides	37
4.2.4	²³⁴ Th adsorption onto mineral surfaces in presence of colloidal material.....	38
4.3	Discussion	39
4.3.1	The influence of functional group composition of polysaccharides on ²³⁴ Th adsorption	39
4.3.2	Partitioning of ²³⁴ Th between dissolved and particulate phase in presence of polysaccharides	41
4.3.3	The effect of natural colloids on the adsorption of ²³⁴ Th onto mineral surfaces ..	42
5	PARTICLE DYNAMIC IN THE MECKLENBURG BAY, BALTIC SEA USING ²³⁴TH AS PARTICLE TRACER	44
5.1	Study area and sampling	44
5.2	Method and material	45
5.2.1	Characterisation of the sediment	45
5.2.2	Critical shear stress velocity (u^*_{cr}) and turbulent kinetic energy (TKE)	46
5.2.3	²³⁴ Th adsorption onto different sediment types in varying hydrodynamic regimes: Resuspension-deposition-experiment.....	47
5.2.4	²³⁴ Th activity, TPM and PC in the water column.....	49
5.2.5	²³⁴ Th activity in the sediment and the mixing coefficient (D_b)	50
5.2.6	Analytical problems - The ingrowths of bismuth-212.....	52
5.2.7	The mixing coefficient (D_b)	54
5.3	Results	55
5.3.1	Hydrography and sediment characteristics of the study area.....	55
5.3.2	Thresholds of sediment motion	57
5.3.3	Resuspension-deposition-experiment.....	57
5.3.4	²³⁴ Th distribution in the Mecklenburg Bay	59
5.3.4.1	²³⁴ Th activities in the water column.....	59
5.3.4.2	Sediment excess ²³⁴ Th and particle mixing.....	60
5.4	Discussion	62
5.4.1	The erodibility of the sediment in the Mecklenburg Bay.....	62
5.4.2	Particle dynamic in the Mecklenburg Bay	65
5.4.3	Particle residence time	66
5.4.4	²³⁴ Th adsorption varying in hydrodynamic regimes and different sediment types.....	68
5.4.5	The transport of ²³⁴ Th from the water column to the sediment	70
5.4.6	Particle reworking in the sediment	74
	SUMMARY AND CONCLUSION	75
	REFERENCES	79
	DANKSAGUNG	XIV
	APPENDIX	XV
	LEBENS LAUF	
	SELBSTSTÄNDIGKEITSERKLÄRUNG	

ABBREVIATIONS

APS	acid polysaccharides
C	carbon
COM	colloidal organic matter
cpm	counts per minute
DOC	dissolved organic carbon
DOM	dissolved organic matter
dpm	disintegrations per minute
EPS	exopolymeric substances
GF/F	glass fibre filters
kDa	kilo Dalton
K _A	distribution coefficient in relation to the surface area
K _d	distribution coefficient in relation to the particle concentration
kV	kilo volt
mab	meter above bottom
MeV	mega electron volt
MWCO	molecular weight cut off
POC	particulate organic carbon
PS	polysaccharide
SD	standard deviation
TEP	transparent exopolymeric particles
²³⁴ Th _d	dissolved thorium-234
²³⁴ Th _p	particulate thorium-234
²³⁴ Th _{tot}	total thorium-234
TPM	total particulate matter

LIST OF TABLES

Table 3.1: The range of particle concentrations used in the experiments, the average surface of the cells (μm^2) of the organic coated particles and the particle surface ($\text{m}^2 \text{g}^{-1}$). Errors indicate a 95 % confidence coefficient. #Labelled error is expressed as standard deviation.	13
Table 3.2: Mineral composition of the fine sediment fraction $<100 \mu\text{m}$ analysed after combustion of the organic material. In total, 2177 particles were analysed using a coupled scanning electron microscope (SEM) and energy dispersive X-ray analysis (EDX) analysis (kindly provided by Rainer Bahlo). The unclassified fraction comprises the particle which could not be clearly identified.....	14
Table 3.3: Pictures and geometric forms (from Hillebrand et al., 1999) of the organic coated particles as well as the equations for the calculation of the surface area. Pictures of <i>Rhodomonas</i> spp. and <i>Synechococcus</i> spp. show the fixed cells of the experiments, while the picture of <i>Surirella</i> spp. represents the preparation of the silica shell by removing the organic matter with H_2O_2	15
Table 3.4: Recoveries of total ^{234}Th after 10 min and 3 h experiments. Errors indicate a 95 % confidence coefficient ($n = 9$, $^{\#}n = 7$).	18
Table 4.1: The chemical description, the molecular weight and the concentration of the polysaccharides (PS) used in the ^{234}Th adsorption experiments are shown. (Description and molecular weight according to Ziervogel and Arnosti, 2007).....	30
Table 4.2: Comparison of added and measured initial PS concentrations in the experiments A. R1, 2 and 3 represent the replicates of each approach.	35
Table 5.1: Position and water depth of the three Stations along a vertical transect in the Mecklenburg Bay, western Baltic Sea. Temperature and salinity were measured with the FSI sensor and water samples were taken from the surface water (SW) and bottom water (BW) column.	44
Table 5.2: Summary of the sediment characteristics of the three study sides in the Mecklenburg Bay. The ranged values represent the minimum and maximum values of the sediment profile.....	56
Table 5.3: Summary of critical shear stress velocities of fluff material from different studies at varying locations.	64
Table 5.4: Residence time (in days) of dissolved ^{234}Th (τ_d) and particle associated ^{234}Th (τ_p) in the water column (SW - surface water, BW - bottom water) and the sediment inventory as well as the dissolved ^{234}Th scavenging rate, particulate ^{234}Th removal rate and the total particulate matter concentration (TPM) of the three stations in the Mecklenburg Bay. Errors are based on error propagation of the SD of the activities or TPM concentration. n.d. = no data, due to no replicated samples. * = the particle residence time of excess ^{234}Th inventory.	67

LIST OF FIGURES

Figure 2.1: Illustration of the ^{234}Th decay of a filter sample including the background activity, due to other beta-emitting radionuclides beside ^{234}Th . C_0 represents the activity at time point of sampling and $C_{(t)}$ show the activity at point of measurement. . 8

Figure 3.1: Previous test of the ^{234}Th uptake with increasing concentration of the fine sediment particles $<100\ \mu\text{m}$. Black dots represent the results of this test and the blue dots show the concentration of the fine sediment fraction in the annular flume experiments..... 11

Figure 3.2: Recovery of the total ^{234}Th activity over time for the particle free run. Errors represent a 95 % confidence coefficient ($n = 5 - 9$)..... 17

Figure 3.3: Total ^{234}Th activity ($^{234}\text{Th}_{\text{tot}}$) over time for *Rhodomonas* spp., *Surirella* spp., *Synechococcus* spp. and the fine sediment fraction $<100\ \mu\text{m}$. Errors represent a 95 % confidence coefficient ($n = 7 - 9$). Note that data at 0 h indicate the initially added ^{234}Th activity based on the calculation of the natural activity in the seawater and the added activity of the ^{234}Th spike. The total ^{234}Th activity after 10 min was determined by collection of particulate and dissolved ^{234}Th simultaneously. The total ^{234}Th activity after 3 h was calculated as the sum of the fractioned ^{234}Th filtration of the particulate and dissolved ^{234}Th 19

Figure 3.4: ^{234}Th adsorption onto different particle types after 3 h experiments. The plots show the fraction of particulate ^{234}Th (3.4-a), the distribution coefficient in relation to the particle concentration ($\log K_d$) (3.4-b) and particle surface ($\log K_A$) (3.4-c) as well as the particulate $C/^{234}\text{Th}_p$ ratio (3.4-d). Errors represent a 95 % confidence coefficient ($n = 7 - 9$). Different lower-case letters indicating significant differences of $P < 0.05$. . 20

Figure 3.5: The $\log K_d$ values of the experiments in relation to the particle concentration. 24

Figure 3.6: Correlations between the percentage of ^{234}Th adsorbed to the particulate fraction against the surface area (3.6-a); the distribution coefficient in relation to the particle concentration ($\log K_d$) and particle surface ($\log K_A$) (3.6-b) and the $C/^{234}\text{Th}$ ratio to $\log K_A$ (3.6-c). Errors represent a 95 % confidence coefficient ($n = 7 - 9$). Statistical analyses show significant correlation of $P < 0.05$ 26

Figure 4.1: Scheme of the ^{234}Th adsorption experiments of part A, B and C. Experiment A determine the adsorption preference of ^{234}Th onto different PS. Experiment B was carried out in order to determine the influence of the PS Fucoïdan on the adsorption process of ^{234}Th onto inorganic mineral surfaces. Experiment C was conducted to describe the adsorption of ^{234}Th to a mineral surface in presence and absence of natural COM. MWCO – molecular weight cut off, kDa – kilo Dalton. 33

Figure 4.2: a: The concentration of the PS in the initial solution and the ultra-filtrate of Fucoïdan, Chondroitin and Pullulan in experiment A. Figure b-d indicate the concentration of Fucoïdan in experiment B of the fine sediment (d), Fucoïdan (e) and Fucoïdan and fine sediment (f) added. Error bars represent the 95 % confidence level of the subsamples ($n = 6 - 9$) for PS analyses..... 36

Figure 4.3: Recovery of ^{234}Th in control run, without adding particles or PS, to determine the ^{234}Th loss onto the container walls und ultrafiltration devices. + and – MB indicate

the recovery in presences or absence of the ultrafiltration membrane (MB). Significance level $P < 0.05$	37
Figure 4.4: Figure a: Percentage of colloidal and dissolved ^{234}Th fraction of Fucoidan, Chondroitin and Pullulan of experiment A. Figure b: Distribution coefficient ($\log K_d$) between the colloidal and dissolved ^{234}Th activity in relation to the colloidal concentration. The ^{234}Th activities are corrected for ^{234}Th loss onto container walls: Errors indicate standard deviation. Significance level $P > 0.05$	38
Figure 4.5: Percentage of particulate, colloidal and dissolved fraction (corrected for ^{234}Th loss onto container walls) of experiment B. Errors indicates standard deviation. Significance level of particulate ^{234}Th $P < 0.05$; dissolved ^{234}Th : $P > 0.05$ and colloidal ^{234}Th : $P < 0.05$	38
Figure 4.6: Results of the experiment C. The percentage of ^{234}Th adsorbed to fine sediment particles (a) and the distribution coefficient- $\log K_d$ (b) in deionized water and natural seawater. Dissolved ^{234}Th samples run in deionized water are corrected for the ^{234}Th loss onto the container walls during 2 h incubation period. Error bars indicate SD of $n = 3$. Significance level $p < 0.05$	39
Figure 4.7: Linear relationship between ^{234}Th activity per μmol of carbon and the ratio of carbon to sulphated group of a monomer of Fucoidan, Chondroitin and Pullulan.	40
Figure 5.1: Map of the Baltic Sea and the Mecklenburg Bay with the Station 23.c, 23.b and 23.o along a vertical transect. Map was processed with Generic Mapping Tool (GMT) 5.1.2 by Stefan Meinecke. Bathymetric data bases on GEBCO-08 data. The figure was prepared with Adobe Illustrator CS6 version 682.	45
Figure 5.2: Experimental set-up of the annular flume experiments. 1: Turbidity-meter, 2: 10 cm sediment cores, 3: Second level, 4: Acoustic Doppler Velocitymeter (Vectrino profiler), 5: Motor, 6: Notebook for data record.....	48
Figure 5.3: Sampling scheme of the experiment including the current velocity just beyond the $u_{cr}^{*initial}$ and beyond $u_{cr}^{*erosion}$ over time and the points of sampling (t_0 - t_5) as well as the time intervals between sampling (Δt_1 - Δt_5). The experiment was split into two phases, the 'resuspension' and 'deposition' phase.....	48
Figure 5.4: Station 23.c (0.5-1 cm - leaching) as an example of the decay curve of beta activity for the original measured activities and the ^{212}Bi corrected decay within ~170 days (a). The beta activity of ^{212}Bi over ~170 days, that grows in by the decay of ^{228}Th of the sample (b).....	52
Figure 5.5: The mass spectrometry plot of station 23.c (0.5-1 cm) as an example of leached sediment sample. ^{232}Th , ^{230}Th and ^{228}Th were identified according to the emitted energy.....	53
Figure 5.6: Thorium- and uranium decay series are illustrated as well the type of radioactive decay and the half-life of the nuclide. Source: world nuclear association (http://www.world-nuclear.org/information-library/safety-and-security/radiation-and-health/naturally-occurring-radioactive-materials-norm.aspx (from: 24.05.2016)) .	54

Figure 5.7: Temperature and salinity profile at the stations along a transect in the Mecklenburg Bay as well as the depth dependent density plot. The point data were extrapolated within the sections.	55
Figure 5.8: 5.8-a: Measured critical shear stress velocity (u^*_{cr}) of initial motion of particles and erosion as well as the calculated u^*_{cr} according to Shields at three stations in the Mecklenburg Bay. 5.8-b: Turbulent kinetic energy (TKE) of initial resuspension and erosion flow regime for the sediments. The errors indicate SD.	57
Figure 5.9: The total particulate matter (TPM) concentration over time during the resuspension and deposition phase (figure 5.3) of three stations along the transect at the Mecklenburg Bay, Baltic Sea. The closed and opened Symbols of each type represent two different current velocities (initial resuspension and significant Erosion). Errors indicate SD TPM concentration. of	58
Figure 5.10: Particle- and particle-associated ^{234}Th ($^{234}\text{Th}_p$) fluxes at two different current velocities of initial resuspension and significant erosion of the sediment surface of three stations along the transect at the Mecklenburg Bay, Baltic Sea. Errors of particles fluxes are based on the error propagation of SD of the total particulate matter (TPM). Errors of $^{234}\text{Th}_p$ fluxes result from error propagation of the standard ^{234}Th error and the SD of the TPM concentration for individual samples (see section 4.2.3).....	59
Figure 5.11: The distribution coefficient ($\log K_d$) at the three stations during the resuspension phase of the experiment. Errors are based on the error propagation of the standard ^{234}Th error and the SD of the TPM concentration for individual samples (see section 4.2.3). Significance levels $P > 0.05$	59
Figure 5.12: Activities of particle associated ^{234}Th ($^{234}\text{Th}_p$), dissolved ^{234}Th ($^{234}\text{Th}_d$), ^{238}U as well as the ratio of total ^{234}Th ($^{234}\text{Th}_{tot}$) and ^{238}U in the water column of the surface und close to the seafloor (<1.5 mab). Closed symbols indicate $^{234}\text{Th}_p$, open symbols $^{234}\text{Th}_d$ and red symbol represents the ^{238}U activity. Errors are expressed as SD.	60
Figure 5.13: ^{234}Th profiles of the sediment from three stations along the transect in the Mecklenburg bay. The white striped area indicating supported ^{234}Th and the dark grey area shows the excess ^{234}Th . Total measured activities are represented as filled black dots. The inventories are calculated from the dry bulk density and are shown in each plot.....	61
Figure 5.14: The observed and modelled $^{234}\text{Th}_{ex}$ activity using the models of Soetaert et al. (1996) as well as the mixing coefficient (D_b) and the injection flux (Flux_{inj}) at the three station in the Mecklenburg Bay. The D_b and Flux_{inj} were calculated from model 3.....	62
Figure 5.15: Linear correlation between the particulate ^{234}Th flux and the total particulate matter (TPM) concentration of the resuspension phase of the resuspension-deposition-experiment. The red dot is not included into the regression due to an expected saturation in ^{234}Th adsorption.	69
Figure 5.16: Scheme of the simple box model used for the calculation of ^{234}Th downward fluxes toward the sediment. The water column is divided into 3 boxes based on the density gradient of figure 5.7. Z_{i-3} indicates the layer thickness of the box. The red arrow represents the downward export fluxes. SW and BW represents the surface water and bottom water sampling depth. The green box illustrates factors that control the ^{234}Th distribution in each box.....	71

Figure 5.17: Cumulative ^{234}Th und total particulate matter (TPM) downward flux in the water column of three stations in the Mecklenburg Bay. The errors are based on the error propagation of SD errors of ^{234}Th activities and TPM concentration.....72

ABSTRACT

Thorium-234 (^{234}Th) has been widely used as a tracer for particle-related processes such as horizontal and vertical particle transport, export fluxes and sediment dynamics. For a long time, it was assumed that the distribution of ^{234}Th in the ocean is mainly controlled by the decay of the mother nuclide Uranium-238 (^{238}U), its own radioactive decay and the export by particles. However, there are increasing indications that the particle and colloidal composition plays an important role in ^{234}Th scavenging processes. To gain insight into the factors that control ^{234}Th scavenging onto particles, both, laboratory experiments and field measurements were conducted.

In the first part of the laboratory experiments, the adsorption of ^{234}Th onto different natural particles was investigated. The particles used differed in surface area and surface quality. *Rhodomonas* spp., *Surirella* spp. and *Synechococcus* spp. represented organic coated particles, while the fine sediment fraction $<100\ \mu\text{m}$ showed a mineral surface. It was expected that these particles differ not only in their surface area, but also in their adsorption properties.

The distribution coefficient (K_d) describes the distribution between particulate and dissolved ^{234}Th phase in relation to the particle concentration and is commonly used to estimate the adsorption of ^{234}Th onto particles. However, the presented study introduces the distribution coefficient (K_A), which describes the distribution of the ^{234}Th phases in respect to the particle surface. In relation to the particle concentration the highest ^{234}Th uptake capacity was found for the fine sediment fraction. However, a strong positive correlation between the percentage of ^{234}Th associated to the particle phase and the particle surface indicated that the surface area plays a crucial role in ^{234}Th adsorption. In relation to the surface area the organic coated particles of *Surirella* spp. and *Rhodomonas* spp. showed a higher ^{234}Th uptake potential compared to the fine sediment particles, which supports the assumption of preferential ^{234}Th adsorption to organic particles. A strong inverse correlation between $\log K_d$ and $\log K_A$ indicates that the use of the particle concentration-based $\log K_d$ does not reflect a suitable proxy to describe ^{234}Th adsorption onto different particles. The experimental results of the first part indicated that different natural particle types have varying ^{234}Th uptake potential in relation to their surface area and quality.

In a second part of the experiments, the influence of natural colloidal matter in the ^{234}Th adsorption process was investigated. It has recently been reported that acid polysaccharides (APS), as one major fraction of the colloidal pool, are strongly associated

to ^{234}Th activity. Therefore, different polysaccharides with varying functional group composition were used for ^{234}Th adsorption experiment. It could be shown that the ^{234}Th adsorption seemed to be increased with increasing amount of sulphated functional groups. This indicated that sulphated groups are most likely involved in the ^{234}Th adsorption process. In addition, the ^{234}Th adsorption onto the fine sediment fraction $<100\ \mu\text{m}$ in presence and absence of one of the polysaccharides as well as the natural colloidal fraction was investigated. The ^{234}Th association to the particles is increased only slightly in the presence of the polysaccharide. However, in presence of the natural colloidal fraction, a significant increase of ^{234}Th adsorption to the mineral surface was observed. I assume that not only one fraction of the colloidal pool is involved in the ^{234}Th scavenging but rather the total spectrum of colloidal matter. These investigations support the assumption of the important rule of colloidal matter in ^{234}Th association to particles and could enhance the understanding of ^{234}Th adsorption behaviour on a molecular level.

The third set of experiments was conducted to understand factors that control ^{234}Th scavenging in the bottom water column. The ^{234}Th adsorption for different sediment types as well as the influence of the hydrodynamic conditions were investigated. The overall observed and pronounced fluffy layer on top of the sediment led to the result that no significant differences in ^{234}Th uptake could be observed between the sediment types as well as in varying hydrodynamic regimes. It is speculated that in presence of a fluffy layer and during moderate resuspension events the ^{234}Th uptake potential could be very similar in the whole study area. These findings showed that the fluffy layer has a greater influence in ^{234}Th scavenging in the bottom water column than previously expected.

In the Mecklenburg Bay, south-western Baltic Sea, a significant increased ^{234}Th and particle flux as well as decreased particle residence time toward the sediment was observed, which indicated high particle dynamic in the bottom water column. This is probably caused by the increasing fraction of sediment material in the bottom water column. It is assumed that the sediment particles act as ballast and therefore, increase the sinking velocity, and also lead to an increased particle surface resulting in increased ^{234}Th uptake potential. Particle dynamics in the bottom water column are therefore higher than in surface waters.

The presented study provides insight into factors that control ^{234}Th scavenging and could have influence on the application of ^{234}Th as a particle tracer and for the interpretation of ^{234}Th -based datasets.

ZUSAMMENFASSUNG

Der Partikel Tracer Thorium-234 (^{234}Th) ist ein häufig genutztes Radionuklid für die Bestimmung von Partikel bezogenen Prozessen, wie dem horizontalen und vertikalen Partikeltransport, partikulären Exportflüsse und der Sedimentdynamik. Es wurde lange Zeit angenommen, dass die Verteilung von ^{234}Th im Ozean keinen anderen Prozessen als dem Zerfall des Elternnuklides Uran-238 (^{238}U), dem eigenen Zerfall und den Export durch Partikel unterliegt. Jedoch mehren sich die Hinweise, dass auch die chemische Zusammensetzung der Partikel und Kolloide eine entscheidende Rolle bei der ^{234}Th Adsorption und deren Transport spielen. Um einen Einblick über die Faktoren zu bekommen die das sogenannten ^{234}Th ‚scavenging‘ kontrollieren, wurden im Rahmen dieser Arbeit sowohl Laborversuche als auch Feld Messungen durchgeführt.

Im ersten Teil wurde in Laborexperimenten die Adsorption von ^{234}Th an verschiedene natürliche Partikeltypen untersucht. Diese Partikel unterschieden sich hinsichtlich ihrer Partikeloberfläche und Partikelqualität. Die einzelligen Mikroorganismen *Rhodomonas* spp., *Surirella* spp. und *Synechococcus* spp. wurden der Gruppe der organischen Partikel zugeordnet, wohingegen die feine Sedimentfraktion mit einer Partikelgröße $<100\ \mu\text{m}$ eine mineralische, anorganische Oberfläche aufweist. Es wurde erwartet, dass die Partikeltypen sich nicht nur hinsichtlich ihrer Partikeloberfläche, sondern auch ihren Adsorptionseigenschaften unterscheiden.

Der Verteilungskoeffizient K_d , welcher die Verteilung von ^{234}Th zwischen der gelösten und partikularen Phase in Bezug auf die Partikelkonzentration beschreibt, wird häufig genutzt um die ^{234}Th Adsorption an Partikel zu bestimmen. In diese Arbeit wird allerdings zusätzlich ein Verteilungskoeffizient, K_A , eingeführt, der die Verteilung der ^{234}Th Fraktionen in Bezug auf die Partikeloberfläche darstellt. In Bezug auf die Partikelkonzentration zeigt die feine Sediment Fraktion die höchste ^{234}Th Aufnahmekapazität. Jedoch deutet ein positiver Zusammenhang der Partikel assoziierten ^{234}Th Fraktion und der Partikeloberfläche darauf hin, dass die Partikeloberfläche eine entscheidende Rolle in der ^{234}Th Adsorption spielt. Dabei weisen die organischen Partikel *Rhodomonas* spp. und *Surirella* spp. das höchste ^{234}Th Aufnahmepotential in Bezug auf ihre Oberfläche auf. Dies unterstützt die Annahme, dass ^{234}Th bevorzugt an organische Oberflächen adsorbiert. Des Weiteren, wurde im Rahmen dieser Arbeit ein starker negativer Zusammenhang zwischen dem $\log K_d$ und $\log K_A$ nachgewiesen. Der auf die Konzentration-bezogene $\log K_d$ scheint demnach kein geeigneter Proxy zu sein um die ^{234}Th Adsorption an Partikel zu beschreiben.

Im zweiten Teil der Experimentreihe wurde der Einfluss von kolloidalen Material auf den ^{234}Th Adsorptionsprozess untersucht. Seit einiger Zeit wird vermehrt über einen Zusammenhang von ^{234}Th Aktivität und Konzentration von sauren Polysacchariden (ASP), als ein Hauptbestandteil des kolloidalen Materials, berichtet. Um die Rolle von Polysacchariden, die sich hinsichtlich ihrer funktionellen Gruppen unterscheiden zu untersuchen, wurden Laborversuche mit verschiedenen kommerziell verfügbaren Polysacchariden durchgeführt. Es konnte eine zunehmende ^{234}Th Adsorption mit zunehmendem Gehalt an Sulfatgruppen im Molekül beobachtet werden. Dies könnte drauf hinweisen, dass Sulfatgruppen eine Rolle in der ^{234}Th Adsorption spielen. Allerdings sind weiter systematische Studien notwendig um auch andere reaktive Gruppen zu identifizieren, die die ^{234}Th Aufnahme beeinflussen. Zusätzlich wurden Experimente zur ^{234}Th Adsorption an die feine Sedimentfraktion in An- und Abwesenheit eines Polysaccharides, sowie des natürlichen kolloidalen Materials untersucht. Die ^{234}Th Assoziation an die Sedimentpartikel war nur leicht erhöht in Anwesenheit des Polysaccharides, jedoch deutlich verstärkt in Präsenz der natürlichen Kolloide. Dies lässt drauf schließen, dass nicht nur eine Komponente des kolloidalen Materials, sondern eher das gesamte Spektrum von Substanzen im ^{234}Th ‚scavenging‘ involviert ist. Die Untersuchungen in Rahmen dieser Arbeit unterstützen die Annahme, dass Kolloide eine wichtige Rolle in ^{234}Th Assoziation an Partikel spielen und können das Verständnis der ^{234}Th Adsorption auf molekularer Ebene verstärken.

Der experimentelle Teil des dritten Abschnittes diente der Untersuchung der Faktoren die das ^{234}Th ‚scavenging‘ in dem vom Sediment beeinflussten Bereich der Wassersäule kontrollieren. Dabei wurde die ^{234}Th Adsorption an verschiedene Sedimenttypen der Ostsee bei unterschiedlichen hydrodynamischen Bedingungen untersucht. Es wurde erwartet das verschiedene Sedimenttypen Unterschiede in der ^{234}Th Adsorption aufweisen und die ^{234}Th Adsorption aufgrund der erhöhten Kollisionswahrscheinlichkeit unter erhöhten Strömungsbedingungen verstärkt ist. Die überall zu beobachteten sehr mobile und stark ausgeprägte ‚fluffy layer‘ auf der Sedimentoberfläche führt dazu, dass eine sehr ähnliches ^{234}Th Aufnahmepotential zwischen den Sedimenttypen festgestellt wurde. Auch konnten keine signifikanten Unterschiede in der ^{234}Th Adsorption in unterschiedlichen hydrodynamischen Regimen nachgewiesen werden. Es kann spekuliert werden, dass in Anwesenheit einer ‚fluffy layer‘ und unter moderaten Strömungsbedingungen das ^{234}Th Aufnahmepotential im gesamten Untersuchungsgebiet sehr ähnlich sein wird. Die Ergebnisse dieser Untersuchung zeigen, dass die Präsenz der ‚fluffy layer‘ einen größeren

Einfluss auf das ^{234}Th ‚scavenging‘ in der bodennahen Wassersäule hat als im Vorfeld erwartet.

In der Mecklenburger Bucht in der südwestlichen Ostsee, konnte eine signifikante Zunahme des ^{234}Th und Partikelflusses sowie eine deutliche Abnahme der Partikelaufenthaltszeiten in der bodennahen Wassersäule nachgewiesen werden. Dies deutet auf eine starke Partikeldynamik in Bodennähe hin, welche wahrscheinlich mit einer zunehmenden Sedimentfraktion in diesem Wasserkörper einhergeht. Es wird angenommen, dass diese als Ballast auf sinkende Partikel wirken und damit die Sinkgeschwindigkeit erhöhen. Im Vergleich zu pelagischen Partikeln, die hauptsächlich organischen Ursprungs sind, kann das ^{234}Th Aufnahmepotential der Sedimentpartikel aufgrund ihrer größeren Partikeloberflächen erhöht sein. Dies führt zu einer verstärkten Partikeldynamik in der bodennahen Wassersäule vor allem in hochdynamischen küstennahen Regionen.

Die vorliegende Arbeit gibt vor allem Einblicke in Faktoren die das ^{234}Th ‚scavenging‘ beeinflussen welche Auswirkungen auf die Anwendung von ^{234}Th als Partikeltracer haben kann und bedeutend für die die Interpretation von ^{234}Th -basierenden Berechnungen sind.

1 INTRODUCTION

The marine carbon cycle is the most important part of the global carbon cycle and is crucial for climate changes (Yin et al., 2006). The transfer of atmospheric carbon dioxide to the ocean interior is related to the export flux of particulate organic carbon (POC). To understand the biogeochemical cycle of carbon in the ocean, investigations of POC export fluxes from the euphotic zone are crucial (Volk and Hoffert, 1985). Over the past several decades, Thorium isotopes have been used to describe particle dynamics and particle export fluxes in aquatic systems (Cochran and Masqué, 2003). On time scales of days to months, the short-lived thorium-234 isotope (^{234}Th) is widely used to trace particle related processes such as particle cycling, mass export fluxes from the upper ocean or fluxes of any component of the total mass (e.g., carbon, nitrogen, silica, etc.), and scavenging in re-suspension processes in the benthic boundary layer (e.g., Buesseler et al., 1992; Turnewitsch and Springer, 2001; Buesseler et al., 2006; Peine et al., 2009). In addition, the ^{234}Th based export flux is commonly used for the calibration of sediment traps (e.g. Lampitt et al., 2008; Lalande et al., 2008; Cochran et al., 2009).

^{234}Th is a highly particle-reactive radionuclide with a half-life of 24.1 d. It is produced by the radioactive decay of its long-lived ($t_{1/2} = 4.468 \times 10^9$ yr), chemically conservative and non-particle reactive parent nuclide uranium-238 (^{238}U) (Santschi et al., 2006 and references therein). If, for a given parcel of water, the scavenging and export rate of ^{234}Th onto settling particles is higher than the ^{234}Th production rate by ^{238}U decay, a radioactive disequilibrium is produced. This disequilibrium provides information about particle dynamics and export fluxes (e.g. Coale and Bruland, 1985; Bacon and van der Loeff, 1989; Buesseler et al., 2006; Peine et al., 2009; Evangelidou et al., 2011; Owens et al., 2015).

The calculation of mass export fluxes (e.g., carbon fluxes) requires the determination of ^{234}Th flux rates based on the extent of the disequilibrium between ^{234}Th and ^{238}U as well as the ratio of ^{234}Th to carbon (the C/ ^{234}Th ratio) on sinking particles. It is generally assumed that large ^{234}Th to ^{238}U disequilibria reflect a higher particle export (Buesseler et al., 2006). However, the calculation of export fluxes includes both the scavenging potential of ^{234}Th onto particles and the export of the particles by vertical or horizontal transport. Former studies assumed that the distribution of ^{234}Th is not appreciably controlled by processes other than ^{238}U decay, its own radioactive decay and the export by particles (Bacon and Anderson, 1982; Cochran et al., 1993). However, Buesseler et al. (2006) reviewed a distinct variation of the C/ ^{234}Th ratio dependent on the region, season, water depth and sampling method which led to large uncertainties in flux estimation using ^{234}Th deficiencies relative

to ^{238}U . Therefore, it appears questionable, whether ^{234}Th represents an appropriate tracer for POC (Buesseler et al., 1992, 1995, Murray et al., 1996). Thus, in order to use ^{234}Th as a particle export tracer it becomes more important to understand the mechanisms that control its particle reactivity. Previous investigations show that the particle composition and especially the particle quality may play a critical role in the scavenging process (Guo et al., 2002a; Chase et al., 2002; Quigley et al., 2002; Hirose et al., 2011). This could subsequently lead to a different ^{234}Th scavenging potential with varying particle composition (Passow et al., 2006). It can be assumed that particles with similar sinking behaviour but varying ^{234}Th uptake potential would generate quite different ^{234}Th to ^{238}U disequilibria, which accordingly may have influence to the calculation of export fluxes.

Despite the common use of ^{234}Th to determine carbon export fluxes, our knowledge of the specific scavenging behaviour of ^{234}Th onto marine organic and inorganic matter, and especially the role of the surface area and structure of particles during this scavenging process, remains relatively scarce. In particular, the adsorption preference of ^{234}Th to different phytoplankton species in the upper ocean, which represent the most important contributor to global carbon fixation and mass export of carbon through the water column (Ritzrau et al., 2001), has not yet been studied in great detail. Chuang et al. (2014) recognized an enhanced adsorption of ^{234}Th in the presence of organic coated living diatom cells compared to its cleaned frustules, which indicates preferential adsorption of ^{234}Th to organic coated particles. Furthermore, the scavenging process to inorganic particles, such as sediment minerals with high specific surfaces, is crucial for a thorough interpretation of benthic processes like re-suspension and lateral particle transport. Laboratory studies by Geibert and Usbeck (2004) illustrated a high ^{234}Th absorption capacity to MnO_2 and smectite compared to other inorganic components such as CaCO_3 and opal. Kretschmer et al. (2010, 2011) reported a strong positive correlation between the ^{234}Th uptake and the surface area of the particles. Therefore, it can be assumed that different surface structures, compositions and particularly surface areas of particles lead to variations in ^{234}Th adsorption. Uncertainties in the interpretation of ^{234}Th -corrected particle fluxes in sediment traps as well as calculated ^{234}Th -based carbon export fluxes from the euphotic zone may indeed be generated by the possible variability of the ^{234}Th distribution among different particles types. On a particle level, this variability may have two major causes: (1) the particle surface area, and therefore the available ^{234}Th uptake potential; and (2) the chemical composition of the particle surface, which reflects a preferential adsorption of ^{234}Th onto a certain type of particle. Therefore, investigations of the ^{234}Th adsorption behaviour to different organic and inorganic particles, with respect to

the specific surface area, are necessary to understand the factors that control the ^{234}Th scavenging process in different sections of the water column and oceanic regions.

On a molecular level, colloids are known to be involved in the metal removing in the ocean (Santschi, 2005). Due to their metal character most radionuclides can be associated to colloidal matter by the formation of chelating complexes (Chuang et al., 2015). Previous studies have recognized that colloidal particles are involved in the scavenging process of ^{234}Th onto particles (e.g. Honeyman and Santschi, 1989; Guo et al., 1994; Baskaran et al., 2003). In a former study Honeyman and Santschi (1989) postulated a “Brownian pumping model” according to which Th(IV) isotopes are transferred to larger filterable particles through coagulation of colloidal intermediates. In addition, it has been observed that the adsorption of ^{234}Th to inorganic surfaces can be modified as a result of organic, surface-active substances coating these surfaces (Santschi et al., 2006). Therefore, it can be assumed that colloidal matters play a critical role in scavenging of trace metals and their transfer from the dissolved to the particulate phase.

It is reported that acid polysaccharides (APS) and siderophores are major components of biomolecules which are involved in metal uptake (Neilands, 1995; Buck et al., 2010; Kraemer et al., 2014). Exopolymeric substances (EPS), produced by bacteria and phytoplankton, represent an important APS rich fraction of colloidal organic matter (COM) and can be attached to the cell surface or are excreted to the environment as free colloids (Passow, 2002b). Both laboratory and field studies demonstrated that ^{234}Th is associated with APS rich components of EPS (Guo et al., 2002b; Santschi et al., 2003; Zhang et al., 2008; Hirose et al., 2011; Xu et al., 2011; Chuang et al., 2014). Some previous studies reported that a strong ^{234}Th -binding ligand in size of ≤ 13 kDa is likely responsible for ^{234}Th removal in the ocean (Guo et al., 1997; Quigley et al., 2002; Alvarado Quiroz et al., 2006). The latter authors suggested that such ligands are able to form clustered structures of ^{234}Th binding complexes including acid functional groups like carboxylic, sulphate and/or phosphate acid. However, there is little known about the specific ligand or preferred functional groups involved in ^{234}Th adsorption. For a better use of ^{234}Th as an oceanographic tracer for particle related processes, systematic studies are needed to investigate the role of COM, including the molecular composition and functional groups on ^{234}Th scavenging.

Shelf regions, continental margins and estuaries once cover a relatively small area of the global ocean, nevertheless more than 90 % of the organic carbon is buried in their sediments. For the biogeochemical cycle of carbon the understanding of particle dynamics

in coastal waters is very important (Hedges and Keil, 1995; Hartnett et al., 1998). Shallow water systems and estuaries are very dynamic regions in particle cycling due to their low water depth and/or the terrestrial input (Bauer et al., 2013). Therefore, the influence of suspended sediment particles plays a crucial role for the biogeochemical particle cycle and the distribution of pollutants (e.g. Bauer et al., 2013; Kersten et al., 2005; Leipe et al., 2005). As introduced above, it is assumed that the particle properties on both molecular and particle level are important for ^{234}Th scavenging processes. Especially in regions of strong terrestrial or lithogenic influence the fact of varying particle types with different adsorption potential increasingly becomes a focus. To describe particle dynamics and quantify particle fluxes in shallow waters and estuaries ^{234}Th is widely applied (e.g. Wei and Murray, 1992; Andersson et al., 1995; Zhang et al., 2004; Kim et al., 2011). To prevent uncertainties in flux calculations and prediction of particle dynamics, the understanding of factors controlling scavenging processes are important in the coastal waters which are strongly influenced by varying conditions and particularly by a large spectrum of natural particle types.

This study presents both laboratory experiments and field measurements with the aim to investigate factors that control ^{234}Th adsorption and to describe the influence for the application of ^{234}Th as particle tracer. The Ph.D thesis is structured in three sections which deal with a specific topic each.

The first section presents laboratory experiments to investigate the ^{234}Th adsorption behaviour onto natural organic coated particles and the fine sediment fraction $<100\ \mu\text{m}$ with special emphasis on the surface area and organic content of the respective particles. Here, the distribution coefficient (K_A) is introduced which reflects the distribution of particulate and dissolved ^{234}Th phase normalised to the particle surface. It is expected that different particle types show variations in ^{234}Th uptake potential with respect to varying particle surface areas and quality. These experiments allow a better understanding of the factors that control the scavenging process of ^{234}Th , which is important for the calculation of export fluxes and particle residence time as well as to describe particle dynamics.

In the second section the ^{234}Th adsorption is investigated on a more molecular level. What is the influence of natural colloidal matter in ^{234}Th adsorption to particles? If polysaccharides represent a major carrier phase, are there differences in association of ^{234}Th between different polysaccharides? What is the role of their functional group composition? To answer these questions controlled laboratory experiments are presented. The aim of the study is to investigate the influence of natural colloidal matter in ^{234}Th

adsorption to particles as well as to estimate the role of the polysaccharide fraction in the colloidal pool for ^{234}Th association. These investigations will enhance the understanding of ^{234}Th adsorption behaviour on a molecular level.

In the third section laboratory experiments and field observation are presented. The laboratory investigations were conducted to understand factors that control ^{234}Th scavenging in the bottom water column. What is the influence of varying current regimes of ^{234}Th scavenging onto natural resuspended particles? Do different sediment types show variations in ^{234}Th uptake potential? It can be expected that increasing current velocities increase the collision frequency of ^{234}Th and suspended sediment particles and lead to an enhanced ^{234}Th adsorption. Due to varying surface areas and/or particle composition it is assumed that particles in the water above different sediment types show variation in the ^{234}Th uptake potential. This could have an influence on the magnitude of the $^{234}\text{Th}/^{238}\text{U}$ disequilibria, which again leads to uncertainties in the calculation of export fluxes.

On the other hand, this section will connect the results of the previous investigated laboratory experiments with field measurements in the coastal water and sediment of the Baltic Sea. The aim is to apply the experimental results in interpretation of the field observations and in the calculation of export fluxes and particle residence time, as well as the distribution of ^{234}Th in the sediment.

The presented study could be relevant for (1) the interpretation of ^{234}Th based data, (2) the application of ^{234}Th as particle tracer and (3) providing suggestions for further investigations.

2 ²³⁴TH METHOD

2.1 Laboratory analyses and measurement via β -counting

The analytical procedure for the total, particulate and dissolved ²³⁴Th is described in Turnewitsch et al. (2008) and predominantly follows methods by van der Loeff and Moore (1999).

For particulate ²³⁴Th, the samples were filtrated at ~ 400 mbar overpressure through polycarbonate filters (142-mm-diameter) with a pore width of 0.4 μm or 1.0 μm . Dissolved ²³⁴Th was co-precipitated in the total volume or subsample of the filtrate by formation of MnO_2 . To form MnO_2 in a volume of 1 litre, 10 – 30 μl of a 25% NH_3 solution, 40 – 60 μl of a KMnO_4 solution (60 g l^{-1}) and 60 – 80 μl of a $\text{MnCl}_2 \cdot 4\text{H}_2\text{O}$ solution (400 g l^{-1}) were added to each sample. Larger sample volumes required adjusted quantities of reagents. If the precipitation resulted in a lighter yellow colour, an additional small portion of the precipitation chemicals were added. Previous tests have shown that the formation of filterable MnO_2 particles in deionised water (section 4) seems to be problematic because most of the MnO_2 particles passed the filter. Probably, this is related to the lack of dissolved organic matter which act as crystallisation germ in the formation of MnO_2 particles. Previous experimental test indicated that a small fraction of seawater is sufficient for the formation of filterable MnO_2 . Therefore, 3 ml of 0.2 μm filtered seawater was added to samples running in deionised water before MnO_2 precipitation. It is assumed that the immediate addition of the small portion of in situ water to the samples have no influence on interpretation of the results. The precipitating MnO_2 particles were allowed to develop for at least 3 h. Subsequently, the MnO_2 particles were filtered via polycarbonate filters with a 1.0 μm nominal pore width by filtration.

To determine the total ²³⁴Th activity of the samples two ways were applied: (1) the total ²³⁴Th activity of the fractioned samples was calculated by summing the separately determined particulate and dissolved ²³⁴Th activity and (2) the total ²³⁴Th content was analysed directly by the simultaneous collection of natural particles and MnO_2 particles on the same filter. Therefore, the unfiltered sample was precipitated with MnO_2 and filtrated (as described above).

Between the two MnO_2 samples the filtration equipment was rinsed with a solution of 10 ml of H_2O_2 l^{-1} in 1 M HCl and with deionised water. For the particulate, dissolved and total ²³⁴Th the volume of the filtered water was determined with volumetric flasks and graduated cylinders.

All of the filters were air-dried, folded in a reproducible way and wrapped in mylar foil. The radioactivity emitted from these sample packages was determined non-destructively in RisøGM-25-5 low-level beta multi-counters. ²³⁴Th is a β-emitter with a half-life of 24.1 days. The emitted electrons have a very weak main beta decay energy of 0.053 MeV (Santschi et al., 2006). However, protactinium-234 (²³⁴Pa), its immediate daughter nuclide with a half-life of 1.17 min, emits a much higher energy with a maximum of 2.3 MeV (Nour et al., 2002). Therefore, the decay of ²³⁴Pa was used for the ²³⁴Th measurements in the presented study. All of the samples were counted as quickly as possible and at least twice within 150 days after sampling. After ~150 days the samples were measured again to determine background counts.

The background activity of all spiked samples showed a high variability of 114.5 % (1.04 ± 1.19 cpm). In the majority of cases (76.6 %), the background activity of the dissolved ²³⁴Th samples was one order of magnitude higher compared to the naturally expected background activities (0.33 ± 0.05 cpm, as noted in Turnewitsch and Springer (2001)). These differences may be partly caused by the minor amounts of uranium trapped in the MnO₂ precipitate, leading to a high background signal. In an additional experiment this assumption was supported by separating the ²³⁴Th and ²³⁸U from the uranium standard solution via an ion exchange column. The background level of the ²³⁴Th separated samples was significantly lower (0.445 ± 0.04 cpm) compared to most of the sample background levels. For this reason, a background level of 0.445 cpm was subtracted from all of the dissolved ²³⁴Th samples.

Total ²³⁴Th activities were corrected for the ingrowth of ²³⁴Th from ²³⁸U during the analytical procedure (see section 2.3). The reported activities are expressed as activity per volume of seawater (dpm l⁻¹). Turnewitsch et al. (2008) reported an extraction efficiency of 99.0 % ± 1.4 % for total ²³⁴Th after a second precipitation and filtration step. The counting efficiency for each detector used here was determined by Robert Turnewitsch by using standard ²³⁸U filters, which were prepared according to van der Loeff and Moore (1999).

The initial total ²³⁴Th activity of the experiments was estimated as the sum of ²³⁸U activity and the activity of the added ²³⁴Th spikes (see section 2.2). The activities of ²³⁸U in seawater were calculated from salinity of the seawater based on the ²³⁸U-salinity-relationship developed by Chen et al. (1986). The seawater used in the experiments was stored several days before use. Therefore, an equilibrium between ²³⁸U and ²³⁴Th of the seawater was assumed.

2.2 Spiking with ²³⁴Th

To provide measurable differences in activity, the experiments were enriched with ²³⁴Th of 14.83 dpm l⁻¹, which represents six times of the activity in the world's ocean. Therefore, the ²³⁴Th activity in the experiments resulted from the natural ²³⁴Th activity (= ²³⁸U, as described in section 2.1) of the seawater (or increased salinity for *Surirella* spp. approach) and the added ²³⁴Th activity of 14.83 dpm l⁻¹. For increasing ²³⁴Th activity a uranium oxide solution (U₃O₈ in 5% HNO₃) (Specpure Uranium Plasma Standard Solution, Alfa Aesar, Karlsruhe) with a concentration of 1000 ± 2 µg ml⁻¹ was used. As described in the Diploma thesis of Stephan Werk (Werk, 2003) the composition of the uranium solution corresponds to the natural isotopic ratio of 99.284 % ²³⁸U, 0.710 % ²³⁵U and 0.0057 % ²³⁴U (Tsoulfanidis and Landsberger, 1995). With a total specific activity of 0.747 dpm µg⁻¹, the standard solution contains ²³⁸U activity of 741.65 ± 1.5 dpm ml⁻¹. To increase the experimental activity to 14.83 dpm l⁻¹ to each litre of seawater 20 µl of the uranium solution was added. Because of the large volume and the use of natural seawater in the experiments of section 3 and 5, the spike was added without neutralization. Prior tests indicated that the pH did not change during the experiments. Due to the lack of a buffer system in deionised water, unfortunately the decreasing pH of the experiments in section 4, compared to natural seawater, was not considered and is discussed in section 4.3.1.

2.3 Determination of ²³⁴Th activity

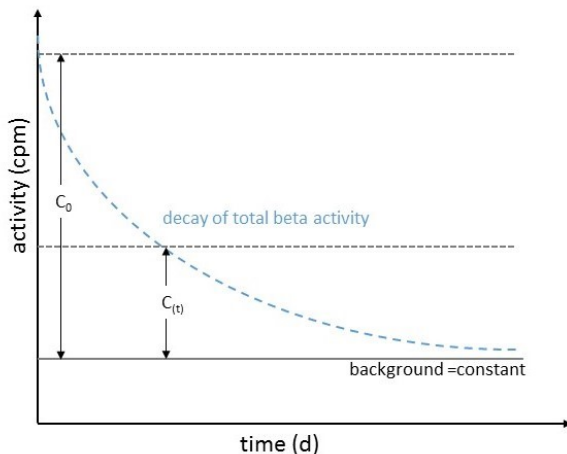


Figure 2.1: Illustration of the ²³⁴Th decay of a filter sample including the background activity, due to other beta-emitting radionuclides beside ²³⁴Th. C₀ represents the activity at time sampling and C_(t) show the activity at point of measurement.

For the determination of the ²³⁴Th activity the samples were measured as soon as possible after sampling and at least 2 times within the decay period. After 150 days, the activity was measured again to determine background activity.

Figure 2.1 shows a scheme of the beta decay which is described by the following equation:

$$C_{(t)} = C_0 e^{-\lambda_{Th} t} \quad (2.1)$$

$$C_0 = \frac{C(t)}{e^{-\lambda_{Th} \cdot t}} \quad (2.2)$$

with: C_0 = ²³⁴Th activity (cpm) at time point of sampling
 $C(t)$ = ²³⁴Th activity (cpm) during measurement at time point t
 λ_{Th} = decay constant of ²³⁴Th
t = time

The ²³⁴Th activity (A_{Th} in dpm l⁻¹) was calculated by the following equation:

$$A_{Th} = \frac{C(t) - C_{BG}}{e^{-\lambda_{Th} \cdot \Delta t} \cdot V \cdot E_c} \quad (2.3)$$

with: C_{BG} = background activity (cpm) measured ~150 d after sampling
 Δt = time between particulate or dissolved ²³⁴Th filtration and ²³⁴Th measurement
V = filtered volume (l)
 E_c = counting efficiency (cpm dpm⁻¹)

The counting efficiency of each detector was determined by Robert Turnewitsch by using standard ²³⁸U filters, which were prepared according to van der Loeff and Moore (1999). The ingrowth of ²³⁴Th from ²³⁸U during experiments until particulate or dissolved filtration was calculated according to the Ph.D thesis of Robert Turnewitsch (1999) and follows the equation:

$$A_{Th-co} = \frac{A_{Th} - A_U \cdot \left(\frac{\lambda_{Th}}{\lambda_{Th} - \lambda_U}\right) \cdot (1 - e^{-[\lambda_{Th} - \lambda_U] \cdot \Delta t_1})}{e^{-[\lambda_{Th} - \lambda_U] \cdot \Delta t_1}} \quad (2.4)$$

with: A_{Th-co} = corrected ²³⁴Th activity for ingrowth from ²³⁸U
 A_U = ²³⁸U activity (dpm l⁻¹)
 Δt = time between particulate or dissolved ²³⁴Th filtration and
 λ_U = decay constant of ²³⁸U
 Δt_1 = time between sampling and particulate or dissolved ²³⁴Th filtration

3 ADSORPTION OF ^{234}Th ONTO PARTICLES WITH VARIABLE SURFACE QUALITIES AND SURFACE AREAS

3.1 Method and material

3.1.1 Particle types and preparation

For the ^{234}Th adsorption experiment, selected natural types of organic and inorganic particles were used. Following the assumption of varying ^{234}Th adsorption capacity onto the surface of different species, two photoautotrophic protozoa in different taxonomic orders were selected, which represent the phytoplankton species: *Rhodomonas* spp. (Cryptophyceae) and *Synechococcus* spp. (Cyanobacteria). In contrast, *Surirella* spp. (Bacillariophyceae), a benthic diatom species, represents an organic coated particle type of the sediment. Furthermore, a different surface structure and composition is expected to be caused by the different functional properties of the benthic diatom *Surirella* spp. compared to the planktonic species *Rhodomonas* spp. and *Synechococcus* spp., is expected. As a representative of inorganic particles with a mineral surface and a main component of marine sediment, we used the fine sediment fraction $<100\ \mu\text{m}$. This fraction can be re-suspended at the marine sediment water interface and remains in suspension over a long period. Together with its high specific surface area it can be assumed that this fine fraction could scavenge a large amount of dissolved ^{234}Th from the water column.

For the experiment, the diatom *Surirella* spp. was cultured in sterile Erlenmeyer flasks under ideal conditions using $F_{1/2}$ medium plus meta silicate (Salinity 31, $10\ ^\circ\text{C}$) in a dark/light cycle of 12:12. In contrast, *Rhodomonas* spp. and *Synechococcus* spp. were cultured in $F_{1/2}$ or BG11 media. These cultures were kept in vented glass bottles, under constant stirring and at room temperature under a dark/light cycle of 12:12 to attain a high biomass in a short period of time.

The fine sediment fraction ($<100\ \mu\text{m}$) was extracted from the Marl layer of beach ridge sediments collected at the Stoltera coast, Baltic Sea. Marl sediment was formed during glacial deposits and contains a large fraction of fine sediment particles in the Baltic sea (Jensen et al., 1999). To separate the fine sediment fraction $<100\ \mu\text{m}$ from the coarse sand fraction, a high plastic bucket was used to suspend the collected sediments. The fine sediment fraction remains in suspension and the supernatant was decanted. The collected supernatant remained for a few days to settle and the clear water was subsequently decanted carefully. The fine sediment fraction $<100\ \mu\text{m}$ was then dried at $60\ ^\circ\text{C}$. After drying, the sediment was pestled and sieved, and the fraction $<100\ \mu\text{m}$ was captured. The

organic material was removed by incineration at 500 °C for 24 h. Two weeks before an experimental run the fine sediment fraction <100 µm was suspended in deionized water to soak.

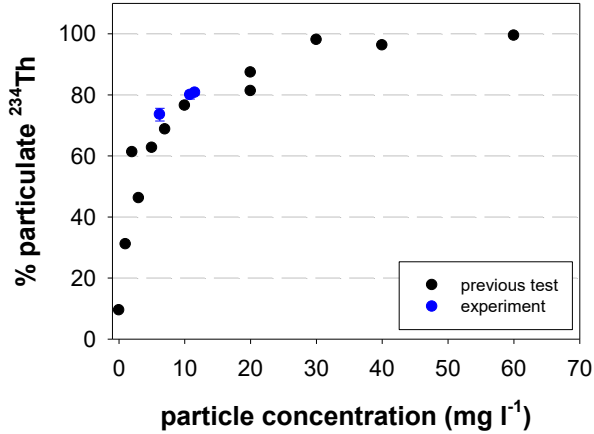


Figure 3.1: Previous test of the ^{234}Th uptake with increasing concentration of the fine sediment particles <100 µm. Black dots represent the results of this test and the blue dots show the concentration of the fine sediment fraction in the annular flume experiments.

of ^{234}Th spiked seawater (total activity: natural ^{234}Th activity of the seawater + ^{234}Th spike of 14.83 dpm l⁻¹, see section 2.1) and was stirred with a magnetic stirrer. Subsequently, the samples were filtered and the activity of particulate and dissolved ^{234}Th was analysed as described in section 2.1. The results showed that ~100 % of the total ^{234}Th activity is associated to the particulate fraction if 30 mg l⁻¹ of fine sediment was added (figure 3.1). The used particle concentration of 6.21 - 11.53 mg l⁻¹ (table 3.1) in the experiments would lead to an excess of ^{234}Th in seawater.

Baltic Sea surface water (salinity 8.0 – 9.45) was collected from the pier in Graal-Müritz or during a cruise of the RV ‘Praunus’ from the coastal Stoltera region. The water was centrifuged (Heraeus centrifuge 17RS, continuous flow Rotor of titanium 8575 at 15000 rpm) and filtered on 142-mm-diameter polycarbonate filters (1.0-µm pore width) at ~400 mbar overpressure to remove large particles. In the experiments, all components smaller than 1.0 µm are considered as part of the dissolved/colloidal fraction, which agrees well with the definition of colloids in Santschi et al. (2006) and references therein. This filtered seawater contains the natural colloidal composition and should display realistic adsorption behaviour (Geibert and Usbeck, 2004). If necessary, the seawater salinity was increased by adding natural sea salt to that amount of the algae culture to avoid bursting of the cells (salinity: *Surirella* spp. 31). To prevent undesirable growth of algae, water was stored dark at 10 °C until the experiments were performed.

To determine the ^{234}Th uptake onto the surface area of the particles, the experiments required an excess of ^{234}Th in the seawater. Due to the large surface area of the fine sediment fraction the saturation of the ^{234}Th uptake at the experimental conditions (^{234}Th enrichment of 14.83 dpm l⁻¹, 3 h incubation time) was tested previously. Therefore, an increasing concentration (0, 1, 2, 3, 5, 7, 10, 20, 30, 40, 60 mg l⁻¹) of the fine sediment fraction was added to 1 litre

3.1.2 Experimental design

The ^{234}Th adsorption experiments were performed in three identically constructed acryl annular flumes (modified after Widdows et al., 1998) filled with 75 litre filtered seawater, which permitted the formation of a uniform current velocity and led to a homogenous particle distribution. In addition, this design reduced analytical error by permitted the analysis of a large volume (2 – 5 litre) for the particle samples. After starting the annular flume, the particle suspension was added (particle concentration see table 3.1) and the rotational velocity was set to visually suspend all of the particles. After 10 – 15 min, one portion (1.5 ml) of spike was added to the flume. A complete mixture of the spike is expected within 10 min. Subsequently, three replicates of 1 litre sub-samples were taken from each flume via a PE spigot and silicone tube to analyse the total ^{234}Th activity directly as described in section 2.1. This value is considered to be the onset of the activity. After 3 h of rotation, water was sampled and analysed for the fraction of particulate and dissolved ^{234}Th activity. Before adding the particles (blank filters) and after the experiment (3 h), 0.5 – 1 litre subsamples were taken to analyse the carbon and nitrogen content. To determine the number and size of the cells, 50 ml of water were sampled and fixed with Lugol solution after the end of the experiment. For each annular flume three sub-samples of all of the analysed parameters were taken. In total, 7 to 9 replicates were processed.

Rhodomonas spp., *Synechococcus* spp., the fine fraction (<100 μm) and particle free analyses were performed in three flumes simultaneously. Because of the slow growth and the resulted low biomasses for the simultaneous use of three flumes, the *Surirella* spp. experiments were conducted on different days. It is noted that sufficient biomass was obtained after 48 – 57 days. Therefore, the three replicates of this particles were conducted in a time lag of ~50 - 60 days.

Previous studies have shown that the adsorption of the extremely particle reactive ^{234}Th onto the walls of the containers and experimental devices is problematic (Baskaran et al., 1992; Moran and Buesseler, 1992a; Geibert and Usbeck, 2004). Prior to the particle experiments, the ^{234}Th spike was added to each of the three flumes without the addition of particles ('particle free run') to test the adsorption onto the walls of the flumes. Samples were taken at subsequent intervals (10 min, 30 min, 1 h, 2 h, 3 h, 5 h) to follow the ^{234}Th activity over time.

Table 3.1: The range of particle concentrations used in the experiments, the average surface of the cells (μm^2) of the organic coated particles and the particle surface ($\text{m}^2 \text{g}^{-1}$). Errors indicate a 95 % confidence coefficient. #Labelled error is expressed as standard deviation.

<i>Rhodomonas</i> spp.	<i>Surirella</i> spp.	<i>Synechococcus</i> spp.	<i>fine sediment fraction</i>
Particle concentration (mg l^{-1})			
3.51 - 3.92	3.39 - 10.44	2.91 - 4.13	6.21 - 11.53
Surface of cell (μm^2)			
128.76 \pm 4.99	1364.52 \pm 71.24	12.55 \pm 0.49	n.a.
Particle surface ($\text{m}^2 \text{g}^{-1}$)			
0.34 \pm 0.02	0.63 \pm 0.09	5.60 \pm 0.70	14.75 \pm 0.62

3.1.3 Particle analyses

3.1.3.1 Total particulate matter and particulate carbon

To determine the total particulate matter (TPM) and particulate carbon (PC or C) content, 0.5 – 1 litre of water was filtered by vacuum at ~200 mbar through pre-combusted (500 °C for 12 h) and pre-weighed 25-mm-diameter Whatman GF/F filters. Approximately 10 ml of deionised water was used to rinse the system and remove sea salt from the GF/F filter. Until further analysis, the filters were kept frozen at -14 °C. As soon as possible, the filters were dried at 60 °C for 24 h and re-weighed to determine the TPM or particle concentration. For the PC analyses, samples were folded in tin foil and measured in a Carlo-Erba CHN Analyzer, as reported in Verardo et al. (1990) with slight modifications. For calibration, acetanilide standards with a carbon content of 71.09 % were measured. Empty pre-combusted GF/F filters were used as filter blanks and were subtracted from the measured carbon values. For the calculation of the PC, the “Blank filters” (i.e., sampled before adding the particles) were subtracted from the particle filters.

3.1.3.2 Elemental analyses of fine sediment <100 μm

For an exact characterization of the mineral composition of the fine sediment fraction <100 μm , an automated quantitative particle analysis was performed using a combined scanning electron microscopy (SEM - MERLIN VP compact) and energy dispersive X-ray

analysis (EDX – AztecEnergy software). The sample was analysed by R. Bahlo at the Leibniz Institute for Baltic Sea Research in Warnemünde.

The samples were prepared by suspending the combusted fine sediment fraction $<100\ \mu\text{m}$ in distilled water und filtering the suspension on Nuclepore filter with a pore size of $0.4\ \mu\text{m}$. The surface of the dried sample was covered by pure carbon to ensure electrical conductivity. For the measurements, a high vacuum, 15 kV electron beam and a working distance of 8.3 mm was applied. A secondary electron detector (Silicon Drift Detector – SDD) was used to acquire the X-ray spectra. Owing to the automated analysis procedure, the resulting large data set was processed for mineral or particle group identification and quantification (counting). The definition of a certain mineral or particle group was based on the elements' composition and concentration or ratios of the analysed particle.

The results of the particle analysis are shown in table 3.2. The fine sediment fraction $<100\ \mu\text{m}$ is dominated by clay minerals (37.1 %), followed by silica (19 %), feldspar (16.3 %) and calcite (11.5 %). Organic particles are less than 0.06 % of the total sample. Other minerals are mainly composed of dolomite and titanium minerals. Within the clay mineral group illite is the main mineral component. With a content of more than 96 %, aluminium-rich silica dominated the silica group.

Table 3.2: Mineral composition of the fine sediment fraction $<100\ \mu\text{m}$ analysed after combustion of the organic material. In total, 2177 particles were analysed using a coupled scanning electron microscope (SEM) and energy dispersive X-ray analysis (EDX) analysis (kindly provided by Rainer Bahlo). The unclassified fraction comprises the particle which could not be clearly identified.

Particle analyses of fine sediment fraction $<100\ \mu\text{m}$			
Percentage (%)		Percentage (%)	
clay minerals	37.08	illite	83.33
		smectite	8.46
		chlorite	7.84
		kaolinite	0.37
silica	19.10	Al rich silica	96.14
		pure silica	3.86
feldspar	16.28		
calcite	11.53		
other	4.94		
not classified	11.07		

3.1.3.3 Particle surface

Depending on the expected cell number, the Lugol fixated samples were transferred into an Utermöhl sedimentation Chamber (annular flume samples) or Bürker chamber (stock culture). Depending on the cell size, the cells were left to settle for 2 – 24 h. Cell numbers were counted under an Olympus CH 20 microscope (at least 100 cells per sample).

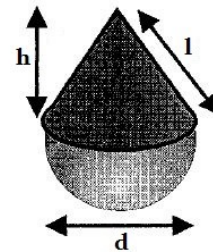
To estimate the surface area of the organic coated particles different geometric forms were assumed according to the recommendation by Hillebrand et al. (1999). Specifically, *Rhodomonas* spp. is represented by a cone and half sphere, *Surirella* spp. is represented by a prism on an elliptic base and *Synechococcus* spp. is represented by a cylinder and two half shares (Table 3.3). The cell size (at least 90 cells) was determined from samples of the fixated stock solution because these samples contained more cells per volume. Cell dimensions were measured under an Olympus BX51 microscope with the corresponding analySIS® Soft Imaging System 3.0 software. Because of the strong deformation of the *Surirella* spp. cells especially the silica shell, which was likely caused by the fixation step, living cells from the culture were analysed.

Table 3.3: Pictures and geometric forms (from Hillebrand et al., 1999) of the organic coated particles as well as the equations for the calculation of the surface area. Pictures of *Rhodomonas* spp. and *Synechococcus* spp. show the fixed cells of the experiments, while the picture of *Surirella* spp. represents the preparation of the silica shell by removing the organic matter with H_2O_2 .

Rhodomonas spp.

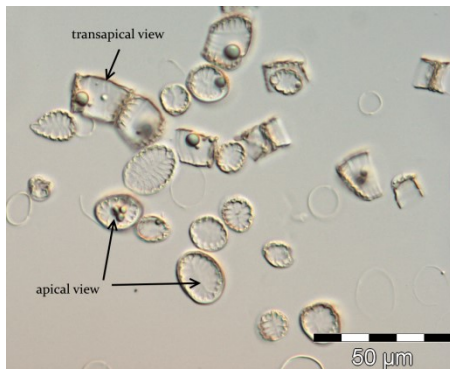


Cone + half sphere

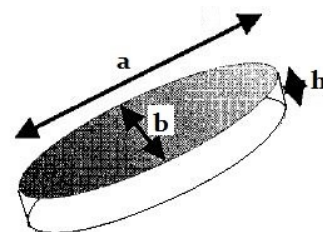


$$A = \frac{1}{2} \cdot \pi \cdot d \cdot (l + d) \quad (3.1)$$

Surirella spp.

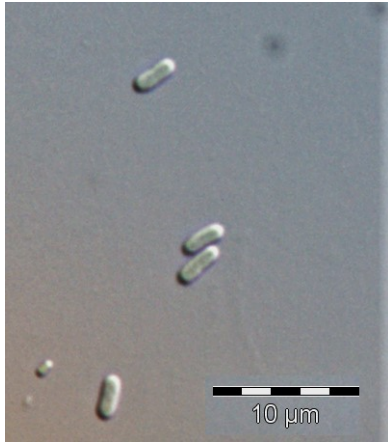


Prism (elliptic base)

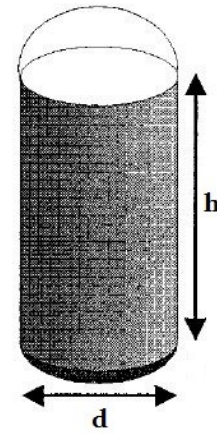


$$A = \frac{1}{2} \cdot \pi \cdot a \cdot b + \frac{1}{2} \cdot \pi \cdot (a + b) \cdot c \quad (3.2)$$

Synechococcus spp.



Cylinder + 2 half sphere



$$A = 4 \cdot \pi \cdot r^2 + 2 \cdot \pi \cdot r \cdot h \quad (3.3)$$

The surface area of the fine fraction $<100 \mu\text{m}$ was determined at the University of Hannover, Institute of Solid Sciences, using the Brunauer-Emmett-Teller Method (BET) of Brunauer et al. (1938). This method based on the adsorption of nitrogen gas molecules on a solid surface. The surface areas of all particle types are summarized in table 3.1.

3.1.4 The distribution coefficients K_d and K_A

Distribution or partition coefficients (K_d) were used to quantify the sorption of radionuclides onto different particles (Chuang et al., 2014).

In this study, the particle specific distribution coefficients (K_d in l kg^{-1}) were calculated according to Chuang et al. (2014) using the measured ^{234}Th activities related to the particle concentration:

$$K_d = \frac{{}^{234}\text{Th}_p}{{}^{234}\text{Th}_d \cdot C_p} \quad (3.4)$$

, where $^{234}\text{Th}_p$ represents the particulate ^{234}Th activity (dpm l^{-1}), $^{234}\text{Th}_d$ represents the dissolved ^{234}Th activity (dpm l^{-1}) and C_p is the particle concentration (kg l^{-1}).

For the calculation of K_d , the equilibrium between the dissolved and particulate phases is required. On the basis of kinetic experiments, Lin et al. (2014) reported an adsorption equilibrium time of 2 h. Thus, an equilibrium time of 3 h was used for all of the present experiments and it is assumed that ^{234}Th between particulate and dissolved phase are in radioactive disequilibrium.

Analog to the K_d , the measured $^{234}\text{Th}_p$ and $^{234}\text{Th}_d$ activities, together with the specific particle surface (A_p), were used to calculate the distribution coefficient K_A .

$$K_A = \frac{{}^{234}\text{Th}_p}{{}^{234}\text{Th}_d \cdot A_p} \quad (3.5)$$

The reported activities are expressed as $\log K_A$ (in l m^{-2}).

3.1.5 Statistics

The results are presented as the mean \pm 95 % confidence interval. For the statistical analyses, the results were tested using ANOVA with a post-hoc test for unequal N (Tukey Honest significant difference test) and normally distributed data. Non-normally distributed data were tested using a rank based Dunn's test. Differences were considered to be significant at $P < 0.05$. Lower-case letters were used to indicate significant differences.

3.2 Results

3.2.1 Recovery and ^{234}Th adsorption onto the container walls

Recoveries of ^{234}Th were calculated as the sum of the measured particulate and dissolved ^{234}Th activity compared to the initial total activity of the experiment as described in section 2.1. The results are shown in table 3.4 and figure 3.2 and 3.3.

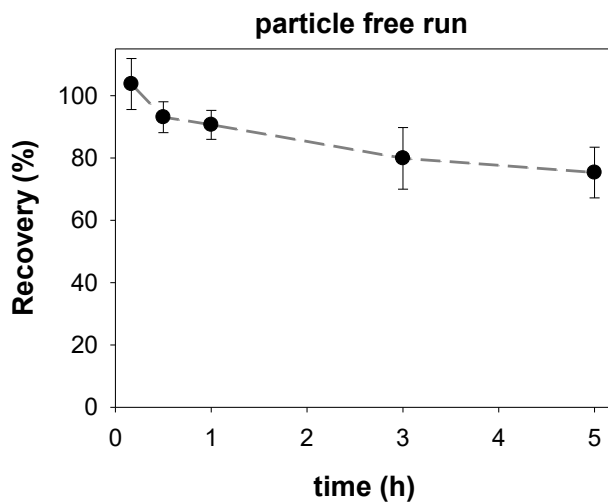


Figure 3.2: Recovery of the total ^{234}Th activity over time for the particle free run. Errors represent a 95 % confidence coefficient ($n = 5 - 9$).

For the particle free run, the results of figure 3.2 indicated a decreasing recovery and a resultant increasing ^{234}Th loss with time (10 min - 5 h), ranging from $\sim -3.7 \pm 0.3$ % to 24.7 ± 2.0 %, which is directly influenced by the longer contact time of dissolved ^{234}Th to the container walls. Total ^{234}Th activity decreased rapidly with a rate of 4.9 ± 0.4 dpm h^{-1} between 10 min and 30 min after starting the experiment. This rate decreased to

0.4 ± 0.04 dpm h^{-1} towards the end of the experiment (between 3 and 5 h). This almost exponential decrease of total ^{234}Th activity indicates an approximate saturation of the container walls with respect to the dissolved ^{234}Th content.

The recoveries of ^{234}Th for the particle runs ranged from 47.3 to 103.8 % (table 3.4). The highest recovery after 10 min (with values >100 %) was found for the experiments involving the fine sediment fraction <100 μm . Significantly lower recovery values (<70 %) were found after 10 min in the experiments for the organic coated particles. Therefore, a ^{234}Th loss of more than 30 % was determined and requires some discussion. In all of the experiments with organic coated particles, the recoveries after 10 min appear to be virtually in the same range. In general, the recoveries decrease from the start of the experiment (after 10 min) to its conclusion (after 3 h).

Table 3.4: Recoveries of total ^{234}Th after 10 min and 3 h experiments. Errors indicate a 95 % confidence coefficient (n = 9, ^a: n = 7).

	Recovery (%)		
	<i>Rhodomonas spp.</i>	<i>Surirella spp.</i>	<i>Synechococcus spp.</i>
10 min	60.54 \pm 4.82	59.47 \pm 12.88	66.39 \pm 6.83
3 h	47.26 \pm 13.58 ^a	57.70 \pm 9.48	57.77 \pm 4.27
Fine sediment fraction			
10 min	103.79 \pm 3.81		
3 h	80.48 \pm 5.20		
Particle free run			
10 min	103.72 \pm 8.16		
30 min	93.04 \pm 4.95		
1 h	90.62 \pm 4.65		
3 h	79.86 \pm 9.88		
5 h	75.31 \pm 8.13		

The results shown in figure 3.3 indicate that some loss of ^{234}Th to the container walls and filtration system occurred. A relatively long contact time of dissolved ^{234}Th to the container walls leads to a decrease of total ^{234}Th activity. In the case of the organic coated particles, a rapid decrease of the total ^{234}Th activity, with a rate in a range of $31.3 - 41.5$ dpm h^{-1} , was measured within the first 10 min after starting the experiment. Subsequently (i.e., between 10 min and 3 h), the ^{234}Th loss appears to essentially stall, approaching a rate of 0.1 to 0.7 dpm h^{-1} . Notably, in the experiment with the fine sediment

fraction $<100\ \mu\text{m}$ a significantly slower decrease of total ^{234}Th activity was found. Within the first 10 min, the ^{234}Th activity decreased at a rate of $3.5\ \text{dpm h}^{-1}$, which is several orders of magnitude lower than the organic coated particles. Between 10 min and 3 h, the ^{234}Th activity loss decreased to a rate of $1.4\ \text{dpm h}^{-1}$.

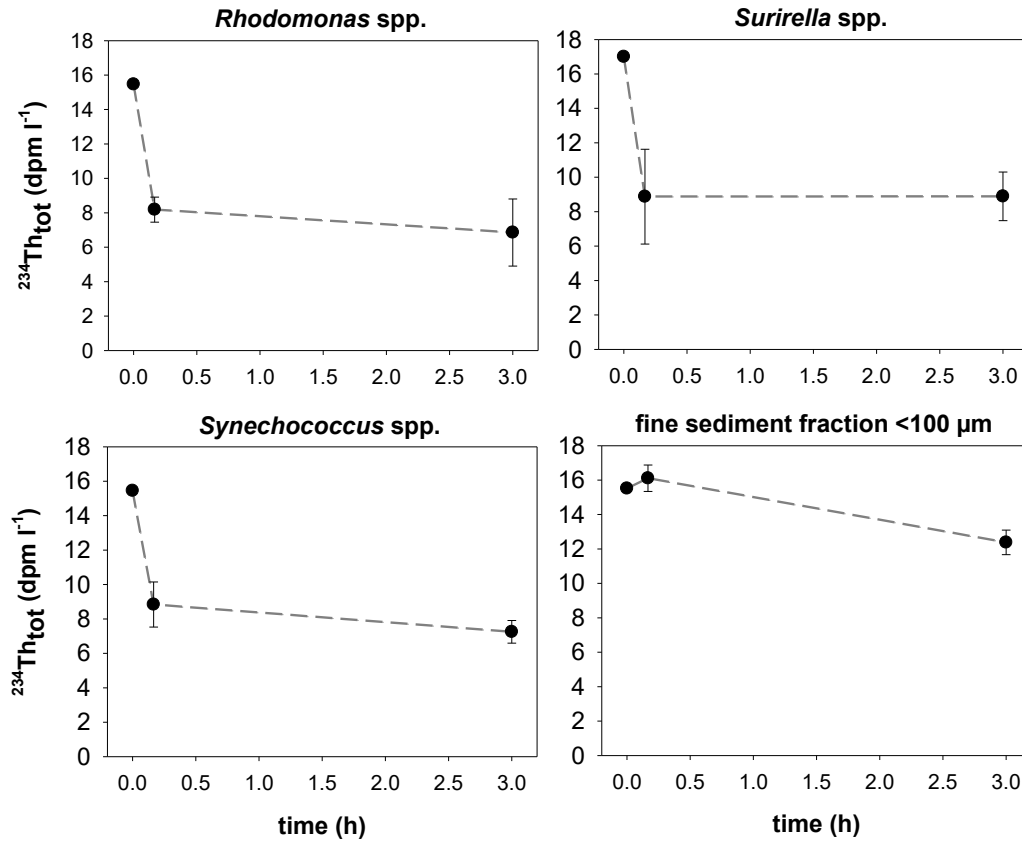


Figure 3.3: Total ^{234}Th activity ($^{234}\text{Th}_{\text{tot}}$) over time for *Rhodomonas* spp., *Surirella* spp., *Synechococcus* spp. and the fine sediment fraction $<100\ \mu\text{m}$. Errors represent a 95 % confidence coefficient ($n = 7 - 9$). Note that data at 0 h indicate the initially added ^{234}Th activity based on the calculation of the natural activity in the seawater and the added activity of the ^{234}Th spike. The total ^{234}Th activity after 10 min was determined by collection of particulate and dissolved ^{234}Th simultaneously. The total ^{234}Th activity after 3 h was calculated as the sum of the fractioned ^{234}Th filtration of the particulate and dissolved ^{234}Th .

3.2.2 ^{234}Th adsorption on different particles

The percentage of particulate ^{234}Th was determined for the ^{234}Th fractioned samples (i.e., particulate and dissolved) after 3 h. It was calculated as the deviation between the activity of particulate ^{234}Th and the sum of the particulate and dissolved ^{234}Th activity (total ^{234}Th) and is illustrated in figure 3.4-a. The fine sediment fraction $<100\ \mu\text{m}$ shows the highest percentages of ^{234}Th adsorbed onto the particle fraction, followed by *Synechococcus* spp., *Rhodomonas* spp. and *Surirella* spp. With a mean of 78.8 %, the fine sediment fraction $<100\ \mu\text{m}$ scavenged a large fraction of the total dissolved ^{234}Th from the water column

within 3 h of the experiment. In contrast, in the organic coated particle experiments, less than half of the total ^{234}Th was adsorbed onto the particle fraction. On average, *Surirella* spp. scavenged 29.1 % of the total ^{234}Th onto the surface of the cells, followed by *Rhodomonas* spp. with 34.8 % and *Synechococcus* spp. with 47.1 %.

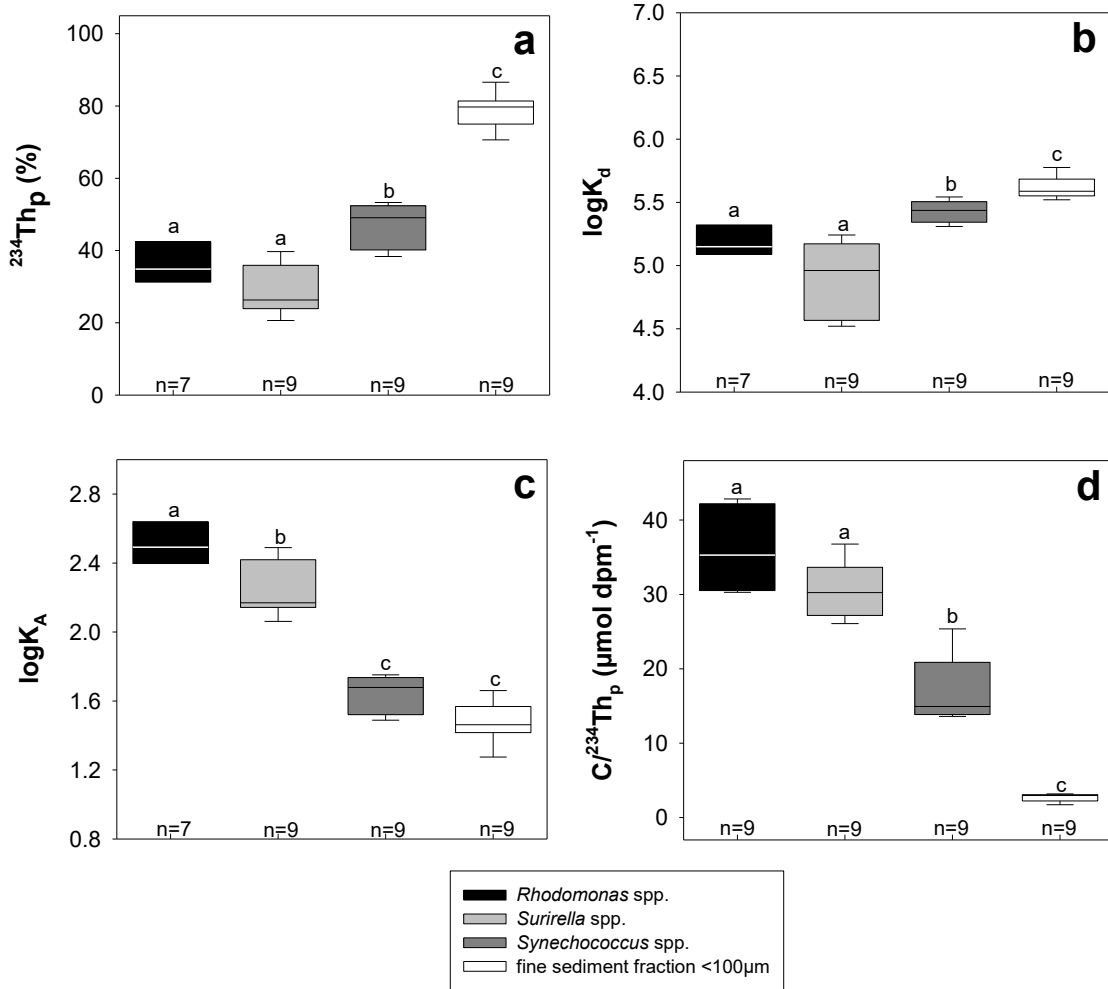


Figure 3.4: ^{234}Th adsorption onto different particle types after 3 h experiments. The plots show the fraction of particulate ^{234}Th (3.4-a), the distribution coefficient in relation to the particle concentration ($\log K_d$) (3.4-b) and particle surface ($\log K_A$) (3.4-c) as well as the particulate $C/^{234}\text{Th}_p$ ratio (3.4-d). Errors represent a 95 % confidence coefficient (n = 7 - 9). Different lower-case letters indicating significant differences of $P < 0.05$.

The concentration based $\log K_d$ values (figure 3.4-b) suggested a trend similar to that of particulate ^{234}Th , with a highest mean value of 5.6 ± 0.1 for the fine sediment fraction <100 µm, followed by *Synechococcus* spp., *Rhodomonas* spp. and *Surirella* spp. The $\log K_A$ values of the three organic coated particles are in the range from 4.9 to 5.4, which are slightly lower compared to the fine sediment fraction <100 µm.

Determining the ^{234}Th adsorption with respect to different surface areas was a major objective of this study. Concentration based results of $\log K_d$ led to the conclusion that most of the dissolved ^{234}Th adsorbs onto the fine sediment fraction <100 µm. However, the

results calculated as $\log K_A$ show a reverse trend, with the highest $\log K_A$ values for *Rhodomonas* spp. (2.5 ± 0.1) and *Surirella* spp. (2.2 ± 0.1) and significantly lower $\log K_A$ values for *Synechococcus* spp. (1.6 ± 0.1) and the fine sediment fraction $<100 \mu\text{m}$ (1.5 ± 0.1) (figure 3.4-c). Therefore, *Rhodomonas* spp. and *Surirella* spp. scavenged more ^{234}Th relative to their surface area compared to *Synechococcus* spp. and the fine sediment fraction $<100 \mu\text{m}$. Furthermore, within the group of organic coated particles, the results indicate significant differences in the adsorption of ^{234}Th to the surfaces.

The particulate carbon to ^{234}Th ratios ($C/^{234}\text{Th}$) show a similar trend to those of $\log K_A$ (figure 3.4-d). The highest ratios were found for *Rhodomonas* spp. ($35.2 \pm 4.2 \mu\text{mol dpm}^{-1}$), closely followed by *Surirella* spp. ($30.5 \pm 2.8 \mu\text{mol dpm}^{-1}$) and *Synechococcus* spp. ($17.2 \pm 3.3 \mu\text{mol dpm}^{-1}$). The fine sediment fraction $<100 \mu\text{m}$ shows a significantly lower $C/^{234}\text{Th}$ ratio (of $2.7 \pm 2.5 \mu\text{mol dpm}^{-1}$). This is related to the lower PC content for the fine sediment fraction.

3.3 Discussion

3.3.1 Variation in ^{234}Th loss between the particle types

A decrease of the total ^{234}Th activity with increasing contact time can be rationalized by the removal of dissolved ^{234}Th to the container walls and the particulate material remaining in the filtration system. The presented findings (table 3.4) are similar to the results from Geibert and Usbeck (2004), which ranged from 40 to 99 %. The presented results show a maximum ^{234}Th loss of more than 30% within the first 10 min for the organic coated particles (table 3.4 and figure 3.3). It is unlikely that this massive loss occurs by the effect of adsorption of dissolved ^{234}Th to the walls alone. Furthermore, this ^{234}Th loss is higher compared to the ^{234}Th loss found without adding particles after 3 h (table 3.4). The experimental results of Baskaran et al. (1992) indicate that natural particles and colloids presented in the experiment act as concurrent surfaces that are available for dissolved ^{234}Th and consequently lead to a reduction of dissolved ^{234}Th adsorption onto the container walls. This is in contrast to the presented findings of higher ^{234}Th loss in presence of organic coated particles compared to the particle free run. Due to the continuously flow conditions in the experiments the particles collisions frequency is enhanced and the formation of aggregates could be encouraged (Jähmlich et al., 2002). Therefore, it can be speculated that aggregation processes of the living cells occurred which changed the sinking behaviour and led to the precipitation of these aggregates (Alldredge and Jackson, 1995; Jähmlich et al., 2002). The resulting removal of particulate

^{234}Th out of the water column would consequently increase the ^{234}Th loss. However, it is also known that under increasing turbulent drag the aggregates can be destroyed or do not have the chance to form (Eisma, 1986). A visual deposition of aggregates and particles to the bottom of the annular flume was not observed. Nevertheless, a formation of aggregated cannot be excluded.

More likely is the assumption that living cells, especially the benthic diatoms which are able to attach to the surfaces (e.g. Hoagland et al., 1993; Wang et al., 2014) and could had removed particulate ^{234}Th out of the water column by sticking to the experimental device. It is speculated that such process is responsible for the enhanced ^{234}Th loss in presence of organic coated particles.

The ^{234}Th loss in presence of the fine sediment particles are reduced compared to the particle free run (table 3.4). Within 10 min after the start of the experiment, the fine sediment fraction $<100\ \mu\text{m}$ appears to shift the ^{234}Th equilibrium between the container walls and the suspended particles almost completely towards the latter. Therefore, the potential loss of ^{234}Th to the container walls becomes reduced. Due to the low organic content of the fine sediment particles, the attachment to the container walls is unlikely. Here, the effect of concurrent adsorption surfaces and the resulting decrease in ^{234}Th loss (Baskaran et al 1992) can be supported.

Notably, the presented results indicate strong differences in ^{234}Th loss between the organic coated particles and the fine sediment fraction $<100\ \mu\text{m}$. Geibert and Usbeck (2004) found similar results, with large variations in the recovery values between different particle types. In that case, however, no reasons for these observations were provided. Here it is concluded that most likely the effect of sticky living cells which attach to the surface of the experimental devices are responsible for the enhanced ^{234}Th loss in presence of organic coated particles. Nevertheless, at this stage a final conclusion cannot given. Rather an outlook for further investigation can be proposed. It would be a benefit to remove the ^{234}Th loss onto container walls by rinsing the devices after the experiments with dilute acid solution and collect this fraction and determine the ^{234}Th activity in this sample. Based on a mass balance for total ^{234}Th used in the experiments the actual ^{234}Th loss could be quantified which provides possible reasons and/or further speculation for the loss.

3.3.2 Affinity of ^{234}Th to different organic coated particles

According to the presented investigations, *Rhodomonas* spp. and *Surirella* spp. show the highest ^{234}Th scavenging intensity per unit surface area (figure 2.4-c), which is likely caused by the large number of ^{234}Th binding sites. Unfortunately, investigation on the chemical composition of the cell surface was not implemented. Therefore, the interpretation in this section based on literature and more speculative assumptions.

Previous studies showed a high affinity of ^{234}Th associated with acid polysaccharides (APS), and its content is used as a proxy for the presence of strong Th-binding ligands (Guo et al., 2002b; Santschi et al., 2003; Zhang et al., 2008; Xu et al., 2009; Hirose et al., 2011; Chuang et al., 2014). APS's in the form of slime or mucilage layers, sheaths or capsules are produced by marine plankton and bacteria (Santschi et al., 2006). Those polysaccharides are likely to be major compounds in the matrix of filamentous extracellular polymeric substances (EPS) and transparent exopolymeric particles (TEP). EPSs and TEPs can be secreted into the environment or coated the cell surface. Released EPSs are part of the marine colloidal pool and are major components involved in the formations of marine aggregates (Passow et al., 2006; Santschi et al., 2006; Fisher et al., 2013). EPSs attached to cell walls are important for the transport of essential growth substances into the cell and for preventing the direct contact of the cell to toxic substances such as heavy metal ions (Pereira et al., 2011, Tourney and Ngwenya, 2014). Because of the surface binding properties of metal ions, EPSs have been the object of several studies in relation to removing toxic heavy metals. Therefore, increasing interest of EPS in the biogeochemical cycle and transport of metals in the environment is observed (see, for example, Gardea-Torresdey et al., 1998; Mari et al., 2009; Pereira et al., 2011; Yilmaz et al., 2012, Ozturk et al., 2014, Tourney and Ngwenya, 2014). However, the exact chemical composition of EPSs and TEPs are largely unknown. The chemical composition and formation rate of microorganism EPSs is known to vary between species, but the essential sugars are identical (Passow, 2002a). However, some studies have indicated that varying growth conditions (e.g. light intensity, increasing salinity, metal toxicity and nutrient supply) may lead to differences in the excretion of EPS and the cell surface quality and quantity (e.g. De Brouwer et al., 2002; Gügi et al., 2015 and references therein). The binding of metal ions depends on such physical properties as pH, contact time and the metal binding capacity (Passow, 2002b; Tourney and Ngwenya, 2014; Pierre et al., 2014). Therefore, it can be speculated that the differences in ^{234}Th adsorption of the organic coated particles are the result of variations in the EPS composition on the cell surface. In the case of the benthic diatom *Surirella* spp., the high adsorption capacity per

surface (see figure 3.4-c) is an indication that the diatoms are surrounded by an exopolymeric polysaccharide gel with an adsorption capacity that is much higher than that of a pure silica surface (Santschi et al., 2006; Chuang et al., 2014). Compared to pelagic cyanobacteria, which produce EPSs primarily to protect their cells from toxic substances (Yilmaz et al., 2012; Ozturk et al., 2014), benthic diatoms secrete an adhesive mucilage to migrate in sediment (e.g. Higgins et al., 2000; Lundkvist et al., 2007). Furthermore, Obst et al. (2009) reported EPSs close to the cell wall of *Synechococcus* spp., which are capable of precipitating minerals (i.e., biomineralization). It is assumed that the different functions of EPSs induce variations in the chemical composition of the cell surface and thus in their ability to scavenge ^{234}Th . In summary, the presented results support the assumption of previous studies that the ability of ^{234}Th to adsorb to different organic coated particles depends on the specific chemical composition of the cell's surface (e.g. Guo et al., 2002b; Quigley et al., 2002, Santschi et al., 2003)

3.3.3 The particle concentration effect

If the partitioning between the dissolved and particulate ^{234}Th phase is controlled only by the equilibrium between these two phases, the distribution should be independent for the

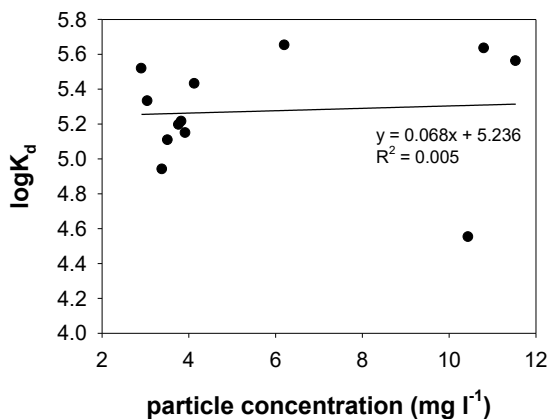


Figure 3-5: The $\log K_d$ values of the experiments in relation to the particle concentration.

particle concentration. However, previous studies have shown that the $\log K_d$ value decrease with increasing particle concentration (e.g. Honeyman et al., 1988; Honeyman and Santschi, 1989; Guo et al., 1997; Lin et al., 2014; Hayes et al., 2015). This well documented so called “particle concentration effect” is probably caused by intermediated role of colloidal matter and/or physical particle-particle interaction (Lin et al 2014). Therefore, it

is assumed that increased particle concentrations lead to increasing colloidal matter concentration, which leads to an increased colloidal ^{234}Th fraction that pass through the filter. On the other hand, the tendency of particles sticks together lead to a decreasing surface area which is available for ^{234}Th scavenging (Henderson et al., 1999).

In the presented study the particle concentrations used differ between the particles types (see table 3.1). To test the effect of particle concentration the $\log K_d$ values were plotted

against the particle concentration (figure 3.5). These findings show no strong variation in $\log K_d$ with increasing particles concentration. This is in contrast to previous studies as mentioned above. A final explanation cannot be given at this stage. However, the particle concentration effect in this study seems to be negligible which is important for the further interpretations of the presented data. It can be concluded that the variations in $\log K_d$ values of the experiments are unaffected by the particle concentration and represents actual differences between the particle types.

3.3.4 ^{234}Th adsorption onto different particles and the influence of surface area

According to the results depicted in figure 3.4-a and 3.4-b, it is assumed that ^{234}Th preferentially adsorbs to the fine sediment fraction $<100\ \mu\text{m}$. Chase et al. (2002) determined strong ^{230}Th scavenging by carbonate and lithogenic materials, but weak ^{230}Th scavenging by opal. Geibert and Usbeck (2004) reported a high ^{234}Th adsorption capacity with respect to smectite (as a representative for clay). This finding agrees well with the presented findings, with the highest percentage of particulate ^{234}Th found in the fine sediment fraction $<100\ \mu\text{m}$. The percentage of particulate ^{234}Th provides information on the distribution of the particulate and dissolved ^{234}Th fraction, but it does not reflect the adsorption capacity with respect to particle concentration, composition or surface area. Instead, the distribution coefficient K_d is based on the particle concentration. Some ^{234}Th distribution values have been reported in the literature, though some must be converted from K_d in $10^6\ \text{kg L}^{-1}$ to $\log K_d$. The results for sediment trap samples reported by Chase et al. (2002) (average $\log K_d$ value 6.6), Roberts et al. (2009) (range from 5.22 to 6.62) and Chuang et al. (2013) (range from 4.17 to 7.08) are in the similar range to the presented values. The latter authors investigated sediment trap samples, which represent a mixture of several different types of particles (e.g., organic coated and inorganic particles). Notably, Chuang et al. (2013) reported increasing $\log K_d$ values with increasing water depth. This could correlate with a higher fraction of degraded material with depth. As shown in figure 3.4-b the $\log K_d$ increases for particles low in PC content. A more recent study investigated the ^{234}Th adsorption of intact living diatom cells from *Phaeodactylum tricorutum* (Chuang et al., 2014). In this case, the $\log K_d$ values were 6.6 – 6.7, which are somewhat higher than the presented findings for *Surirella* spp. (figure 3.4-b), which may be related to different surface structures as already discussed in section 3.3.2. In general, K_d values are calculated based on the particle concentration of the sample, but they are not related to the surface area or composition of the particles. This representation

changes completely with respect to the surface area (see figure 3.4-b and c). The specific surface of the fine sediment fraction $<100\ \mu\text{m}$ ($14.72\ \text{m}^2\ \text{g}^{-1}$) is much higher than the organic coated particles ($0.34\text{--}5.6\ \text{m}^2\ \text{g}^{-1}$). Therefore, it is not surprising that the fine sediment fraction is able to scavenge a larger percentage of dissolved ^{234}Th (figure 3.4-a). The percentage of ^{234}Th adsorbed to the particulate phase increases with increasing surface area (figure 3.6-a). This supports the assumption of Kretschmer et al. (2010 and 2011) who postulated that the capacity of ^{234}Th adsorption for sediment particles is a function of the surface area. Therefore, it is concluded that larger surfaces may increase the uptake potential for ^{234}Th .

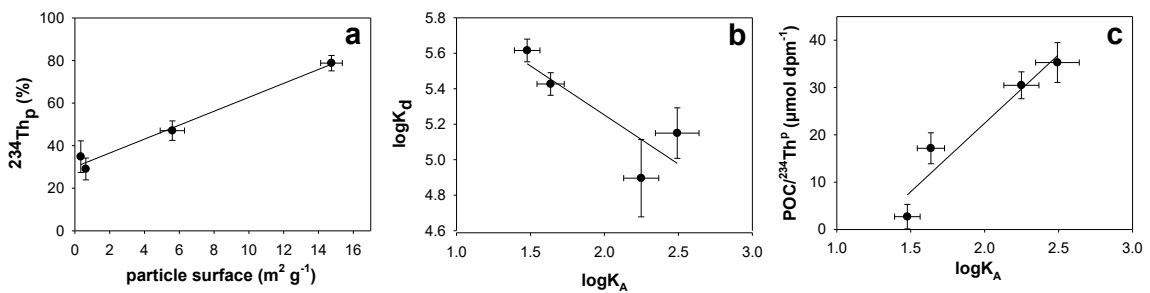


Figure 3.6: Correlations between the percentage of ^{234}Th adsorbed to the particulate fraction against the surface area (3.6-a); the distribution coefficient in relation to the particle concentration ($\log K_d$) and particle surface ($\log K_A$) (3.6-b) and the $C/^{234}\text{Th}$ ratio to $\log K_A$ (3.6-c). Errors represent a 95 % confidence coefficient ($n = 7 - 9$). Statistical analyses show significant correlation of $P < 0.05$.

In general, ^{234}Th adsorption on mineral surfaces is related to ion exchange processes. ^{234}Th adsorbs on minerals to balance the negative charge on the surface. For instance, clay minerals have a high specific surface because of their interlayer areas, which can interact with surface reactive metals such as ^{234}Th . The potential adsorption sites of clay minerals are: (1) the basal surface; (2) the edges of the layers; and (3) in the case of expanding clays, the internal interlayers (Cornell, 1993). The fine sediment fraction $<100\ \mu\text{m}$ of the experiments is composed of a large percentage of clay mineral (table 3.2), which could have a large ^{234}Th uptake potential. Quartz and calcite are known to be relatively inactive with respect to metal adsorption because of their uncharged surfaces (Cornell, 1992). Therefore, it can be suggested that these compounds of the fine sediment fraction $<100\ \mu\text{m}$ are less involved in ^{234}Th uptake.

This study examined the adsorption of ^{234}Th in relation to the surface area of different natural organic coated particles in comparison to inorganic particles, which reflect an extension of already investigated sediment particles (Kretschmer et al., 2010, 2011). A strong negative linear correlation between the concentration-based $\log K_d$ value and the surface-based $\log K_A$ value (see figure 3.6-b) was observed. According to these results concerning particle surface, it can be concluded that the surface area of particles is more

crucial in ^{234}Th adsorption as the particle concentration. Nevertheless, depending on scientific question being ask, different parameters to describe ^{234}Th scavenging become appreciated. For the question which particle component shows the highest ^{234}Th scavenging potential, then the $\log K_d$ and the percentage of particulate ^{234}Th do not represent a suitable proxy. The presented results support the notion of the importance of surface areas in ^{234}Th adsorption, but the few experiments presented herein do not allow us to offer a definitive conclusion. The effects of surface area and quality must be further validated by additional investigations on a wide range of particle surfaces.

3.3.5 Importance for natural Environment

The presented results do not allow an exact prediction of the ^{234}Th adsorption behaviour in natural environments. However, they do provide a suitable approximation of the factors that control the scavenging process of natural particles. Because of their high surface area, clay minerals adsorb a large fraction of ^{234}Th compared to organic coated particles. This could be important for the interpretation of ^{234}Th scavenging processes and ^{234}Th -based calculations (e.g., residence time, export fluxes, etc.) in different oceanic regions or within different depth zones of the water column. Seasonal variability in carbon fluxes could result from changing phytoplankton compositions, for example during bloom events where a dominant species acts as the main carrier for particulate matter (e.g., diatom blooms). In addition, uncertainties in ^{234}Th -based calculations caused by varying ^{234}Th adsorption behaviour on different types of particles could lead to regional variations of carbon fluxes; for example, when open ocean conditions are compared to regions of strong terrestrial input (e.g., coastal zones, estuaries and atmospheric deposition of particles). Furthermore, for the characterization of hydrodynamic events close to the seafloor (i.e., re-suspension/deposition events) (Turnewitsch et al., 2008, Peine et al., 2009), ^{234}Th scavenging of a large fraction of ^{234}Th by fine sediment particles must be considered. Not only varying particle types with more or less efficient aggregation and/or sinking behavior could generate large $^{234}\text{Th}/^{238}\text{U}$ disequilibria in the water column, but also the particle surface plays a crucial role. Both would reflect a strong particle load compared to processes in the upper ocean water column, especially in the euphotic zone. For instance, if for a given set of particles with equal particle concentration and sinking behavior, one particle type shows a higher surface area compared to the other, that particle would virtually generate a larger $^{234}\text{Th}/^{238}\text{U}$ disequilibria and therefore a stronger particles load.

In addition, investigations to describe carbon dynamics in the ocean often requires $\text{C}/^{234}\text{Th}$ ratio, in which the particle composition influence the ratio. We observed a strong positive correlation between $\log K_A$ and $\text{C}/^{234}\text{Th}$ content (figure 3.6-c). Therefore, there may be a relationship between $\text{C}/^{234}\text{Th}$ and the particle surface, which would mean that the chemical composition indirectly reflects the particle surface. However, it must be noted that we investigated only a few types of particles compared to the spectrum of natural particles and that the simple method of characterising cells according to geometric forms does not including the organic coating of the cells. Actual cell surfaces are much more complex and structured. Nevertheless, this study provides a first insight into the ^{234}Th scavenging process with respect to different natural organic coated and inorganic particles and the importance of their surfaces area and quality.

4 THE INFLUENCE OF COLLOIDS ON ^{234}Th SCAVENGING WITH RESPECT TO VARYING FUNCTIONAL GROUPS IN THE POLYSACCHARIDE FRACTION

4.1 Method and material

4.1.1 Colloidal substances and experimental conditions

Three parts of laboratory experiments were conducted to describe the influence of colloids, especially the polysaccharide (PS) fraction, in ^{234}Th scavenging. The experimental procedure is illustrated in figure 4.1 and is described in section 4.1.2. To prevent the involvement of other colloidal molecules in the adsorption process, the experiments with added PS were performed in deionised water. To provide measurable ^{234}Th activities, the experiments were enriched with ^{234}Th to 14.83 dpm l^{-1} as described in section 2.2.

For the ^{234}Th adsorption experiment A (figure 4.1), three types of commercial available PS, differing in their molecular structure, were used. Due to the assumption of varying ^{234}Th adsorption capacity related to different functional reactive groups of the macromolecule, different PS (Fucoidan, Chondroitin and Pullulan) were selected. Table 4.1 summarises the chemical characterisation of molecules used in the experiment. The concentrations of the PS added to the experiment were applied according to the natural dissolved organic carbon (DOC) concentration in the ocean. DOC represents the major fraction of the dissolved organic matter (DOM) pool. Therefore, the abundance of DOM has generally been determined as DOC (Ogawa and Tanoue, 2003). The distribution of DOC concentration in ocean depends on the oceanic region, water depth and season (spring bloom). For central oceanic region values of $30 - 90 \mu\text{mol DOC l}^{-1}$ were reported (e.g. Ogawa and Tanoue, 2003; Bauer and Carlson, 2002). For near shore environments and high productive oceanic regions, the concentration of DOC increases to $>100 \mu\text{mol DOC l}^{-1}$ (e.g. $131 \mu\text{mol l}^{-1}$ coastal Gulf of Mexico, Guo et al., 1994; $>300 \mu\text{mol l}^{-1}$ in the Baltic Sea, Aarnos et al., 2012). In this study, a DOC concentration of $100 \mu\text{mol l}^{-1}$ was applied for the adsorption experiments. The concentrations of the PS added to the experiment were calculated according to the ratio of the natural ^{234}Th activity (2.5 dpm l^{-1}) to the assumed DOC concentration of $\sim 100 \mu\text{mol DOC l}^{-1}$. Note that PS concentrations of the results were converted to the carbon concentrations of the molecules and were expressed in $\mu\text{mol C l}^{-1}$. As described in section 2.2 the ^{234}Th activity in the adsorption experiments was increased to $\sim 15 \text{ dpm l}^{-1}$, which is 6 times higher compared to the natural ^{234}Th concentration. To maintain the natural ratio of ^{234}Th to DOC concentration the PS concentration was increased correspondingly to the ^{234}Th activity (15 dpm l^{-1} to $600 \mu\text{mol l}^{-1}$). The

concentrations used in the experiments were calculated based to the molecular weight of the PS's and are listed in table 4.1.

Table 4.1: The chemical description, the molecular weight and the concentration of the polysaccharides (PS) used in the ^{234}Th adsorption experiments are shown. (Description and molecular weight according to Ziervogel and Arnosti, 2007).

	Description	Molecular weight (kDa)	Added concentration (mg l ⁻¹)
Fucoidan	Sulfated fructose polysaccharide	~100	22.62
Chondroitin	Sulfated polymer of N-acetylgalactosamine and glucuronic acid	63	21.56
Pullulan	α (1,6) maltotriose polymere	71.5 and smaller fractions	16.42

In experiment B (figure 4.1) the adsorption of ^{234}Th onto an inorganic mineral surface in presence and absence of Fucoidan was determined. The fine sediment fraction <100 μm was extracted from marl layer of the beach ridge sediments, collected at the Stoltera coast, Baltic Sea as described in section 3.1.1. The concentration of the fine sediment fraction used in the experiment (7 mg l⁻¹) was derived from the previous tested ^{234}Th uptake potential with increasing particle concentration of the fine sediment fraction <100 μm as described in section 3.1.1 and figure 3.1. The concentration of Fucoidan was calculated as described above.

Experiment C (figure 4.1) was performed to investigate the adsorption of ^{234}Th onto mineral surfaces in presence and absence of colloidal matter. In situ Baltic Sea surface water (salinity: 13.3) was collected during a cruise of the RV 'Poseidon' from the Mecklenburg Bay. To exclude pre-existing particles, water was filtered through a filter of 0.2 μm pore size. All components smaller than 0.2 μm are considered to be part of the dissolved and colloidal fraction, agreeing well with the definition of colloids in Santschi et al. (2006) and references therein. The filtered seawater contains the natural colloidal composition and should provide a realistic impression on the adsorption behaviour in a natural system compared to the adsorption in absence of natural colloidal material (deionised water). To prevent undesirable growth of algae and microorganisms, filtered seawater was stored in the dark at 5 °C until experimental run. To create similar conditions for both, seawater and deionised water, the pH of the deionised water was increased with NaOH to ~8. The pH was observed over the whole period of incubation and was frequently adjusted in case that the pH decreased again.

4.1.2 Experimental design

4.1.2.1 Experiment A - ^{234}Th adsorption onto different PS (single-sorbent)

Experiment A was conducted to determine the adsorption preference of ^{234}Th onto different PS. A scheme of the adsorption experiment is shown in figure 4.1. Three replicates of 1 litre of ^{234}Th spiked deionised water were added to an aliquot weighted bulk of the PS (see table 4.1). Quigley et al. (2001) reported an initial equilibration time of ^{234}Th uptake to COM in the order of minutes, whereas the coagulation of the ^{234}Th -colloid-complexes was reported to need hours. Therefore, the samples were incubated at room temperature for an absorption time of 1 h with frequent mixing. To separate the PS's from deionised, water a cross flow ultrafiltration X-Flo76 (Novasep) was used. The cross-flow ultrafiltration based on the tangentially continuous flow of the sample across the ultrafiltration membrane. Material smaller than the pore size of the membrane was collected in the filtrate. The major advantage of this method is to process a relatively large sample volume at minimum time. The cross-flow ultrafiltration unit was preconditioned with ~200 ml deionised water in order to remove possible PS contamination from the membrane. After an incubation time of 1 h the samples were ultra-filtered through a polyether sulfone membrane. It is recommended to use a membrane with a molecular weight cut off (MWCO) of 2 - 3 times smaller than the molecular size of the separated molecules (personal communication of Carol Arnosti). According to the molecular weight of the PS (table 4.1) membranes of a MWCO of 30 kDa (Fucoidan and Chondroitin samples) or 10 kDa (Pullulan samples) were used.

The activity of the dissolved ^{234}Th in the filtrate was determined and is described in the section 2.1 (see also special notes to experiments in deionised water in this section). The initial total ^{234}Th activity was determined by measurement of the total activity in the ^{234}Th spiked deionised water. The activity of the ^{234}Th phase adsorbed onto PS (colloidal phase) was calculated as the difference between the initial measured activity and dissolved ^{234}Th phase activity.

4.1.2.2 Experiment B - ^{234}Th adsorption onto fine sediment in presence of Fucoidan (binary-sorbent)

Experiment B (figure 4.1) was carried out in order to determine the influence of PS (Fucoidan) on the adsorption process of ^{234}Th onto inorganic mineral surfaces. Three replicates of 1 litre of ^{234}Th spiked deionised water were added to plastic containers filled with (1) the fine sediment fraction (particle size <100 μm) (7 mg l⁻¹), (2) Fucoidan and (3)

Fucoidan and fine sediment fraction (particle size $<100\ \mu\text{m}$) ($7\ \text{mg l}^{-1}$). According to kinetic experiments of Lin et al. (2014), an adsorption equilibrium time of 2 h was used. A similar equilibrium time has also been reported in studies of Quigley et al. (2001), Guo et al. (2002a) and Roberts et al. (2009) which make the results of the presented study comparable. The samples with the added fine sediment fraction were stirred with a magnetic stirrer. After incubation of 2 h, the fine sediment fraction $<100\ \mu\text{m}$ was collected by particulate filtration. To separate Fucoidan from the dissolved fraction, the samples were ultra-filtrated (as describe in section 4.1.2.1). The particulate and dissolved ^{234}Th fraction as well as the initial ^{234}Th activity was samples and measured as described in section 2.1. The initial ^{234}Th activity was determined by measurement of the total activity in the ^{234}Th spiked deionised water. The activity of the colloidal ^{234}Th fraction was calculated by subtracting the sum of particulate and dissolved ^{234}Th activities from the initial ^{234}Th activity.

4.1.2.3 *Experiment C - ^{234}Th adsorption onto fine sediment in presence of natural COM (binary-sorbent)*

The experiment C (figure 4.1) was conducted to describe the adsorption of ^{234}Th to a mineral surface in presence and absence of natural COM. Therefore, three replicates of 1 litre ^{234}Th spiked in situ water and deionised water were added to plastic containers that contained $\sim 7\ \text{mg l}^{-1}$ of the fine sediment fraction $<100\ \mu\text{m}$ and stirred with a magnetic stirrer. After 2 h of incubation the fine sediment fraction was separated by filtration and the activity on the particulate filter was determined. The dissolved ^{234}Th activity was analysed according to the description of section 2.1.

4.1.2.4 *Control run- ^{234}Th loss onto container walls*

Previous studies have shown that the adsorption of the extremely particle reactive ^{234}Th onto container walls and experimental devices is problematic (Baskaran et al., 1992; Moran and Buesseler, 1992b; Geibert and Usbeck, 2004). A control run without adding any PS or mineral particle was processed to determine the ^{234}Th loss onto container and filtration devices.

In addition, the ^{234}Th adsorption was determined in respect to increasing adsorption surfaces of the analytical devices. The contact surfaces were: (1) the experimental container only (plastic bottle of 1 litre volume), (2) the experimental container and the

ultrafiltration device without an ultrafiltration membrane (-MB) and (3) with inserted ultrafiltration membrane (+MB). The samples were incubated in the container for 2 h before further procedures. Therefore, the control run was conducted in the same way as the experiments of PS and particles. The results were used to correct ^{234}Th activities in experimental run with deionised water for the ^{234}Th loss onto the container walls.

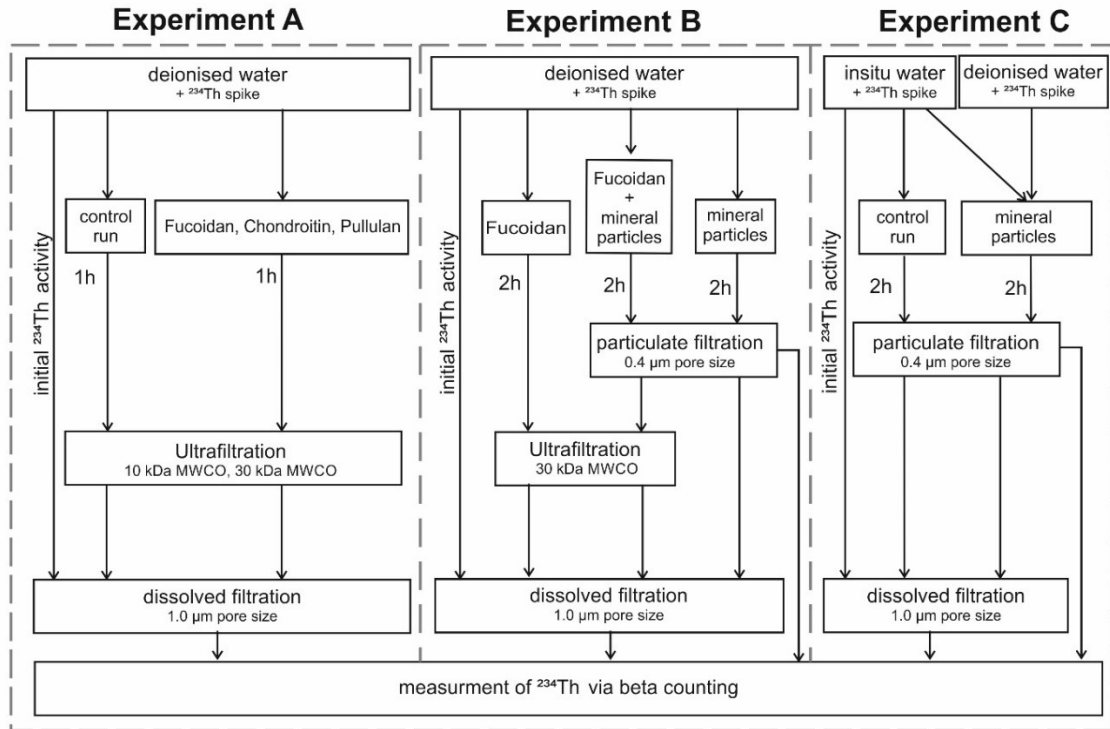


Figure 4.1: Scheme of the ^{234}Th adsorption experiments of part A, B and C. Experiment A determine the adsorption preference of ^{234}Th onto different PS. Experiment B was carried out in order to determine the influence of the PS Fucoidan on the adsorption process of ^{234}Th onto inorganic mineral surfaces. Experiment C was conducted to describe the adsorption of ^{234}Th to a mineral surface in presence and absence of natural COM. MWCO - molecular weight cut off, kDa - kilo Dalton.

4.1.3 Determination of the polysaccharide concentration

The PS concentration was measured before ultra/particulate filtration to determine the initial PS concentration of the experiment. To assure that no PS passes the ultrafiltration membrane and to estimate whether the PS interacts with fine sediment fraction, PS concentration was additionally measured in the ultra-filtrate and particulate filtrate.

One method frequently used in order to determine total dissolved mono- and polysaccharides concentration in marine samples is the TPTZ (2,4,6-tripyridyl-s-triazine) method, which is described in detail in Myklestad et al. (1997). The method is based on an oxidation reaction reducing Fe^{3+} to Fe^{2+} and can be determined colorimetrically after conditioning with the chromogen TPTZ. The resultant $\text{Fe}(\text{TPTZ})_2^{2+}$ complex is responsible

for the violet colour of the reaction. Monosaccharides with a reducing group will react directly in this method. For non-reducing sugars and polysaccharides, first, it is necessary to hydrolyse the glycosidic bonds to produce a number of reducing monomers according to their degree of polymerisation. Therefore, 1 ml of sample or standard was hydrolysed with 0.5 ml 1 M HCl in a glass ampoule and was placed in a dry oven over night at 100°C. The analytical TPTZ-procedure was conducted as described in Myklestad et al. (1997). All samples were run in triplicates. As standard solutions, the appropriate PS used in the experiment was prepared in increasing concentration.

4.1.4 ^{234}Th fractions and distribution coefficient

The activities of particulate and dissolved ^{234}Th fractions were measured directly via beta-counting. The activity of the PS fraction was calculated based on the subtraction of (1) the dissolved or (2) the sum of dissolved and particulate fraction activity from the initial activity.

The distribution coefficient (K_d) describes the partitioning of radionuclides between particulate and dissolved phase in relation to the particle concentration and has been applied for investigations of adsorption behaviour of various particle reactive elements in seawater (Guo et al., 1997; Quigley et al., 2001; Guo et al., 2002a; Geibert and Usbeck, 2004; Lin et al., 2014; Lin et al., 2015). In the present study, the K_d value is also used in relation to the colloidal concentration and will be called K_c . K_d/K_c were calculated using the following equation:

$$K_{d/c} = \frac{{}^{234}\text{Th}_{p/c}}{{}^{234}\text{Th}_d \cdot C_{p/c}} \quad (4.1)$$

, where ${}^{234}\text{Th}_{p/c}$ represents the particulate or colloidal and ${}^{234}\text{Th}_d$ the dissolved ${}^{234}\text{Th}$ activity (dpm l^{-1}), while $C_{p/c}$ is the particle or colloidal concentration (kg l^{-1}). The dimension of K_d values is l kg^{-1} and is expressed in this study as $\log K_d$.

4.1.5 Statistics

The results are presented as mean values and the errors indicating the standard deviation (SD) of the mean. For the statistical analyses, the comparison of two groups was

conducted by running a t-test. When comparing more than two groups an ANOVA was carried out. Differences were considered to be significant at $P < 0.05$.

4.2 Results

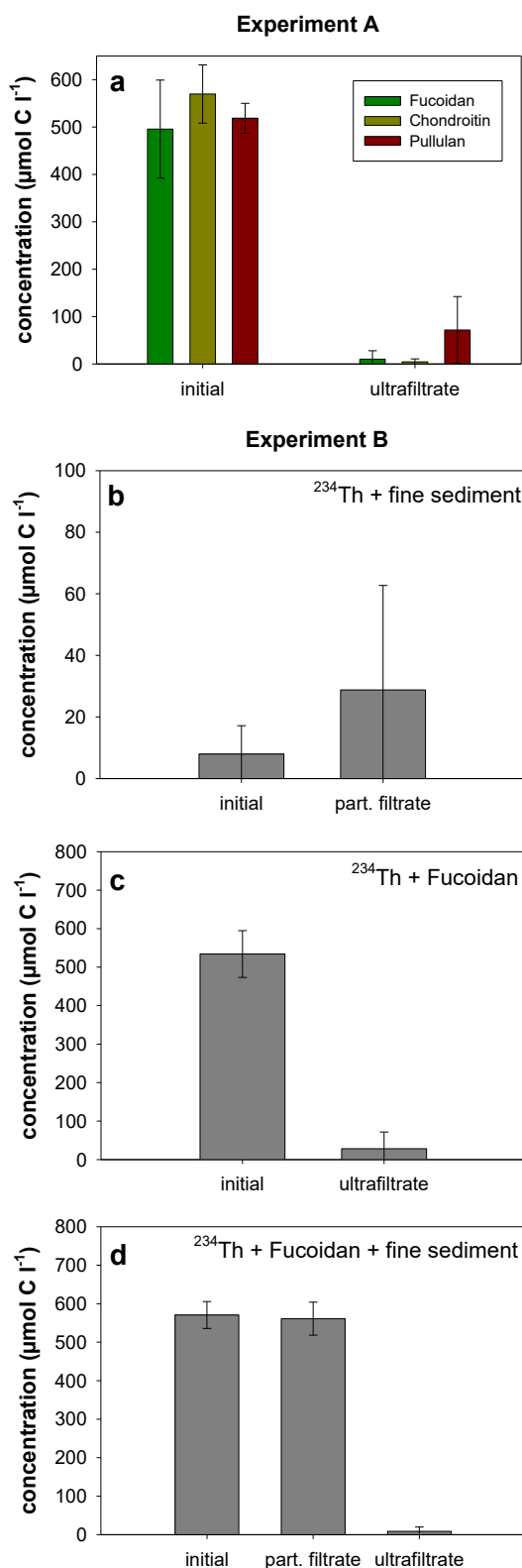
4.2.1 Concentration of polysaccharides

The actual added concentration (in $\mu\text{mol C l}^{-1}$) of the experiments was calculated from the amount of weighed PS.

In experiment A, the measurements of PS concentration of the initial solution show some discrepancies compared to the added concentrations (table 4.2). In most of the samples the measured concentration is somewhat lower compared to the added concentration, except of Chondroitin R₁. In the replicate sample R₂ containing Fucoidan the measured concentration is nearly half of the added concentration. It is assumed that the measured concentration is affected by errors due to the possible incomplete hydrolyses of the PS. This is supported by the standard curve of the PS compared to the monomer Glucose (not shown here) which indicate an incomplete hydrolysis. For further calculations, the added PS concentration is used.

Table 4.2: Comparison of added and measured initial PS concentrations in the experiments A. R₁, 2 and 3 represent the replicates of each approach.

	Replicate	concentration [$\mu\text{mol C l}^{-1}$]	
		Added	Measured
Fucoidan	R 1	623.3	595.3 \pm 29.6
	R 2	597.9	350.5 \pm 37.6
	R 3	614.8	574.4 \pm 92.2
Chondroitin	R 1	598.6	675.3 \pm 30.3
	R 2	604.0	503.7 \pm 29.8
	R 3	604.4	530.4 \pm 36.1
Pullulan	R 1	603.4	507.8 \pm 20.9
	R 2	600.2	529.6 \pm 43.6



To ensure that no PS passes the ultrafiltration membrane the PS concentration was measured in the ultrafiltrate (figure 4.2-a). In experiment A and in relation to the error bars, no molecules passed the membrane. In experiment Band samples without added Fucoïdan, no significant PS concentration can be observed (figure 4.2-b). The average initial measured PS concentration of Fucoïdan in figure 4.2-c and d is $534.1 \pm 60.8 \mu\text{mol C l}^{-1}$ and $570.6 \pm 34.9 \mu\text{mol C l}^{-1}$. In the ultrafiltrates, no significant PS concentrations is found. Therefore, it is concluded that Fucoïdan did not pass the ultrafiltration membrane. In the binary sorbent experiment, where Fucoïdan and the fine sediment fraction was represented, (figure 4.2-d) the PS concentration does not change significantly after particulate ^{234}Th filtration. This indicates that there is no association of Fucoïdan onto fine sediment particles.

Figure 4.2: a: The concentration of the PS in the initial solution and the ultra-filtrate of Fucoïdan, Chondroitin and Pullulan in experiment A. Figure b-d indicate the concentration of Fucoïdan in experiment B of the fine sediment (d), Fucoïdan (e) and Fucoïdan and fine sediment (f) added. Error bars represent the 95 % confidence level of the subsamples ($n = 6 - 9$) for PS analyses.

4.2.2 ^{234}Th lost onto container walls

Figure 4.3 shows the recovery of ^{234}Th with increasing steps of the experiment. The recovery decrease with each additional experimental step. Therefore, highest ^{234}Th recovery of $83.6 \pm 10.7 \%$ is found for the container incubation only. This indicates a ^{234}Th

loss of 16.4 ± 10.7 % onto the container walls. The recovery decrease to 67.4% when the samples additionally pass the ultrafiltration device without adding a membrane and decrease further to 50.8 ± 8.2 % if an additional membrane is presented. Therefore, a ^{234}Th

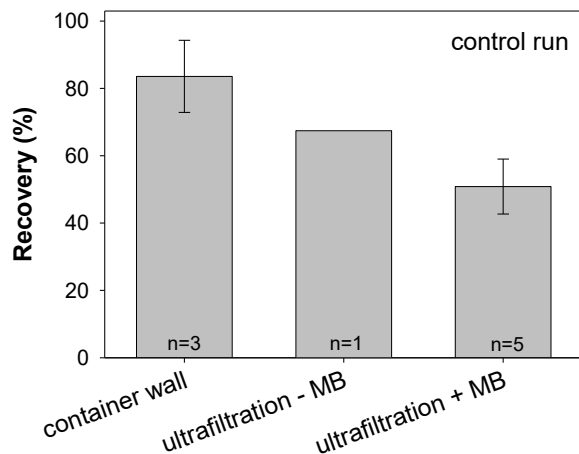


Figure 4.3: Recovery of ^{234}Th in control run, without adding particles or PS, to determine the ^{234}Th loss onto the container walls und ultrafiltration devices. + and - MB indicate the recovery in presences or absence of the ultrafiltration membrane (MB). Significance level $P < 0.05$.

container walls during 2 h incubation. Due to the presence of natural COM in the seawater which is known to influence the ^{234}Th loss onto container walls (Baskaran et al., 1992) the ^{234}Th activities of the seawater experiments are not corrected. For a detailed description see section 3.3.1.

4.2.3 ^{234}Th adsorption onto different polysaccharides

Most of the total ^{234}Th in the experiment is adsorbed onto the PS fraction (figure 4.4). The differences detected between the different PSs used is only weak. The largest fraction of ^{234}Th is adsorbed to Fucoïdan with 74.7 ± 14.1 %, followed by Chondroitin with 67.4 ± 9.9 % and Pullulan with 59.7 ± 5.5 %. This suggests an adsorption preference of ^{234}Th onto Fucoïdan compared to the other PS. A similar trend is observed for the distribution coefficient (K_c). Fucoïdan shows the highest $\log K_c$ values of 5.1 ± 0.3 . Slightly decreasing $\log K_c$ values are found for Chondroitin ($\log K_c$ 5.0 ± 0.2) and Pullulan ($\log K_c$ 5.0 ± 0.1). However, in relation to the standard deviation of the percentage of ^{234}Th fraction and $\log K_c$, the differences between the PS's are of minor importance.

loss of 24.6 % onto the membrane is observed. The results suggest a significant ^{234}Th loss with increasing contact of ^{234}Th to adsorption surfaces. To prevent an overestimation of the colloidal and underestimation of the dissolved fraction, dissolved ^{234}Th activities are corrected for the ^{234}Th loss of 49 % after ultrafiltration through a membrane. For samples run in deionised water without ultrafiltration (experiment B and C: only mineral surface added) the ^{234}Th activities are corrected for the 16.4 % loss onto the

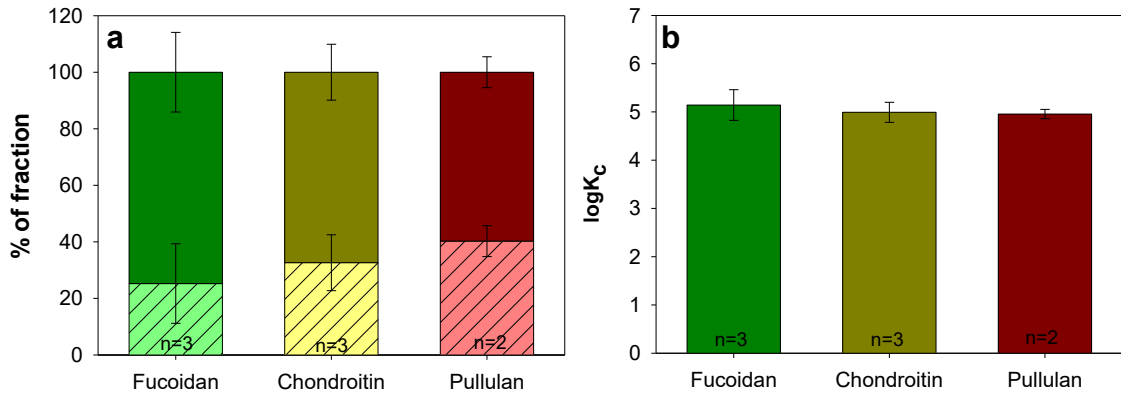


Figure 4.4: Figure a: Percentage of colloidal and dissolved ^{234}Th fraction of Fucoidan, Chondroitin and Pullulan of experiment A. Figure b: Distribution coefficient ($\log K_c$) between the colloidal and dissolved ^{234}Th activity in relation to the colloidal concentration. The ^{234}Th activities are corrected for ^{234}Th loss onto container walls: Errors indicate standard deviation. Significance level $P > 0.05$.

4.2.4 ^{234}Th adsorption onto mineral surfaces in presence of colloidal material

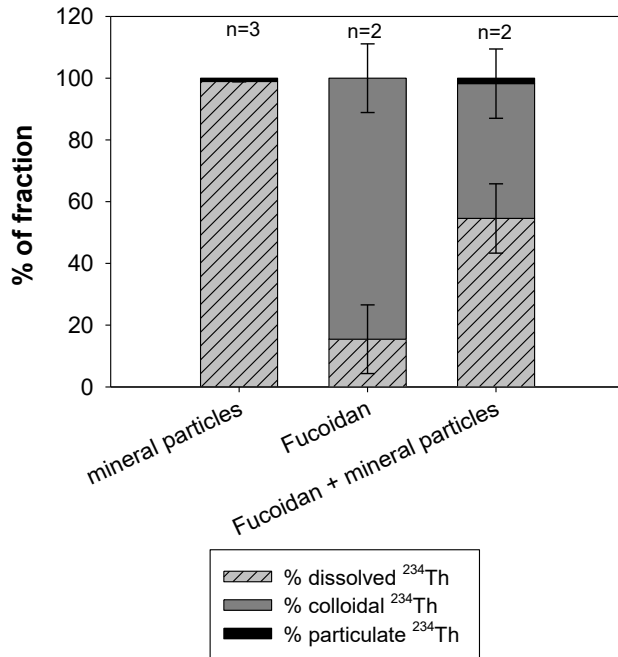


Figure 4.5: Percentage of particulate, colloidal and dissolved fraction (corrected for ^{234}Th loss onto container walls) of experiment B. Errors indicates standard deviation. Significance level of particulate ^{234}Th $P < 0.05$; dissolved ^{234}Th : $P > 0.05$ and colloidal ^{234}Th : $P < 0.05$.

According to the results presented in figure 4.5 and in the presence of Fucoidan, the particulate ^{234}Th fraction adsorbed to the minerals surface is slightly increased by almost 40 %. Hence, it can be assumed that the adsorption of ^{234}Th onto mineral surfaces is increased in presence of Fucoidan. However, in the approach with fine sediment added, only 1.1 ± 0.1 % of the total ^{234}Th is adsorbed onto the particles. More than 98 % of the total ^{234}Th remains in the dissolved phase. Therefore, in deionised water and in absence of Fucoidan nearly no ^{234}Th is

adsorbed onto the fine sediment fraction. Nevertheless, in all cases the largest fraction of ^{234}Th is found in the colloidal or dissolved phase. In the combined approach (Fucoidan + mineral surface) the colloidal ^{234}Th phase is with 43.7 ± 11.2 % somewhat lower compared

to 84.5 ± 11.1 % where only Fucoïdan is available. In presence of these mineral surface, the colloidal ^{234}Th phase decreases and the dissolved ^{234}Th phase increases.

Figure 4.6 shows the adsorption of ^{234}Th onto fine sediment fraction in deionised water compared to seawater. The percentage of ^{234}Th adsorbed to the fine sediment particles in seawater (40.4 ± 10.3 %) is several orders of magnitude higher compared to deionised water (2.9 ± 1.5 %). In addition, the $\log K_d$ value is significantly lower in COM free samples. The results of experiment C show a significant increase in ^{234}Th adsorption to mineral surfaces in presence of natural colloidal material.

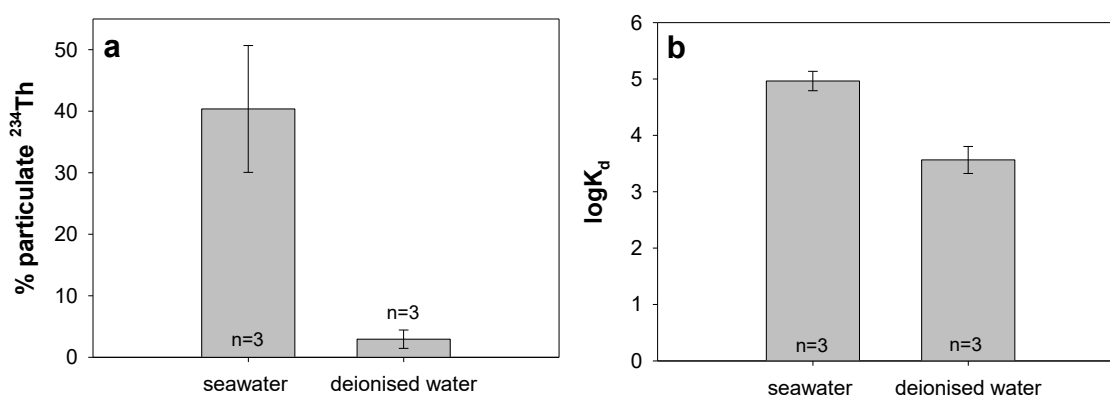


Figure 4.6: Results of the experiment C. The percentage of ^{234}Th adsorbed to fine sediment particles (a) and the distribution coefficient- $\log K_d$ (b) in deionized water and natural seawater. Dissolved ^{234}Th samples run in deionized water are corrected for the ^{234}Th loss onto the container walls during 2 h incubation period. Error bars indicate SD of $n = 3$. Significance level $p < 0.05$.

4.3 Discussion

4.3.1 The influence of functional group composition of polysaccharides on ^{234}Th adsorption

Several studies have demonstrated a strong relationship between acid polysaccharides (APS) content and ^{234}Th removal (e.g. Guo et al., 2002b; Quigley et al., 2002; Azetsu-Scott and Niven, 2005). Chuang et al. (2015) found $\log K_c$ values of the natural COM in mean of 5.05 ± 0.2 and for exopolymeric substances (EPS) extracted from laboratory cultured diatom species in the range of 5.13 - 5.33. These findings agree well with the results presented here for the PS (figure 4.4-b). Lin et al. (2015) reported $\log K_c$ values for APS of 6.76 and 6.38 in experiments conducted in natural seawater. Quigley et al. (2002) experimental findings show $\log K_c$ values for commercial PS in the range of 5.3 - 8.1 (in NaClO_4 solution or artificial seawater 34 PSU, pH 8). These findings are somewhat higher compared to the presented results in figure 4.4-b. The differences likely occur because of

varying experimental conditions (pH 8, natural and artificial seawater) compared to the present study (pH ~4.5, deionised water). It should also be noted that the pH in the presented study (~4.5 pH) is somewhat lower compared to experiments in natural seawater. The sorption of ions to particle depends strongly on pH. Cations generally show an increasing sorption behaviour with increasing pH, whereas the sorption of anions to particles increases with decreasing pH (Santschi et al., 2006 - and references therein). There are some recent studies that show an increasing Th(IV) sorption with increasing pH from 0 - 4 and a maintained level of Th(IV) sorption with pH > 4 (Tan et al., 2007; Xu et al., 2015; Kaynar et al., 2015). Xu et al. (2015) explained the decreasing Th(IV) sorption with increasing acidification of the medium by the partial protonation of the active groups and the competition of H_3O^+ ions for the adsorption side of the sorbent. According to the finding of these authors, in the presented experiments (pH of ~4.5) optimal sorption conditions can be expected. However, the variations of $\log K_c$ compared to Lin et al. (2015) cannot exclude the pH effect. Similar experimental conditions would lead to an increasing comparability. In addition, the commercially available PS used in these experiments could have different chemical properties compared to the natural PS.

According to our results Fucoïdan seems to have higher adsorption capacity compared to Chondroitin and Pullulan (figure 4.4). In general, functional groups are known to be involved in the metal ions adsorption to PS (Alvarado Quiroz et al., 2006). These

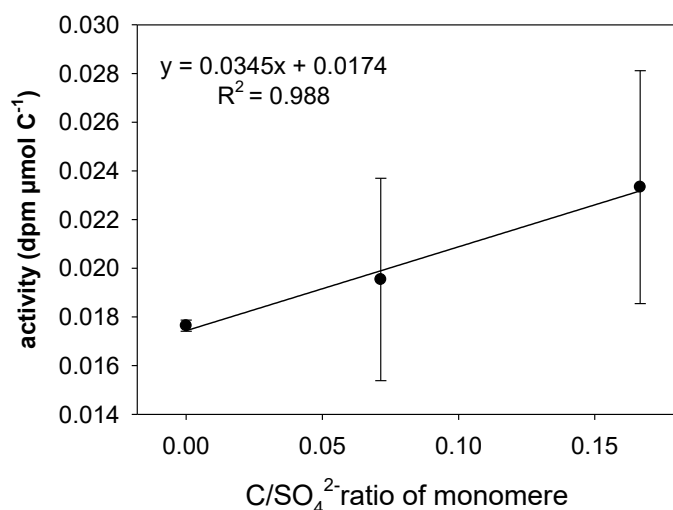


Figure 4.7: Linear relationship between ^{234}Th activity per μmol of carbon and the ratio of carbon to sulphated group of a monomer of Fucoïdan, Chondroitin and Pullulan.

functional groups react with the metal through chelation and/or ion-exchange (Xu et al., 2014 - and references therein). As an A- type metal, Th(IV) shows a high binding constant to oxygen-containing functional group (Santschi et al., 2006). Xu et al. (2014) demonstrated that amine and hydroxyl functional groups are involved in the adsorption of Th(IV) to the sorbent. Alvarado Quiroz et al.

(2006) reported that a possible ^{234}Th binding ligand consists of parts of carboxyl, sulphate and/or phosphate groups. In the presented study, a positive correlation between the ^{234}Th activity in $\text{dpm } \mu\text{mol } \text{C}^{-1}$ and the ratio of $\text{C}/\text{SO}_2^{-4}$ of the monomer, which is proportional to

the $\text{C}/\text{SO}_2^{-4}$ ratio of the whole molecule, was observed (figure 4.7). Fucoïdan, which contains several sulphated groups compared to Chondroitin and Pullulan shows a higher adsorption capacity of ^{234}Th . According to these findings it can be concluded that the ^{234}Th adsorption increases with increasing number of sulphated groups in the molecule which indicates that sulphated groups are involved in the adsorption process. According to this experiment, it cannot be excluded that other functional groups are also influence the ^{234}Th adsorption. In addition, the very similar $\log K_c$ values of the PS used in this study indicate no varying adsorption preference of ^{234}Th to different functional group composition. This is in line with the findings of Quigley et al. (2002). The authors also found no significant differences between commercial PS with carboxyl and those with sulphate groups. According to the presented results, rather the numbers of functional groups (e.g. SO_2^{-4}) determine the ^{234}Th uptake (figure 4.7). Additional experiments should clarify the role of colloids of other molecular composition (e.g. amino acids and humic acids) and of the numbers of functional groups in the molecule.

The observation, that ^{234}Th is most likely associated to functional groups in biomolecules, is relevant, on the one hand, for the influence of COM in the ^{234}Th scavenging process, as discussed below. On the other hand, variation in functional group composition on particle surfaces, especially EPS on living cells (e.g. microorganisms and phytoplankton) can lead to variations in ^{235}Th uptake capacity which is discussed in detail in section 3.3.2.

4.3.2 Partitioning of ^{234}Th between dissolved and particulate phase in presence of polysaccharides

Some studies reported that a large fraction of ^{234}Th is associated to COM (Baskaran et al., 1992; Guo et al., 1997). This agrees well with the presented findings of experiment B, where a large fraction of the total ^{234}Th pool is adsorbed onto the PS Fucoïdan (figure 4.5). The results also show an enhanced ^{234}Th adsorption to mineral surfaces in presence of Fucoïdan. APS are known to rapidly coat non-living particles (Decho, 1990). This leads to the assumption of an enhanced ^{234}Th adsorption onto mineral surfaces in the presence of APS. Guo et al. (2002b) and Santschi et al. (2003) reported a positive correlation between $^{234}\text{Th}/\text{POC}$ and APS content. The authors postulated that the APS content controls not only the amount of ^{234}Th sorption, but also the rates of coagulation of particles. Also Tan et al. (2007) found a positive effect of humic and fulvic acid in the Th(IV) adsorption to TiO_2 nanoparticles. However, as shown in figure 4.5, the particulate ^{234}Th fraction is still weak in comparison to the dissolved and colloidal fraction. In this experiment only Fucoïdan was available to represent the colloidal fraction. Therefore, it can be assumed

that not only one component of the total COM pool is responsible for ^{234}Th scavenging to particles. More likely the whole mixture of COM leads to an enhanced adsorption of ^{234}Th onto mineral surfaces. This agrees with the finding of experiment C and will be discussed in the following section 4.3.3.

As already mentioned above, it is conceivable that the commercial available PS such as Fucoïdan does not show the properties and chemical composition of natural PS in colloidal matter. Therefore, for future investigations, it is recommended to conduct such experiments with naturally available fractions of COM (PS, amino acids, humic acids etc.) to identify the most important fraction in ^{234}Th adsorption. This would help to understand the mechanisms that control ^{234}Th scavenging on molecular level which would lead to an improved knowledge for the application of ^{234}Th as particle tracer.

4.3.3 The effect of natural colloids on the adsorption of ^{234}Th onto mineral surfaces

Marine colloids are important in the marine carbon cycling in the ocean due to their dispersing and complexing capacity (e.g. Amon and Benner, 1994). The adsorption experiments of ^{234}Th to mineral particles in the presence or absence of COM attested the important role of COM in the ^{234}Th scavenging process onto particles. ^{234}Th adsorption is significantly higher in the presence of COM, (figure 4.6) which leads to the assumption that COM may act as organic carrier phase in ^{234}Th adsorption onto particles. Former studies of Honeyman and Santschi (1989) postulated a model according to which ^{234}Th adsorbs onto particles by a colloidal intermediate. It is assumed that the association of ^{234}Th to inorganic particles can be the result from coating of organic, surface active substances like COM (Passow et al., 2006). If inorganic particles are coated with an organic film, which is mostly negative charged, the surface properties and reactivity of the particles are completely changed. Therefore, it can be expected that metal ion (mostly positive charged) sorption is modified by associated COM to less reactive particles (Santschi et al., 2006 - and references therein). The results of the presented study strongly support this assumption. Therefore, it can be assumed that the adsorption capacity to mineral surfaces is enhanced in presence of COM and colloidal substances act as an organic intermediate in ^{234}Th scavenging.

On the next level, these findings would have influence on the ^{234}Th based calculations of particle or carbon fluxes as well as for data interpretations. It has been observed that the $\text{C}/^{234}\text{Th}$ ratio varied significantly with region, season, water depth and particle size (e.g. Guo et al., 2002b; Buesseler et al., 2006, Passow et al., 2006). Mineral surfaces coated with

organic, reactive substances could increase the ^{234}Th uptake capacity relative to the carbon concentration. Therefore, the $\text{C}/^{234}\text{Th}$ would vary depending on the abundance, composition and reactivity of the COM which are associated to particles.

According to the presented results, it can be concluded that COM likely acts as an organic carrier phase on a molecular level for ^{234}Th scavenging and can enhance the ^{234}Th uptake potential of less reactive, inorganic surfaces. Such findings are essential in order to improve the interpretation and understanding of biogeochemical cycles of particles and their components like carbon. With this information, better models could be constructed that are based on radioisotopes for carbon flux and particle dynamics in the ocean.

5 PARTICLE DYNAMIC IN THE MECKLENBURG BAY, BALTIC SEA USING ^{234}Th AS PARTICLE TRACER

5.1 Study area and sampling

During two cruises on 26th August 2014 with the Vessel “Praunus” and 24th September 2015 with “Goor II”, three stations were sampled along a vertical transect in the Mecklenburg Bay, western Baltic Sea (figure 5.1, table 5.1). In August 2014 sediment cores were sampled with the Multicorer (MUC) to determine sediment parameter such as: grain size, water content, porosity, dry bulk density, carbon content and chlorophyll-*a* content (not shown here, appendix figure I). The sliced sediment samples were stored deep frozen until further analyses. In addition, intact sediment cores were transported to the laboratory carefully and without disturbing the surface to investigate the critical shear velocity (u_{cr}^*) and turbulent kinetic energy (TKE) as well as the adsorption of ^{234}Th onto different sediment types in varying hydrodynamic conditions. Until experimental run the cores were kept in darkness and in situ temperature.

During the cruise in September 2015 water and sediment samples were taken in order to determine ^{234}Th activities and the calculation of residence time. A Falmouth Scientific Inc. (FSI) sensor with a pump mounted on the device was used to measure conductivity, temperature and pressure as well as to take water samples. At each station, approximately 20 litre seawater were collected at the surface and close to the seafloor (<1.5 meter above bottom, mab) for ^{234}Th and PC analyses. Sediment cores were taken to determine the ^{234}Th activity in the sediment described in section 5.2.5. Therefore, the single slices of 5 to 8 parallel sediment cores of each station were mixed to minimise the effect of patchiness. The sediment samples were stored cool at 6 - 7 °C until analyses.

Table 5.1: Position and water depth of the three Stations along a vertical transect in the Mecklenburg Bay, western Baltic Sea. Temperature and salinity were measured with the FSI sensor and water samples were taken from the surface water (SW) and bottom water (BW) column.

Station	Position		Water depth (m)	Water sample (m)	Temperature (°C)	Salinity	
	Latitude	Longitude					
23.c	54° 01.599' N	11° 03.905' E	15.2	SW	0.89	14.86	13.62
				BW	14.34	15.10	16.41
23.b	54° 02.160' N	11° 03.758' E	20.3	SW	0.88	14.82	13.84
				BW	19.01	13.73	19.15
23.o	54° 03.498' N	11° 03.291' E	22.9	SW	0.94	14.90	13.97
				BW	22.30	13.64	20.34

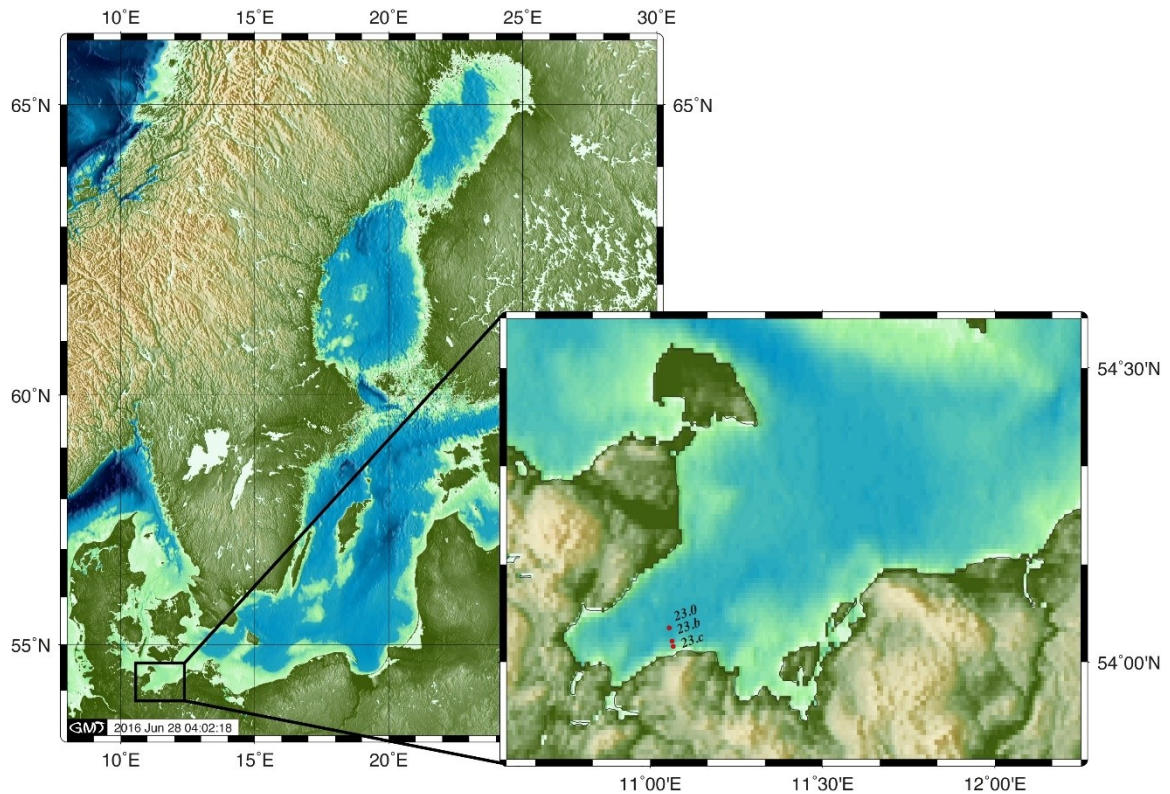


Figure 5.1: Map of the Baltic Sea and the Mecklenburg Bay with the Station 23.c, 23.b and 23.o along a vertical transect. Map was processed with Generic Mapping Tool (GMT) 5.1.2 by Stefan Meinecke. Bathymetric data bases on GEBCO-08 data. The figure was prepared with Adobe Illustrator CS6 version 682.

5.2 Method and material

5.2.1 Characterisation of the sediment

To characterise the sediment, different sediment parameter was analysed. Grain size was estimated by wet sieving of at least 100 g fresh sediment using sieves with mesh width of 1000, 500, 250, 125 and 63 μm . The median was determined using the cumulative curve. To estimate water content (in %), porosity (ϕ) and dry bulk density, 5 ml of each layer of the sediment were sampled, wet weighted and dry weighted. The total carbon content was analysed, after sediment drying and pestling, in a Carlo Erba C/N analyser. The analyses followed the description in section 3.1.3.1. A detailed description of methods characterising the sediment is given by Bale and Kenny (2005)

5.2.2 Critical shear stress velocity (u^*_{cr}) and turbulent kinetic energy (TKE)

Research on sediment dynamics and erosion started with the studies of Hjulström, (1935) and Shields, (1936). The critical shear stress velocity (u^*_{cr}) is the threshold value which determines the initial movement of particles (incipient motion). The initial sediment motion depends on characteristics of the sediment (grain size, density, packing, sorting, shape ect.), the fluid (density and viscosity) and the flow conditions (current velocity and turbulent stresses) (Miller et al., 1977). The turbulent kinetic energy (TKE) is the mean kinetic energy per mass unit accumulated in turbulent flows (Pope, 2000).

In an annular flume filled with seawater a 10 cm sediment core was carefully inserted (3 replicates of each station) without disturbing the sediment surface. The current velocity was measured with a Vectrino Profiler (Nortek AS) in a 3 cm cell directly above the sediment surface which enabled the recording of a current profile. The current profiler measures the current velocity and direction (x, y and z) in multiple layers in the water column. The principle mechanism of current measuring is based on the doppler shift effect where an acoustic signal of a definite frequency is transmitted and the pulse is reflected by suspended particles in the water column. This reflection changes the frequency of the pulse proportional to the current velocity. The detector receives the pulse and the current velocity is calculated.

In the experiment, current velocity was increased in steps of $\sim 0.8 \text{ cm s}^{-1}$ with an exposing time of 5 min. Two thresholds of critical shear stress velocities were defined analogue to Ziervogel and Bohling (2003): (1) initial particle transport ($u^*_{cr-initial}$) and (2) erosion ($u^*_{cr-erosion}$) of surface sediment particles. The detection of the thresholds was carried out by visual observation using a zoom camera focused on the sediment surface. Initial particle transport was noted when particles started to roll over the sediment (bed load transport). An erosion was reached when particles from the sediment surface were resuspended into the overlying water. The calculation of the shear stress velocity (u^*) and TKE was carried out by Michelle Dietz using the software MATLAB and is described in the Master thesis of Michelle Ditze (2015).

The TKE was calculated as follows:

$$TKE = \frac{1}{2} \cdot \rho \cdot (\overline{u'^2} + \overline{v'^2} + \overline{w'^2}) \quad (5.1)$$

, where ρ is the density of the water, u' , v' and w' are the turbulent fluctuations in x, y and z direction of the coordinate system.

The shear stress velocity (u^*) was calculated using the following equation:

$$u^* = \sqrt{\frac{p}{\tau_0}} \quad (5.2)$$

, where τ_0 is the shear stress and can be calculated as $\tau_0 = 0.2 \cdot \text{TKE}$.

In addition to the experimental data the results were compared to theoretical u_{cr}^* (u_{cr}^* -shields) based on grain size and the Shield parameter as described in Ziervogel and Bohling (2003) and largely followed by Soulsby and Whitehouse (1997). The theoretical critical shear stress velocity was calculated as described in Ziervogel and Bohling (2003):

$$u_{cr-shields}^* = \sqrt{\frac{\theta_{cr} \cdot g \cdot (p_s - p_w) \cdot d}{p_w}} \quad (5.3)$$

θ_{cr} – Shield parameter (dimensionless)

g – Gravity constant (9.81 m s^{-2})

p_s – Density of the sediment (for quartz sand: 2.65 kg m^{-3})

p_w – Density of the water (kg m^{-3})

d – Mean grain size (m)

The Shield parameter for cohesionless grains was calculated as follows:

$$\theta_{cr} = \frac{0.3}{1 + 1.2 \cdot D_*} + 0.055(1 - \text{EXP}[-0.02 \cdot D_*]) \quad (5.4)$$

, with the dimensionless grain size $D_* = \left(\frac{g \cdot p'}{v^2}\right)^{1/3} \cdot d$ (5.5), where p' is the relative density (dimensionless), $p' = (p_s - p_w)/p_w$ (5.6) and v is the kinematic viscosity of water ($10^{-6} \text{ m}^2 \text{ s}^{-1}$).

5.2.3 ²³⁴Th adsorption onto different sediment types in varying hydrodynamic regimes: Resuspension-deposition-experiment

For the determination of ²³⁴Th adsorption onto different sediment types in varying hydrodynamic regimes annular flume experiments were conducted. One day before the experiment, three 10 cm sediment cores were carefully inserted in the annular flume filled with 77 - 78 L in situ water (figure 5.2). The flume was started at a very weak velocity to allow for careful mixing of the water mass. Before starting the experiment, three replicate water samples of 0.7 - 1 litre were taken for total particulate matter (TPM) and carbon and

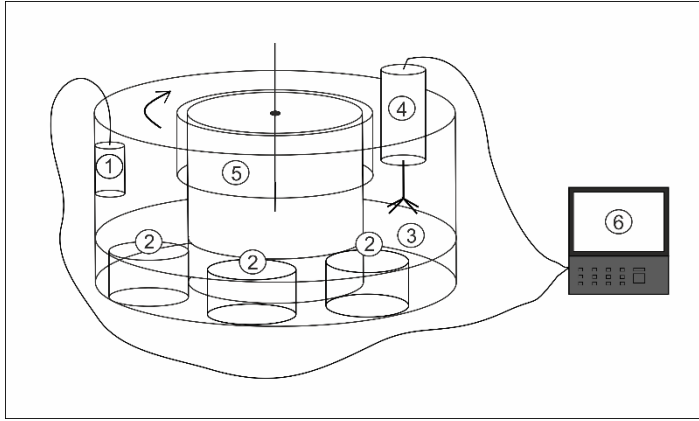


Figure 5.3: Experimental set-up of the annular flume experiments. 1: Turbidity-meter, 2: 10 cm sediment cores, 3: Second level, 4: Acoustic Doppler Velocitymeter (Vectrino profiler), 5: Motor, 6: Notebook for data record.

nitrogen analyses ('Blank filters'). An appropriate amount of uranium standard was added to increase the natural ^{234}Th activity with 14.8 dpm l^{-1} (see section 2.2). The flume was covered with a black foil overnight to prevent additional growth of algae. The next day, before starting the experiment, 3 litre of water were taken to determine the initial particulate and dissolved ^{234}Th activity. The current velocity was adjusted individually for each sediment type to the previously determined different current velocities: 1. just beyond the $u_{cr-initial}^*$ and 2. beyond the $u_{cr-erosion}^*$ (see section 5.3.2). Samples for ^{234}Th , TPM concentration and PC content were collected in varying time intervals over a period of 3 h. Figure 5.3 shows the experimental sampling scheme. During the first 1 h (Δt_1) of the experiment the sediment surface was resuspended ('resuspension phase'). At the end of that phase water samples for PC (3 X 0.5 litre) and particulate and dissolved ^{234}Th (1 X 5 litre) were collected and the

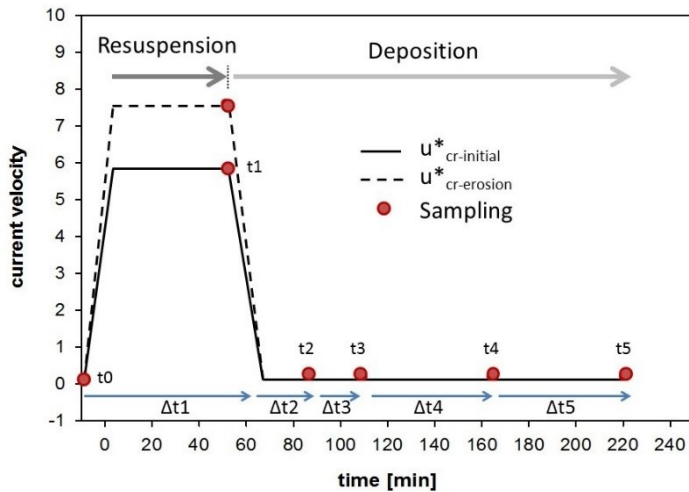


Figure 5.2: Sampling scheme of the experiment including the current velocity just beyond the $u_{cr-initial}^*$ and beyond $u_{cr-erosion}^*$ over time and the points of sampling (t_0 - t_5) as well as the time intervals between samplings (Δt_1 - Δt_5). The experiment was split into two phases, the 'resuspension' and 'deposition' phase.

flume was switched off. After stopping the current velocity samples for ^{234}Th and PC were taken over increasing time intervals (30 min, 1 h, 2 h and 3 h). This phase is called 'Deposition phase' ($\Delta t_2 - \Delta t_5$). ^{234}Th activity, TPM concentration and PC content were analysed as

described in section 2.1 and 3.1.3.1.

Due to the lack of time and logistic possibilities ^{234}Th subsamples were analysed only for one experiment (23.0 at current velocity of initial resuspension). The resulting variabilities in ^{234}Th activity were applied as standard error

for all other experiments. Therefore, the errors (based on error propagation) of the experiment are a combined effect of this standard error for the ^{234}Th measurements and the individual error of the TPM measurements of each sample (3 replicates).

Unfortunately, it must be assumed that the adsorption process during the resuspension and deposition phase was not completed. There were two processes which interfered with each other, the continued adsorption of dissolved ^{234}Th to particles and sedimentation/deposition of the particles. Therefore, the particle flux (in $\text{g m}^{-2} \text{h}^{-1}$) and ^{234}Th flux (in $\text{dpm m}^{-2} \text{h}^{-1}$) was calculated within each time interval (Δt_1 - Δt_5) according to the following equations:

$$\text{particle flux} = \frac{(TPM_{t_n} - TPM_{t_{n-1}}) * h}{(t_n - t_{n-1})} \quad (5.7)$$

, where TPM_{t_n} and $TPM_{t_{n-1}}$ are the total particulate matter (TPM) concentration at the time points t_n - t_5 and h represents the height of the water column. The ^{234}Th flux was calculated by multiplication of the particles flux with the average of the associated particulate ^{234}Th activities.

5.2.4 ^{234}Th activity, TPM and PC in the water column

After sampling, the water samples were acidified with concentrated HCl to a $\text{pH} < 2$ to prevent growth of bacteria and phytoplankton and adsorption of ^{234}Th onto container walls. Before analyses the pH was adjusted to 8 - 9 with a respective volume of ammonia. For particulate ^{234}Th ($^{234}\text{Th}_p$) analyses water samples were centrifuged using a continuous flow centrifuge (Heraeus Contifuge Stratos Centrifuge from Thermo Scientific TM) at the Leibniz Institute of Baltic Sea Research. The remaining particulate material in the rotor (Titanium – Rotor 3049) was carefully resuspended and filtered through 142-mm-diameter polycarbonate filters (0.4 μm pore width) at ~200 mbar underpressure. Dissolved ^{234}Th ($^{234}\text{Th}_d$) was co-precipitated in 10 litre of the filtrate by formation of MnO_2 and subsequent filtration at ~400 mbar overpressure. The activity of ^{238}U was calculated according to Chen et al. (1986). For detailed methodical information see section 2.1.

The PC content in 3 replicates of 1 litre water sample was determined as described in section 3.1.3.1.

5.2.5 ^{234}Th activity in the sediment and the mixing coefficient (D_b)

To determine sedimentary ^{234}Th activity the leaching method was applied. In contrast to the total dissolution of the sediment using HNO_3/HF the leaching method extracts the radionuclide associated with organic matter and which are adsorbed onto the surface of the mineral (Siddeeg et al., 2014). Siddeeg et al. (2014) reported specific activities of ^{234}Th extracted by leaching, relative to the total dissolution in a range of 30 - 75 %. In this study, the research focus is on particle associated ^{234}Th and therefore the use of the leaching method seemed to be sufficient.

Sedimentary ^{234}Th was determined according to a combined procedure reported by Aller and Cochran (1976), Anderson and Fleer (1982), Fleer (1991) and van der Leoff and Moore (1999) and is described in the Ph.D thesis of Robert Turnewitsch (1999).

A subsample of the sediment samples was dried overnight at 60 °C and grounded in an agate mortar. An appropriate amount of dry sediment was weighted to 46 ml FEP centrifuge tubes with ETFE screw closure. To determine the extraction efficiency during the procedure 1 ml of a 10 dpm ml⁻¹ ^{230}Th spike was added and the sediment was dried again over night. Each sample was leached with 33 ml 6 M HCl at 90°C for 4 h and the sediment-acid mixture was mixed every half an hour. The suspension was centrifuged and the supernatant was decanted into 90 ml PFA cups. The remaining sediment was washed with 10 ml 6 M HCl and the supernatant was also transferred into the cups. The 6 M HCl solution was evaporated to dryness using a heating plate and the residue was dissolved in 8 ml 6 M HCl overnight. The sample was transferred to centrifuge tubes and 25% NH_4OH was added until a stable precipitate was formed (at pH of 8 - 8.5). The precipitation is based on formation of $\text{Fe}(\text{OH})_3$ and contains thorium and uranium. Natural sediment should contain enough Fe to precipitate thorium. However, for reagent blanks, where not enough Fe is expected to for the precipitation, 50 of μl purified FeCl_3 solution (50 g l⁻¹ Fe^{3+}) was added. For the preparation of the purified FeCl_3 solution 121 g $\text{Fe}(\text{Cl})_3 \cdot 6 \text{H}_2\text{O}$ was dissolved in 500 ml 8 M HCl. In a glass separatory funnel, the solution was extracted 3 times in 167 ml isopropylether. The isopropylether phase containing FeCl_3 and FeCl_3 was back extracted 2 times with 250 ml 0.1 M HCl. The $\text{Fe}(\text{OH})_3$ precipitate of the samples was washed twice with 16 - 20 ml deionised water and dissolved again in 6 M HCl. The precipitation and washing procedure was repeated once and the precipitate was dissolved with 9 M HCl.

The ion exchange column (20 cm length, 0.8 cm inner diameter) was filled with AG1 X8 100 - 200 mesh anion exchange resin and conditioned with at least 30 ml (3 X column capacities) of 9 M HCl (chloride column). The sample was added and the column was

rinsed with 20 ml 9 M HCl. Uranium and iron were trapped on the resin and the eluate contains thorium. The thorium eluate was evaporated and dissolved in 20 ml 8 M HNO₃ overnight. The following ion exchange column (nitrate column) was prepared in the same way as the chloride column but 8 M HNO₃ was used for conditioning. In the nitrate form, the anion exchange resin collects thorium, while most other elements including lead and sea salt pass through. Therefore, the eluate was discarded and the column was rinsed with 9 M HCl where thorium was removed from the resin and was collected. The HCl eluate was evaporated to dryness and dissolved in 8 M HNO₃ overnight. This step was repeated by using a short nitrate column (10 cm length) and the HCl eluate was evaporated again and the remaining material was dissolved in 8 M HNO₃ overnight. The HNO₃ solution was evaporated to a small drop. The small drop was taken up with 1 ml of 0.01 M HNO₃ and transferred into the electroplating cell. The cup was rinsed with 2 X 1 ml 2 M NH₄Cl buffer (pH 2) and 1 ml of saturated ammonium-oxalate solution. Electroplating was conducted on silverplanchets with 23 mm diameter according to van der Loeff and Moore (1999).

²³⁴Th activities were measured via beta counting, while ²³⁰Th activities were counted in an alpha spectrometer. Beta counter and alpha spectrometer were crosscalibrated by Robert Turnewitsch during his Ph.D thesis (1999) using ²³⁸U planchets, where ²³⁸U was in secular equilibrium with ²³⁴Th. The cpm ratio between beta and alpha counting was 2.162 ± 0.065. It meant that for each ²³⁸U count in the alpha spectrometer 2.162 ²³⁴Th counts in the beta counter could be measured. The crosscalibration is necessary for the calculation of the correction factor (C). The correction factor consists of the activity lost during leaching (extraction efficiency) as well as the counting efficiency of the beta counter und alpha spectrometer and the crosscalibration following the equation:

$$C = \frac{cpm_{\alpha-230Th\ spike}}{dpm_{\alpha-230Th\ spike}} * \frac{cpm_{\beta-234Th\ planchet}}{cpm_{\alpha-238U\ planchet}} \quad (5.8)$$

$$C = \frac{cpm_{\alpha-230Th\ spike}}{dpm_{\alpha-230Th\ spike}} * 2.165 \quad (5.9)$$

, where the sample specific $cpm_{\alpha-230Th\ spike}$ to $dpm_{\alpha-230Th\ spike}$ represents the measured ²³⁰Th activity (cpm) of the spike in the alpha spectrometer and the added ²³⁰Th activity (dpm). The $cpm_{\beta-234Th\ planchet}$ to $cpm_{\alpha-238U\ planchet}$ expresses the measured ²³⁴Th activity in beta - counter to the measured ²³⁸U activity in the alpha spectrometer of the ²³⁸U planchet

(crosscalibration: 2.162 ± 0.065). The measured sample activities of ^{234}Th (in cpm) were divided by the correction factor (C).

Sedimentary excess ^{234}Th ($^{234}\text{Th}_{\text{ex}}$) is defined as the ^{234}Th unsupported by the decay of the parent ^{238}U . It is supplied by particles scavenging ^{243}Th from the overlying water column and transporting into the sediment. $^{234}\text{Th}_{\text{ex}}$ was calculated by subtracting the activity supported ($^{234}\text{Th}_{\text{sup}}$) by its parent nuclide, ^{238}U , from the total Thorium activity in the sample. Activities of ^{238}U were not analysed but in most studies $^{234}\text{Th}_{\text{ex}}$ was reported within the uppermost sediment layer. It can be assumed that in coastal water sediments no $^{234}\text{Th}_{\text{ex}}$ could be found below 5 cm (e.g. Aller and Cochran, 1976; Gerino et al., 1998; Baumann et al., 2013). Therefore, the activity in the deepest sediment layers were assumed to be $^{234}\text{Th}_{\text{sup}}$ and were subtracted from the total measured activity to calculate $^{234}\text{Th}_{\text{ex}}$.

5.2.6 Analytical problems - The ingrowths of bismuth-212

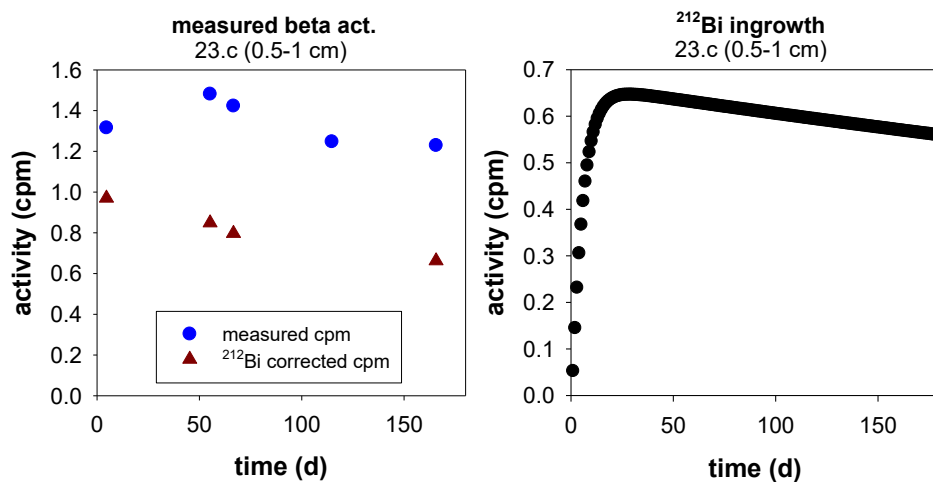


Figure 5.4: Station 23.c (0.5-1 cm - leaching) as an example of the decay curve of beta activity for the original measured activities and the ^{212}Bi corrected decay within ~170 days (a). The beta activity of ^{212}Bi over ~170 days, that grows in by the decay of ^{228}Th of the sample (b).

During repeated ^{234}Th measurements of the samples an unusual ^{234}Th decay was observed. Figure 5.4-a shows an example of the beta decay curve of the original measured activity (blue dots) of station 23.c 0-0.5 cm. The activity increases during the first 50 days after sampling and afterwards it decreases slightly. It is strongly suggested that another nuclide must have grown in. This assumption is supported by the mass spectrometer plot of this example shown in figure 5.5. Not only the peak of the ^{230}Th spike could be found but also two other additional main peaks. It can be expected, that after the leaching procedure and the separation steps using columns, most other elements, except thorium, have been

removed. According to the emitted energy, two additional natural thorium isotopes (^{232}Th and ^{228}Th) could be identified in the samples.

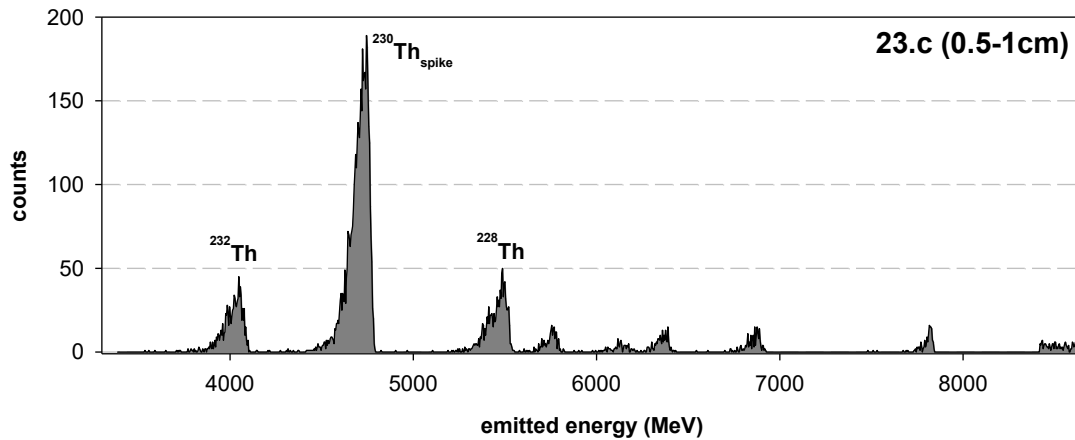


Figure 5.5: The mass spectrometry plot of station 23.c (0.5-1 cm) as an example of leached sediment sample. ^{232}Th , ^{230}Th and ^{228}Th were identified according to the emitted energy.

The identified thorium isotopes decay by emitting alpha particles and therefore had no influence on the beta signal of ^{234}Th . However, the ingrowths of some beta emitting progenies of ^{232}Th and ^{228}Th could have disturbed the ^{234}Th signal. For the identification of the disturbing nuclides it has to be considered that 1. the progeny emitted beta particles, 2. the emitting beta energy is high enough for detection and 3. the half-life of nuclides of the decay series is short enough to allow beta emitting daughter nuclides could have grown in during ~ 170 d of the measurement period. The influence of the beta emitting progenies of ^{230}Th and ^{232}Th within the decay series should be negligible due to the long half-life of ^{230}Th and ^{232}Th itself (figure 5.6). However, within the decay series of ^{228}Th bismuth-212 (^{212}Bi) could be identified as a beta particle emitting progeny (figure 5.6) with an emitting energy (2.252 MeV) similar to that of ^{234}Th daughter ^{234}Pa (2.195 MeV). Waples et al. (2003) described that one of the major problems associated with beta counting of ^{234}Th was the ingrowths of beta producing progeny from ^{228}Th . Therefore, it is highly likely that the ingrowths of ^{212}Bi is the main cause for the unusual decay of ^{234}Th samples. In figure 5.4-b it is shown that the activity of ^{212}Bi reaches a maximum after ~ 24 days and decreased slightly after that. This agrees with the decay of the beta activity of the sample (figure 5.4-a, blue dots). The ^{212}Bi activity (in cpm) of each time point of measurement was calculated from the activity of ^{228}Th measured in alpha spectrometer. ^{212}Bi decays with an emission of alpha (36 %) and beta (64 %) particles. However, ^{212}Bi emits different beta particles with varying energy level. The low energy particles are not available for detection. It is assumed, that only the high energy beta particles can be detected. That

means only 55.4 % of total ^{212}Bi activity decays with high energy beta particles (Brown, 2005; Martin, 2007).

All beta counter measurements were corrected for the ingrowths of the high beta energy particles of ^{212}Bi (55.4 %). In most cases the corrected ^{234}Th decay curves are significantly more suitable (figure 5.4-a, red dots). Therefore, ^{212}Bi seems to represent the largest fraction of the ingrowths of other nuclides. However, additional disturbing nuclides which influence the ^{234}Th beta signal cannot be excluded and therefore some uncertainties remain. The problem of ingrowths of other nuclides is not noticed for a two-point measurement (start and background) of the ^{234}Th activity. It is therefore recommended to measure beta activity at least 3 - 4 times during the decay period.

In this study, all sedimentary ^{234}Th data are corrected for the ingrowths of ^{212}Bi .

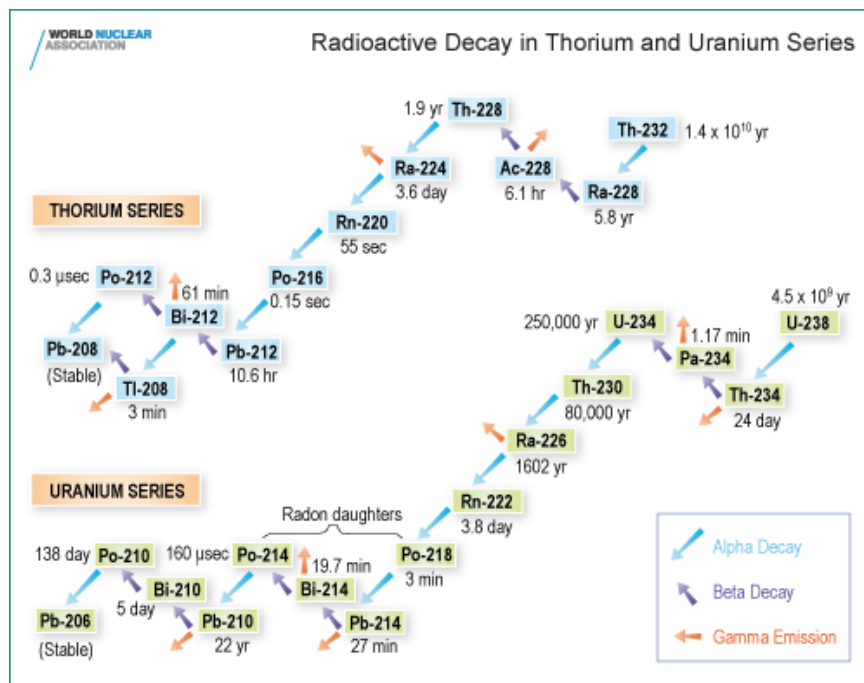


Figure 5.6: Thorium- and uranium decay series are illustrated as well the type of radioactive decay and the half-life of the nuclide. Source: world nuclear association (<http://www.world-nuclear.org/information-library/safety-and-security/radiation-and-health/naturally-occurring-radioactive-materials-norm.aspx> (from: 24.05.2016))

5.2.7 The mixing coefficient (D_b)

The particle mixing intensity can be estimated by modelling the sediment distribution of a particle-reactive radionuclide, such as ^{234}Th . In this study the models of Soetaert et al., 1996 were used to quantify sediment mixing. These models consist of hierarchical families of local and non-local exchange models, where each member of the hierarchy includes all

processes of the previous model and one or two additional processes. The models are based on the following assumptions: (1) steady state, which means a constant supply of ^{234}Th ; (2) continuous nonlocal mixing and (3) no porosity gradients. In addition the model needs the decay rate of ^{234}Th (10.5 y^{-1}) and the sedimentation rate (western Baltic Sea 0.2 cm y^{-1} , Leipe et al. (2005) and references therein) and works on the principle of the best fit for the simplest exchange model.

The distribution of the tracer in the simplest model (model 1) is influenced only by the flux, sedimentation rate and the decay. Mixing by organisms is not considered. Model 2 adds the diffusive exchange but no nonlocal mixing. The following model added nonlocal processes and different conditions were considered (Soetaert et al., 1996).

In this study, the best fit for the sediment profiles was used to calculate the D_b from each sediment. The results were presented as measured $^{234}\text{Th}_{\text{ex}}$ data compared against profiles generated with the best fit model.

5.3 Results

5.3.1 Hydrography and sediment characteristics of the study area

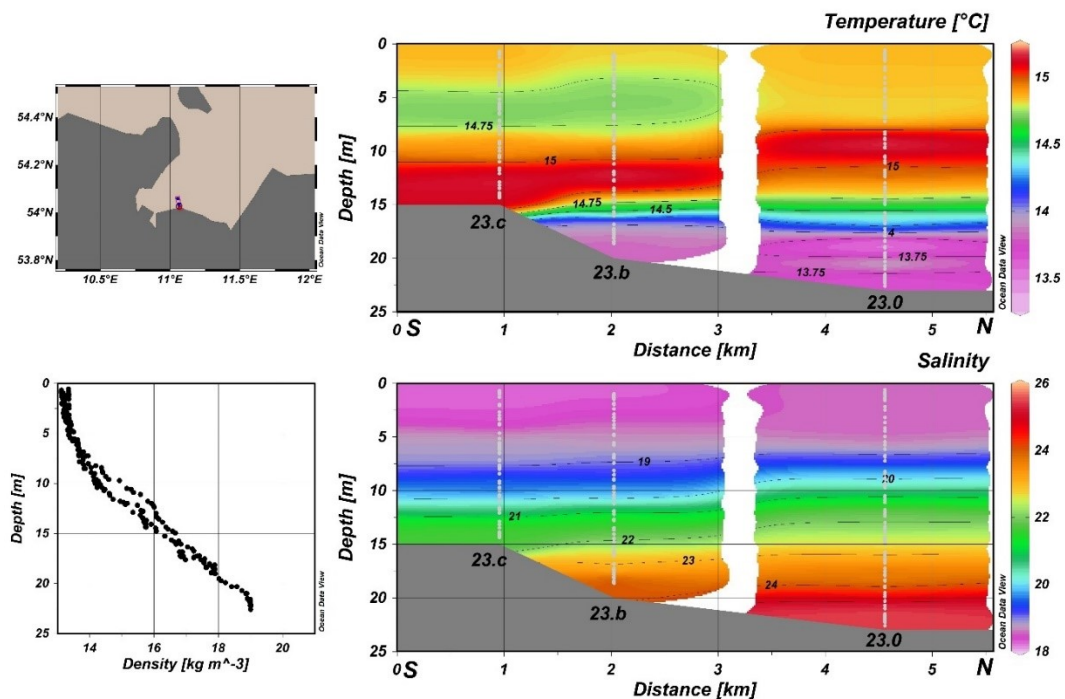


Figure 5.7: Temperature and salinity profile at the stations along a transect in the Mecklenburg Bay as well as the depth dependent density plot. The point data were extrapolated within the sections.

In September 2015, the temperature in the water column varies from 13.4 in the bottom water column to 15.2 °C at the surface. At all stations, the salinity increases towards the

bottom. For example, at Station 23.0 the salinity increases with water depth from 13.9 at the surface to 20.4 in the bottom water column (figure 5.7). Depending on water depth the bottom water salinity varies between the stations from 16.4 at station 23.c to 20.3 at station 23.0 (table 5.1, figure 5.7). The density vs. depth profile shows a mixed surface water mass down to ~8 m, followed by a strong density gradient and an additional mixed bottom water mass to ~1.5 mab. A stratification of the water column is governed by the pronounced salinity/density gradient which is produced by episodic saline inflow from the North Sea into the basins of the Baltic Sea.

According to the sediment parameters, the stations differ clearly from each other (table 5.2). Station 23.c shows low water content, high dry bulk density, low carbon and nitrogen content as well as a high median grain size. This represents typical medium sand sediment. In contrast station 23.0 shows a high water content and low dry bulk density and low median grain size. According to the Udden-Wentworth-scale (Wentworth, 1922) this sediment can be classified as a silt sediment. The water content and organic content increase with increasing distance to the coast, while median grain size and dry bulk density decrease. Therefore, these stations represent three different sediment types of the Baltic Sea. According to these results it can be expected that there are also differences in ²³⁴Th uptake potential.

Table 5.2: Summary of the sediment characteristics of the three study sites in the Mecklenburg Bay. The ranged values represent the minimum and maximum values of the sediment profile.

Station	Median grain size (µm)	Sediment type	Water content (%)	Dry bulk density (g cm ⁻³)	C-content (mg g ⁻¹ dry Sed.)	N-content (mg g ⁻¹ dry Sed.)
23.c	330.37	medium sand	29.5 - 17.5	1.63 - 1.27	3.32 - 1.50	0.42 - 0.19
23.b	147.25	fine sand	53.8 - 22.9	1.48 - 0.65	10.41 - 4.39	1.02 - 0.50
23.0	44.76	silt	83.1 - 73.0	0.31 - 0.19	53.87 - 48.08	6.48 - 5.74

5.3.2 Thresholds of sediment motion

Figure 5.8 shows the results of the determination of the measured u_{cr}^* compared to the

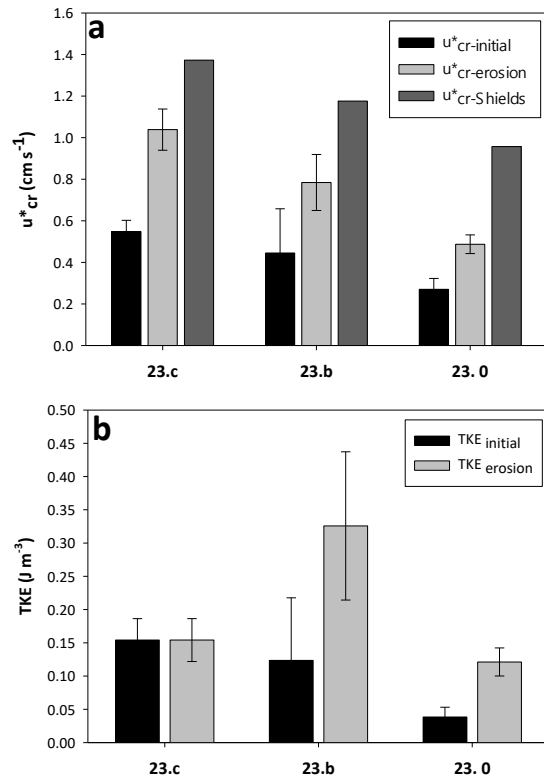


Figure 5.8: 5.8-a: Measured critical shear stress velocity (u_{cr}^*) of initial motion of particles and erosion as well as the calculated u_{cr}^* according to Shields at three stations in the Mecklenburg Bay. 5.8-b: Turbulent kinetic energy (TKE) of initial resuspension and erosion flow regime for the sediments. The errors indicate SD.

calculated u_{cr}^* according to Shields (based on grain size) as well as the TKE of the three stations in the Mecklenburg Bay. The initial particle motion can be observed at $0.27 - 0.55 \text{ cm s}^{-1}$, while erosion is determined between 0.49 and 1.04 cm s^{-1} . Both, the initial particle motion and erosion decrease with increasing distance to the coast. In all cases the calculated u_{cr}^* of Shields is somewhat higher compared to the measured values.

For TKE no clear trend can be observed. Both initial and erosion TKE of station 23.c are in the same range of $0.15 \pm 0.03 \text{ J m}^{-3}$. The initial TKE decreases with increasing water depth, while highest TKE for erosion is found at station 23.b with $0.33 \pm 0.11 \text{ J m}^{-3}$. At station 23.b and 23.0 TKE increases towards erosion.

5.3.3 Resuspension-deposition-experiment

As shown in figure 5.9, during the resuspension phase (Δt_1 , figure 5.3) the particulate matter concentration strongly increases. Highest values of particulate matter ($44.0 \pm 1.1 \text{ mg l}^{-1}$) in suspension is found during strong erosion conditions of station 23.0. The particle concentration strongly decreases within 30 min after the resuspension phase (Δt_2 , figure 5.3) with a decreasing rate in the range of 0.03 to $-1.17 \text{ mg min}^{-1}$. This rate decreases over time to almost ~ 0 (Δt_5 : $0.003 - 0.02 \text{ mg min}^{-1}$) at the end of the experiment. In general, decreasing rates during experiments under erosion conditions are higher compared to initial resuspension. After 3 h, the particle concentration is in the range of 2.1 to 4.3 mg l^{-1} . In relation of the decreasing particle concentration, a clear trend between the stations cannot be observed.

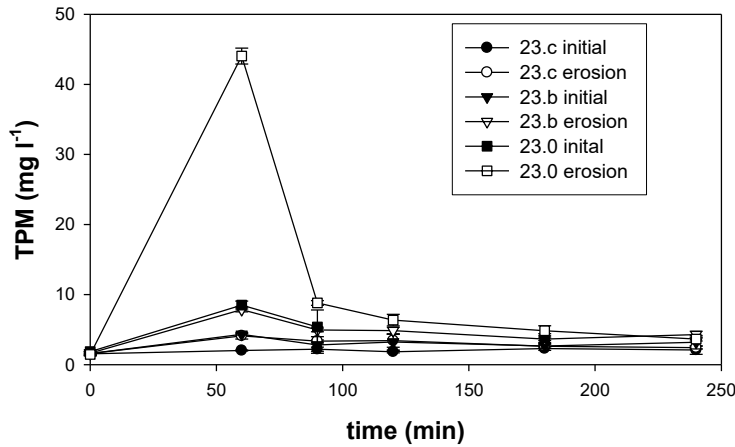
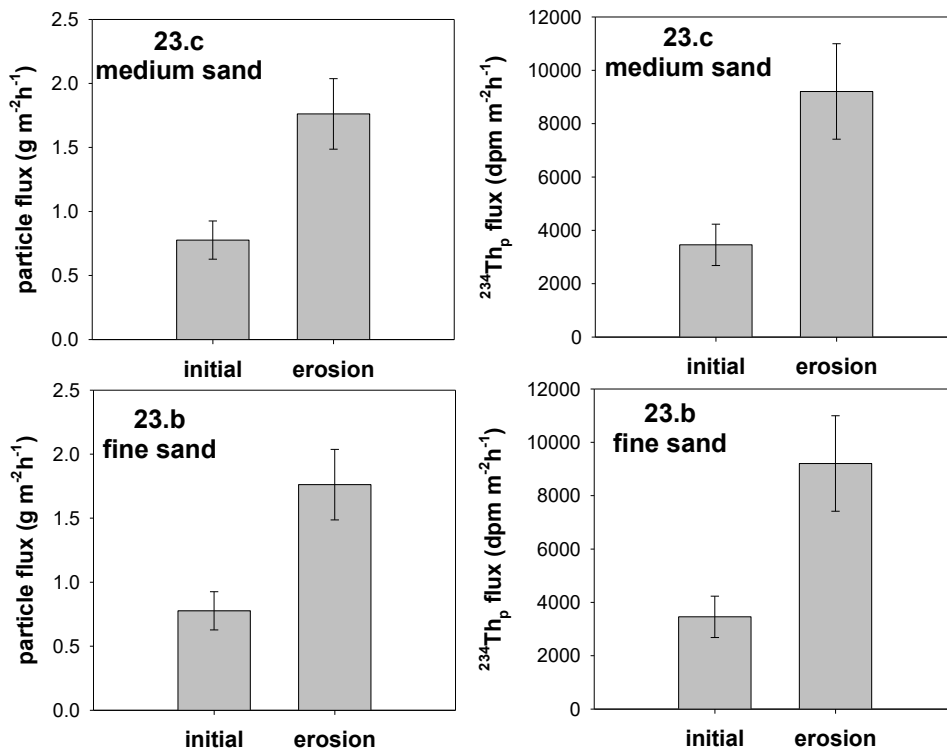


Figure 5.9: The total particulate matter (TPM) concentration over time during the resuspension and deposition phase (figure 5.3) of three stations along the transect at the Mecklenburg Bay, Baltic Sea. The closed and opened Symbols of each type represent two different current velocities (initial resuspension and significant Erosion). Errors indicate SD TPM concentration. of

Figure 5.10 shows the particle – and ²³⁴Th fluxes during the resuspension phase (Δt , figure 5.3) of the three sediment types at current velocity of initial resuspension and significant erosion. In general fluxes are increased at erosion condition velocities. Station 23.0 shows significant higher particle and ²³⁴Th_p fluxes at both initial and erosion flow conditions with maximum values of $12.1 \pm 1.1 \text{ g m}^{-2} \text{ h}^{-1}$ and ²³⁴Th fluxes $26681 \pm 2894 \text{ dpm m}^{-2} \text{ h}^{-1}$ followed by $1.8 \pm 0.3 \text{ g m}^{-2} \text{ h}^{-1}$ and $9205 \pm 1790 \text{ dpm m}^{-2} \text{ h}^{-1}$ at station 23.b and $0.7 \pm 0.1 \text{ g m}^{-2} \text{ h}^{-1}$ and $2344 \pm 442 \text{ dpm m}^{-2} \text{ h}^{-1}$ at station 23.c.



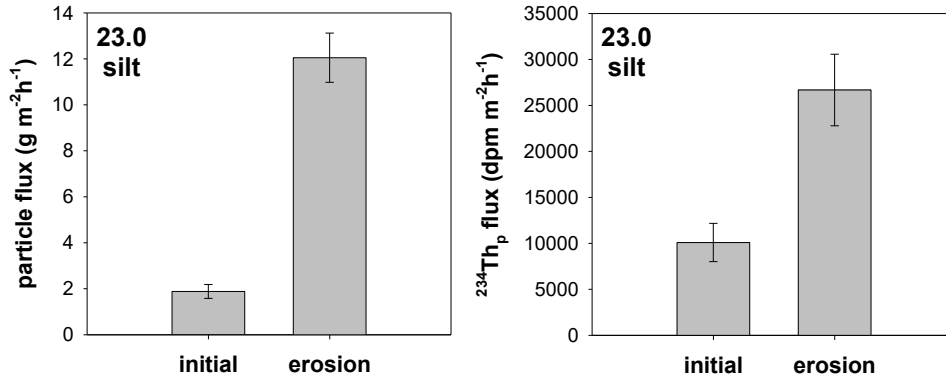


Figure 5.10: Particle- and particle-associated ^{234}Th ($^{234}\text{Th}_p$) fluxes at two different current velocities of initial resuspension and significant erosion of the sediment surface of three stations along the transect at the Mecklenburg Bay, Baltic Sea. Errors of particles fluxes are based on the error propagation of SD of the total particulate matter (TPM). Errors of $^{234}\text{Th}_p$ fluxes result from error propagation of the standard ^{234}Th error and the SD of the TPM concentration for individual samples (see section 4.2.3).

The distribution coefficient (K_d) describes the partitioning of particulate and dissolved ^{234}Th in relation to the particle concentration. Figure 5.11 shows the $\log K_d$ during the resuspension phase at the three stations. $\log K_d$ does not vary between initial resuspension and erosive current conditions at the sandy station and is in the same range from 5.7 ± 0.8 to 6.1 ± 0.5 . Station 23.0 shows a somewhat lower $\log K_d$ of 4.6 ± 0.4 and 5.3 ± 0.5 . The $\log K_d$ of erosion is slightly weaker than the initial sample. However, all tests for significances (ANOVA on ranks) between initial and erosion samples of the station show no significant differences.

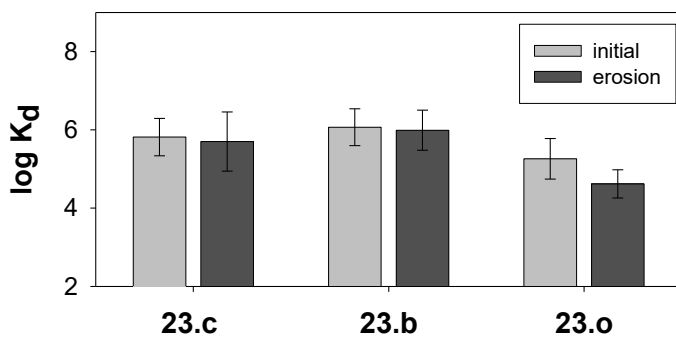


Figure 5.11: The distribution coefficient ($\log K_d$) at the three stations during the resuspension phase of the experiment. Errors are based on the error propagation of the standard ^{234}Th error and the SD of the TPM concentration for individual samples (see section 4.2.3). Significance levels $P > 0.05$.

5.3.4 ^{234}Th distribution in the Mecklenburg Bay

5.3.4.1 ^{234}Th activities in the water column

Activities of particle associated ^{234}Th ($^{234}\text{Th}_p$), dissolved ^{234}Th ($^{234}\text{Th}_d$), ^{238}U as well as the ratio of total ^{234}Th ($^{234}\text{Th}_{\text{tot}}$) and ^{238}U in the water column are shown in figure 5.12. The salinity-derived activities of ^{238}U increase from 0.968 dpm l^{-1} at the surface to 1.417 dpm l^{-1}

in the bottom water column. In general, $^{234}\text{Th}_p$ and $^{234}\text{Th}_d$ activities are very similar at all stations and sampled water depths. $^{234}\text{Th}_p$ range from 0.17 dpm l⁻¹ to 0.25 dpm l⁻¹ and $^{234}\text{Th}_d$ varies from 0.35 dpm l⁻¹ to 0.48 dpm l⁻¹. In the surface water, station 23.0 shows a slightly increased $^{234}\text{Th}_d$ activity.

At all sampled water depths, the ratio of total ^{234}Th and ^{238}U activities is well below 1 and ranged from 0.49 to 0.68. This means that strong radioactive disequilibria are pronounced in the whole water column.

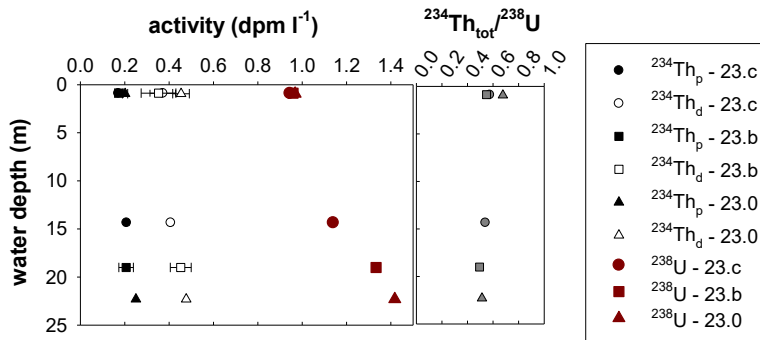


Figure 5.12: Activities of particle associated ^{234}Th ($^{234}\text{Th}_p$), dissolved ^{234}Th ($^{234}\text{Th}_d$), ^{238}U as well as the ratio of total ^{234}Th ($^{234}\text{Th}_{tot}$) and ^{238}U in the water column of the surface and close to the seafloor (<1.5 mab). Closed symbols indicate $^{234}\text{Th}_p$, open symbols $^{234}\text{Th}_d$ and red symbol represents the ^{238}U activity. Errors are expressed as SD.

5.3.4.2 Sediment excess ^{234}Th and particle mixing

The results for sedimentary ^{234}Th are shown in figure 5.13. In this study, the supported ^{234}Th was not directly measured. However, as described in section 5.2.5 it is assumed that the lowermost sediment layers only comprise the supported ^{234}Th . For station 23.c and 23.b there are some problems with this assumption, due to the strong minimum of total measured activity in 1 - 2 cm sediment depth followed by an increasing and relatively constant activity down to 10 cm (figure 5.13). If it is assumed that the lowermost sediment layers represent only supported ^{234}Th and this value would be subtracted from the total activity, it is likely that excess ^{234}Th would be underestimated. Kersten et al (2005) showed varying ^{238}U activity in the sediment with lower activities in the surface sediment by almost a half. Boryto and Skwarzec (2014) and Skwarzec et al (2004) found that in the southern Baltic, vertical diffusions processes of uranium from the sediment into the bottom water, through the pore water, occur. Aller and Cochran (1976) discussed the phenomenon of increasing uranium concentration with sediment depth. The authors described uranium depletion in the surface sediment due to oxygenation effects. Under oxygenated conditions uranium exist in the dissolved form of U^{6+} compared to reduced conditions in the deeper sediment layers, where uranium is reduced to U^{4+} by precipitation of Fe or Mn hydroxides. In this state, it is almost insoluble and cannot be exchanged with the overlaying water by diffusion, while the soluble form of uranium can

be exchanged with the overlying water column. In this study, sediments of station 23.c and 23.b are sandy and most likely permeable. It is strongly assumed that such diffusive exchange processes also took place at these sites and led to a depletion of ^{238}U in the superficial layers of the sediment. As a result of increasingly reduced conditions, the ^{238}U activities increase in the deeper sediment (figure 5.13). Therefore, within the uppermost 2 cm of the sediment the minimum is assumed to represent $^{234}\text{Th}_{\text{sup}}$, while below 2 cm the last data points are set to be $^{234}\text{Th}_{\text{sup}}$. At station 23.o it is assumed that the ^{238}U depletion in the uppermost sediment layer does not exist due to the impermeable character of this sediment type and the expected reduced conditions for these sediment type. This assumption is supported by the absence of a minimum within the topmost 2 cm of total activity found at station 23.o. The resulting $^{234}\text{Th}_{\text{ex}}$ of 23.c and 23.b are highest at the sediment water interface of 0.16 and 0.31 dpm g^{-1} and decrease with increasing sediment depth down to 1.5 cm depth. At station 23.o and 23.b a decrease of $^{234}\text{Th}_{\text{ex}}$ with increasing depth and a subsurface maximum between 3 - 5 cm and 3.5 - 8.75 cm is observed. Highest $^{234}\text{Th}_{\text{ex}}$ activity of 0.37 dpm g^{-1} is found at the sediment water interface of station 23.o. In general, this station shows highest $^{234}\text{Th}_{\text{ex}}$ activities per g dry sediment (figure 5.13).

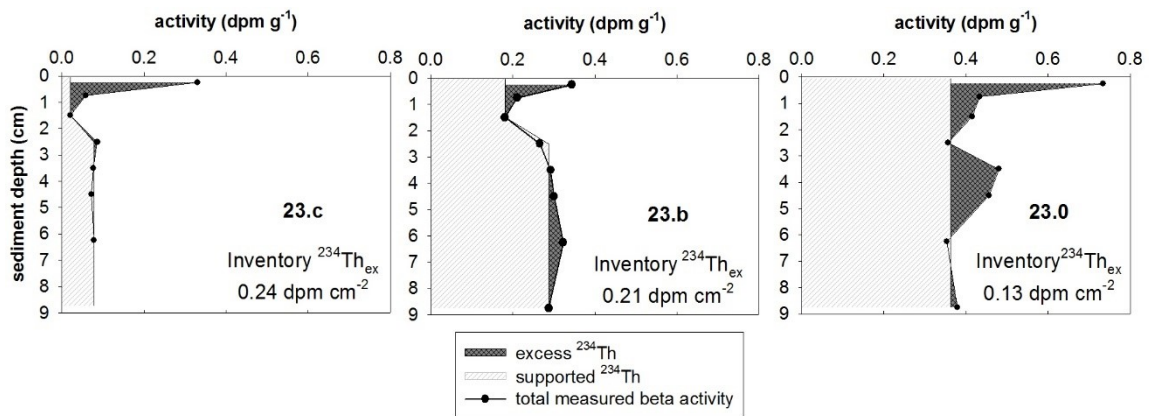


Figure 5.13: ^{234}Th profiles of the sediment from three stations along the transect in the Mecklenburg bay. The white striped area indicating supported ^{234}Th and the dark grey area shows the excess ^{234}Th . Total measured activities are represented as filled black dots. The inventories are calculated from the dry bulk density and are shown in each plot.

$^{234}\text{Th}_{\text{ex}}$ inventory was calculated based on the dry bulk density and the thickness of the sediment layer. The inventory of $^{234}\text{Th}_{\text{ex}}$ increases from station 23.o to 23.c (figure 5.13).

The results of describing particle mixing using the models of Soetaert et al (1996) are shown in figure 5.14. The best fit for station 23.c and 23.b is model 3. Model 3 includes not only the sedimentation, the decay and diffusive mixing, but also the nonlocal injection of the flux at a depth L, where two layers are considered (from 0 to L and from L to ∞) (Soetaert et al., 1996). For station 23.o the best fit is given for model 1 (figure 3.14). This

model describes that the distribution of the tracer is influenced only by the flux from the overlying water column, the sedimentation rate and the decay of the tracer. In model 1 the biological activities are not considered. However, the $^{234}\text{Th}_{\text{ex}}$ sediment profile shows two strong subsurface maxima in 1 - 2 cm and 2.5 - 6 cm, which indicates biological activity. The model of Soetaert et al (1996) cannot handle with two subsurface maxima. It is assumed that the model 1 is not suitable for station 23.0 to describe the distribution of ^{234}Th and possible artefacts seem to exist. Therefore, the best fit for the simplest model is applied for Model 3 at this station.

In general, the D_b values increase with increasing water depth. Highest D_b of $2.35 \text{ cm}^2 \text{ y}^{-1}$ is found at station 23.0 followed by 23.b and 23.c. The injection flux is highest at station 23.b followed by 23.0 and 23.c. The measured and modelled profiles fit very well at station 23.c and 23.b. For 23.0 some discrepancy can be found between modelled and measured $^{234}\text{Th}_{\text{ex}}$ due to the second injection depth as described above. Therefore, it can be assumed that the calculated D_b of $2.35 \text{ cm}^2 \text{ y}^{-1}$ is somewhat underestimated.

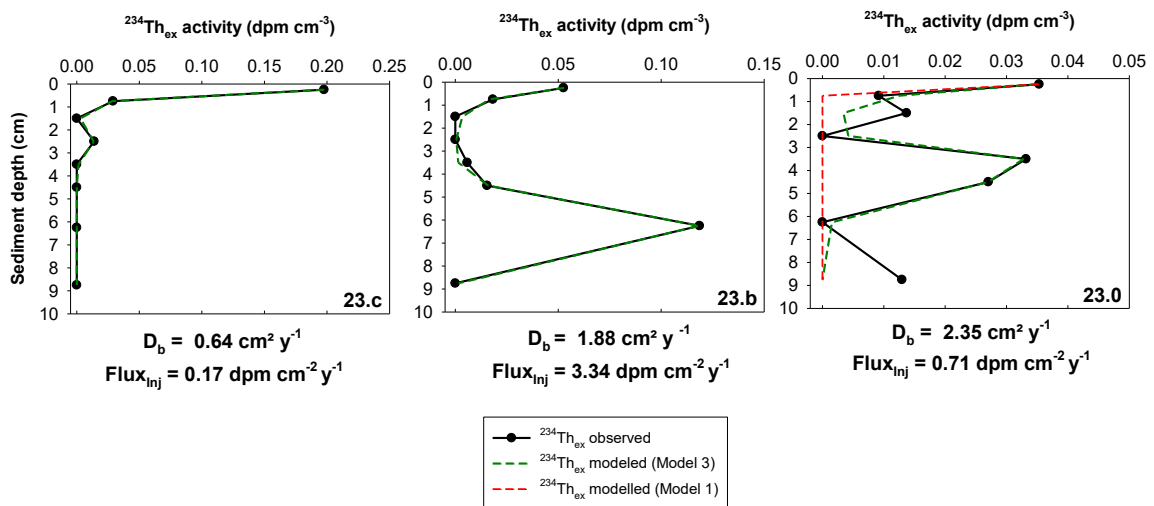


Figure 5.14: The observed and modelled $^{234}\text{Th}_{\text{ex}}$ activity using the models of Soetaert et al. (1996) as well as the mixing coefficient (D_b) and the injection flux (Flux_{inj}) at the three station in the Mecklenburg Bay. The D_b and Flux_{inj} were calculated from model 3.

5.4 Discussion

5.4.1 The erodibility of the sediment in the Mecklenburg Bay

The morphology of the western Baltic seafloor is characterised by sills and basin structures formed during the Pleistocene and Holocene transgression. The Mecklenburg Bay is a basin with a maximum depth of 28 m (Köster and Lemke, 1996). The distribution of the sediments in the Baltic Sea is affected by multiple flooding and draining events

resulting from the different postglacial uplift of the basins (Niedermeyer et al., 2011). The major source of sediment material in the south-western Baltic Sea is glacial till. The input of sediment into the Baltic is mainly caused by erosion of the coast followed by river discharge and air dust deposition as a minor part (Köster and Lemke, 1996). The distribution pattern of the sediment, especially the grain size is controlled by erosion, transport and deposition regimes. Zones of fine sediment accumulation are located below the wave influenced level. In shallow coastal water intensive sediment transport takes place due to the high hydrodynamic regime (Tauber and Lemke, 1995) which leads to a sorting towards coarser sediments.

The results of this study (figure 5.8) agree very well with the reported u_{cr}^* of Ziervogel and Bohling (2003) for stations in the Mecklenburg Bay between Kühlungsborn and Warnemünde. To the best of my knowledge, this study is the only one which experimentally determined u_{cr}^* in the Mecklenburg Bay. The authors found initial particle transport of the fine sand sediment (similar to the station 23.b of the presented study) in a similar time of year in the range of 0.35 to 0.6 cm s^{-1} and the erosion thresholds of 0.7 to 0.8 cm s^{-1} . Their findings are in the same range as the observed values ($u_{cr-initial}^*$: 0.45 cm s^{-1} ; and $u_{cr-erosion}^*$: 0.78 cm s^{-1}) from station 23.b of the presented study. At their fine sediment (mud) station (comparable to station 23.o of this study) initial particle motion ranged from 0.3 to 0.5 cm s^{-1} and mean erosion was detected at 0.62 cm s^{-1} which agrees very well with the finding of this study of 0.27 cm s^{-1} for $u_{cr-initial}^*$ and 0.49 cm s^{-1} $u_{cr-erosion}^*$ at station 23.o.

The strong discrepancy between the measured and the calculated thresholds are likely due to the existence of a fluffy layer on the sediment surface at all stations. Shields theoretical values are calculated only from the grain size and the very labile and loose bound particles are not being considered. Fluff material is presented at the sediment-water interface and consisted mainly of detrital particles settled from the overlying water (Lund-Hansen et al., 2002). In contrast to the underlying sediment (in this study sand or silt), the fluff material can be resuspended at lower critical shear stress velocities (Stolzenbach et al., 1992; Leipe et al., 2000). Therefore, the low critical shear stress velocity of this study can be explained by the presence of a fluffy layer located on the top of the sediment surface. Table 5.3 shows the comparison of critical shear stress velocities of fluffy material with other studies. The measurements of critical shear stress velocities of these studies showed that the thresholds are in same range for $u_{cr-erosion}^*$ presented in this study (figure 5.8).

Table 5.3: Summary of critical shear stress velocities of fluff material from different studies at varying locations.

u_{cr}^* (cm s^{-1})	Location/Experiment	Method	Citation
<i>initial</i> 0.3-0.5 <i>erosion</i> 0.5-0.8	south-western Baltic sea	annular flume	this study
0.4-1.2	NW western European continental margin	erosion chamber	Thomsen and Gust, 2000
0.4-0.8	sieved sediment and phytodetritus	laboratory channel flume	Beaulieu, 2003
0.4-0.5	south-western Baltic Sea	erosion chamber	Jähmlich et al., 2002

At the silt station 23.0 a strong and at least 0.5 cm thick fluff layer was observed while the fluff of the sandy station was rather represented as loose flocks on top of the sediment surface. Additionally, at the silt station the erosion of large aggregates could be observed. Thomsen and Gust (2000) showed that the erosion probability increases with increasing particle size. Therefore, it can be concluded that the large aggregated particles at station 23.0 eroded by lower u_{cr}^* as shown in figure 5.8.

Based on the results of this study it is concluded that the calculated u_{cr}^* of Shields (based on the mean diameter of the sediment) compared to the measured u_{cr}^* could lead to variations in sediment transport due to the presence of a fluffy layer which can be resuspended in reduced flow conditions. Especially the application of models to describe transport of sedimentary material (e.g. Kuhrts et al., 2004; Bobertz et al., 2009), which required the critical shear stress velocity, could be underestimated if fluff material is present on the natural sediment surface. Based on model studies, Bohling (2005) reported an erosion risk during storm events in the shallow water areas of the Mecklenburg bay of up to 87 % and less than 10 % in areas of water depth of more than 23 m. This author ignored the fluffy layer in the model run and only the underlying sediment was referred to surface sediment. According to the results of this study and the previous study of Ziervogel and Bohling (2003) it can be assumed that the erosion risk would increase if the fluffy layer is included in the model. It is recommended that thresholds of sediment motion should be measured directly instead of theoretically estimated. At least, reported thresholds of fluff material should be taken into account by using model approaches to determine sedimentary transport processes.

5.4.2 Particle dynamic in the Mecklenburg Bay

The overall $^{234}\text{Th}/^{238}\text{U}$ ratios of well below one (figure 5.12) indicate a strong depletion of ^{234}Th activities by particle scavenging and removal from the water column. This is very typical for shallow coastal environments as found elsewhere (e.g. Wei and Murray, 1992; Kersten et al., 1998, Forster et al., 2009; Evangelidou et al., 2011; Ma et al., 2014). In the Mecklenburg Bay Kersten et al. (1998) and Forster et al. (2009) found $^{234}\text{Th}/^{238}\text{U}$ ratios of 0.2 - 0.5 and 0.09 - 0.19. The results of 0.5 - 0.7 in the presented study are near the upper end of the range. The particulate and especially the dissolved ^{234}Th values of this study (figure 5.12: $^{234}\text{Th}_p$ 0.17 - 0.25 dpm l⁻¹; $^{234}\text{Th}_d$ 0.35 - 0.47 dpm l⁻¹) are slightly higher compared to Kersten et al. (1998) ($^{234}\text{Th}_p$ 0.05 - 0.55 dpm l⁻¹; $^{234}\text{Th}_d$ 0.09 - 0.41 dpm l⁻¹) and Forster et al. (2009) ($^{234}\text{Th}_p$ 0.08 - 0.11 dpm l⁻¹; $^{234}\text{Th}_d$ 0.02 - 0.11 dpm l⁻¹). The ^{238}U activities are in the same range of 0.9 - 1.4 dpm l⁻¹ in this study and 0.9 - 1.7 dpm l⁻¹ and 1.0 - 1.5 dpm l⁻¹ in Kersten et al. (1998) and Forster et al. (2009) which indicates no influence of varying salinity and therefore different ^{238}U activities between the studies. Natural variability could explain the differences between these three studies in the same sampling area. However, the relative strong discrepancy to Forster et al. (2009) could also result from the different sampling methods used (filtration versus continuous-flow centrifuge). Compared to the results of Kersten et al. (1998) the $^{234}\text{Th}_p$ activities of the presented investigations are in good agreement but the $^{234}\text{Th}_d$ of this study are near the upper end of the range found by Kersten et al. (1998). In both studies the continuous-flow centrifuge was used for the determination of $^{234}\text{Th}_p$, but Kersten et al. (1998) used a different analytical method to extract $^{234}\text{Th}_d$ from the centrifugate. It can be assumed that the method of MnO_2 precipitation to extract $^{234}\text{Th}_d$ (van der Loeff and Moore, 1999) from the filtrate used in this study is more efficient compared to other techniques. In previous studies, it has been reported that $^{234}\text{Th}_d$ is removed by this procedure with an efficiency of nearly 100 % (e.g. van der Loeff and Moore, 1999; Turnewitsch and Springer, 2001; Turnewitsch et al., 2008). Therefore, it can be assumed that possible higher extraction efficiency could result in higher $^{234}\text{Th}_d$ activities.

The discrepancies in ^{234}Th activities to the previous studies in the same area is most likely result from a combined effect of both, natural variability and the methodological differences. Despite these discrepancies, it can be concluded that the pronounced total $^{234}\text{Th}/^{238}\text{U}$ disequilibrium, which occurred throughout the whole water column, strongly indicates very dynamic ^{234}Th scavenging and particle export in the shallow water of the Mecklenburg Bay.

5.4.3 Particle residence time

The distribution of $^{234}\text{Th}_p$ and $^{234}\text{Th}_d$ to ^{238}U indicates considerably scavenging of $^{234}\text{Th}_d$ from the water column and export into the sediment. Therefore ^{234}Th -derived residence time were calculated from the following definitions and equations (according to Forster et al., 2009):

The scavenging residence time, τ_d , is the characteristic time that $^{234}\text{Th}_d$ takes to be transferred into the particulate phase.

$$\tau_d = \frac{1}{k_a} = \frac{{}^{234}\text{Th}_d}{\lambda_{234} \cdot ({}^{238}\text{U} - {}^{234}\text{Th}_d)} \quad (5.10)$$

, where k_a is the rate constant of net absorption of $^{234}\text{Th}_d$ onto particles (scavenging rate); $^{234}\text{Th}_p$, $^{234}\text{Th}_d$ and ^{238}U are the activities of the respective fraction and λ_{234} is the radioactive decay constant of ^{234}Th (0.02876 d^{-1}).

The residence time of particle associated ^{234}Th , τ_p , is the time before $^{234}\text{Th}_p$ is being exported from a given water layer.

$$\tau_p = \frac{1}{\lambda_p} = \frac{{}^{234}\text{Th}_p}{\lambda_{234} \cdot {}^{238}\text{U} - \lambda_{234} \cdot ({}^{234}\text{Th}_d + {}^{234}\text{Th}_p)} \quad (5.11)$$

, where λ_p is the rate constant for the removal of $^{234}\text{Th}_p$ (removal rate).

These equations are based on the assumption that the pool of $^{234}\text{Th}_p$ is maintained by the uptake from $^{234}\text{Th}_d$ from the solution to particles, its radioactive decay and particle export. Kersten et al. (1998) showed that these steady-state equations to calculate residence times are acceptable for the Baltic environment.

The following table 5.4 shows the scavenging and particle-associated residence time in the water column and sediment as well as the scavenging rate, removal rate and the TPM concentration. For the calculation of the particle-associated residence time of $^{234}\text{Th}_{ex}$ (Inventory) in the sediment the equation 5.11 was used. Therefore, it was assumed that all ^{234}Th in the sediment was presented in the particulate phase ($^{234}\text{Th}_d = 0$).

Table 5.4: Residence time (in days) of dissolved ^{234}Th (τ_d) and particle associated ^{234}Th (τ_p) in the water column (SW - surface water, BW - bottom water) and the sediment inventory as well as the dissolved ^{234}Th scavenging rate, particulate ^{234}Th removal rate and the total particulate matter concentration (TPM) of the three stations in the Mecklenburg Bay. Errors are based on error propagation of the SD of the activities or TPM concentration. n.d. = no data, due to no replicated samples. * = the particle residence time of excess ^{234}Th inventory.

		scavenging residence time (τ_d) (d)	particle- associated residence time (τ_p) (d)	$^{234}\text{Th}_d$ scavenging rate (k_a) (d^{-1})	$^{234}\text{Th}_p$ removal rate (λ_p) (d^{-1})	TPM (mg l^{-1})
23.c	SW	22.60 ± 3.52	14.79 ± 2.30	0.044	0.068	2.28 ± 0.09
	BW	19.32 ± 1.24	13.78 ± 0.89	0.052	0.073	1.99 ± 0.15
	Sediment		16.73			
23.b	SW	20.20 ± 5.00	13.97 ± 3.45	0.050	0.072	1.32 ± 0.08
	BW	17.87 ± 3.40	10.64 ± 2.03	0.056	0.094	1.53 ± 0.23
	Sediment		2.22			
23.o	SW	30.68 ± 3.10	22.41 ± 2.26	0.033	0.045	1.32 ± 0.19
	BW	17.64 ± n.d.	12.62 ± n.d.	0.057	0.079	1.60 ± 0.19
	Sediment		4.97			

The residence time of dissolved and particle-associated ^{234}Th in the water column are in the range of 17.64 and 30.68 days and 10.64 and 22.41 days (table 5.4). This is somewhat higher compared to residence times found in the same area from Kersten et al. (1998) and Forster et al. (2009), who reported values in the order of <10 days and <5 days for dissolved ^{234}Th and particle associated ^{234}Th residence time in the range of 1.3 – 20.1 days and 2 – 4 days. The particle-associated ^{234}Th residence time of the presented study is near the upper end of the results of Kersten et al. (1998). However, dissolved ^{234}Th residence times are almost one order of magnitude higher compared to the previously mentioned studies. This is due to the relatively high dissolved ^{234}Th activities of this study compared to Kersten et al. (1998) and Forster et al. (2009) as discussed in section 5.4.2. Nevertheless, the residence times of dissolved and particle associated ^{234}Th in the space of 10 days to a few weeks, compared to more than 100 days in open ocean conditions (e.g., Charette and Moran, 1999), indicates a high level of particle dynamics which is typical for coastal waters.

The scavenging and particle associated residence times in the water column are overall higher in surface water compared to bottom water (table 5.4). This decrease in residence times with increasing water depth is also reflected in a higher scavenging and removal rate and in bottom water, probably due to higher particle concentration resulting from resuspension events. These findings agree with those of Kersten et al. (1998) who also

found lower scavenging residence time in the bottom water of the Mecklenburg Bay. The particle concentrations of this study, however, are only slightly enhanced at station 23.b and 23.o (table 5.4). At station 23.c the TPM concentration even decreases towards the bottom. This small increase or decrease in TPM concentration in the bottom water column is rather in contrast to the assumptions of lower scavenging and particle-associated residence time with increasing particle concentration and cannot be the only explanation. Turnewitsch and Graf (2003) and Forster et al. (2009) found that the organic matter content in the near bottom water column of the south-western Baltic tends to be low and the mineral and lithogenic fractions are increased which indicated transport of sediment particles in the water column. In the presented study, the particulate organic content of the water samples is also lower in the bottom water (see appendix Table VII) which indicated an increasing fraction of sediment particles in the bottom water column. According to the experiments in section 3 it can also be speculated that resuspended sediment particles with a large surface could have a higher ^{234}Th uptake potential which would lead to a higher scavenging rate in bottom water. This is in agreement with scavenging rates in table 5.4 which shows higher values for the bottom water column. The increasing scavenging rates would in turn lead to decreasing residence time of dissolved ^{234}Th in bottom water column compared to the upper water column. On the other hand particles with a high ^{234}Th uptake potential (in this case sediment particles) might also indirectly increase the scavenging rate but also the $^{234}\text{Th}_p$ removal rates due to ballasting effect of mineral particles (Armstrong et al., 2001).

It is concluded that the decreasing particle-associated residence time and the increasing $^{234}\text{Th}_p$ removal rate in bottom water column could be due to both the higher ^{234}Th uptake potential of sediment particles and the ballasting effect of the resuspended mineral particles. Therefore, particles with a higher surface area resuspended in the water column might influence the ^{234}Th scavenging rate and therefore indirectly affects the residence time.

5.4.4 ^{234}Th adsorption varying in hydrodynamic regimes and different sediment types

According to the results of the ^{234}Th -resuspension-deposition experiment the ^{234}Th flux during resuspension seems to be highest at station 23.o, but the particle fluxes are also highest at this station (figure 5.10). This strongly indicates that the ^{234}Th fluxes during the resuspension-phase are an effect of the total particle concentration. The higher the

particle concentration in suspension, the higher the ^{234}Th fluxes. This is supported by a strong linear correlation between the particle concentration and the ^{234}Th fluxes as shown in figure 5.15. The red dot represents the value during significant erosion conditions of

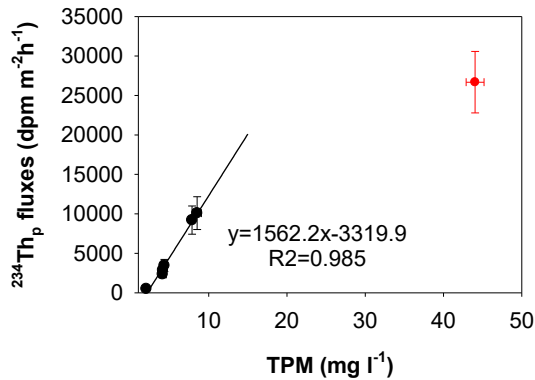


Figure 5.15: Linear correlation between the particulate ^{234}Th flux and the total particulate matter (TPM) concentration of the resuspension phase of the resuspension-deposition-experiment. The red dot is not included into the regression due to an expected saturation in ^{234}Th adsorption.

station 23.0 and is not included into the regression. Here the effect of adsorption saturation can be assumed. The particle surface is saturated in ^{234}Th and no more ^{234}Th can be absorbed. This also explains the low $\log K_d$ value of this station (figure 5.11). According to the finding in figure 5.15 the ^{234}Th fluxes seems to depend only on the

particle concentration and a particle surface effect of the sediments cannot be estimated. In this case, it would mean that the ^{234}Th uptake potential of the suspended material is similar at all stations. This is in contrast to

the findings of section 3.3.4, where particles with higher surface area showed higher ^{234}Th uptake capacity. However, as discussed in section 5.4.1, all sediment types showed a strongly developed fluffy layer at the surface of the sediment. Therefore, it can be assumed that only the fluffy layer was resuspended, which shows a very similar ^{234}Th adsorption behaviour due to the similar chemical composition and therefore similar particle properties. This assumption is supported by the very similar decreasing rates of the particle concentration (figure 5.9) during the deposition phase. According to the varying sinking properties, it is expected that the fine sediment enhanced in organic material at station 23.0 remains very long in suspension compared to the quartz particles at station 23.b and 23.c. This could not be observed, which indicated that the resuspended material was very consistent in the sinking behaviour.

According to the findings in section 3.3.4 it is expected that also the sediment types varying in surface area and/or ^{234}Th uptake potential could show variations in $\log K_d$. However, the $\log K_d$ of figure 5.11 shows no significant differences between the stations which supports the assumption that only fluff material was resuspended during the experiment. It is speculated that sediment particles with expected varying surface areas were not taken into account. In addition, no varying $\log K_d$ values between initial resuspension and erosive flow conditions can be observed. This indicates that the ^{234}Th adsorption behaviour in different hydrodynamic conditions seem to be very similar.

According to the experimental findings in this study it can be concluded that the fluff material shows an enhanced mobility in particle exchange processes at the sediment-water interface than previously expected. This leads to a high spatial redistribution of material in the study area. Therefore, it can be assumed that during moderate near bottom current velocities in the Mecklenburg bay, where only fluffy material is resuspended, no differences in ^{234}Th uptake potential can be observed between different sediment types due to the expected varying composition and properties of the resuspended material. However, it is conceivable that during very strong storm events large amounts of the underlying sediment material are resuspended which could lead to an increasing ^{234}Th uptake potential in the bottom water column of areas covered with clay minerals compared to areas consisting mainly of quartz sediment. Nevertheless, it has to be taken into account that the fluffy layer can be very different in composition and surface area compared to the pelagic particles which could change the adsorption condition for ^{234}Th in the bottom water column. According to the experimental findings in this study ^{234}Th shows no varying adsorption behaviour for different hydrodynamic regimes.

5.4.5 The transport of ^{234}Th from the water column to the sediment

The $^{234}\text{Th}/^{238}\text{U}$ disequilibrium is primarily used for the determination of particle export from the upper water column. To calculate the fluxes of ^{234}Th , an expression of ^{234}Th activity with time ($\partial^{234}\text{Th}/\partial t$) is required. Based on Owens et al. (2015) the following equations can be used to describe ^{234}Th fluxes:

$$\frac{\partial^{234}\text{Th}}{\partial t} = \lambda_{234}({}^{238}\text{U} - {}^{234}\text{Th}_{\text{tot}}) - P + V = 0 \quad (5.12)$$

, where ^{238}U and $^{234}\text{Th}_{\text{tot}}$ is the activity of ^{238}U and total ^{234}Th , λ_{234} is the decay constant of ^{234}Th , V is the sum of advective and vertical diffusive fluxes of ^{234}Th and P is the export of ^{234}Th on sinking particles. In a steady state system, it is assumed that $\partial^{234}\text{Th}/\partial t$ is equal to zero. A steady state system can be assumed in the presented case because of the continuity of the pronounced disequilibria throughout the water column and the absence of strong activity gradients between the stations. In periods of significant ^{234}Th changes, e.g. during phytoplankton blooms, the non-steady state effects would become more important. However, the samples were taken during one day of the cruise; dramatic

changes in ^{234}Th activities cannot be expected. In addition, a non-steady state would require sampling of ^{234}Th in different time spans, which was not possible on this cruise. Due to the absence of clear horizontal gradients of ^{234}U , $^{234}\text{Th}_d$ and $^{234}\text{Th}_p$ throughout the water column (figure 5.12), the horizontal advective transport as well as the horizontal turbulent diffusion can be neglected.

Based on the equation 5.13 a cumulative downward flux, P_{Th} , of particle associated ^{234}Th towards the sediment was calculated according to Forster et al. (2009):

$$P_{\text{Th}} = \lambda_{234} \int_0^z ({}^{238}\text{U} - {}^{234}\text{Th}_{\text{tot}}) dz \quad (5.13)$$

The cumulative downward flux is based on a simple box model which is describe in figure 5.12.

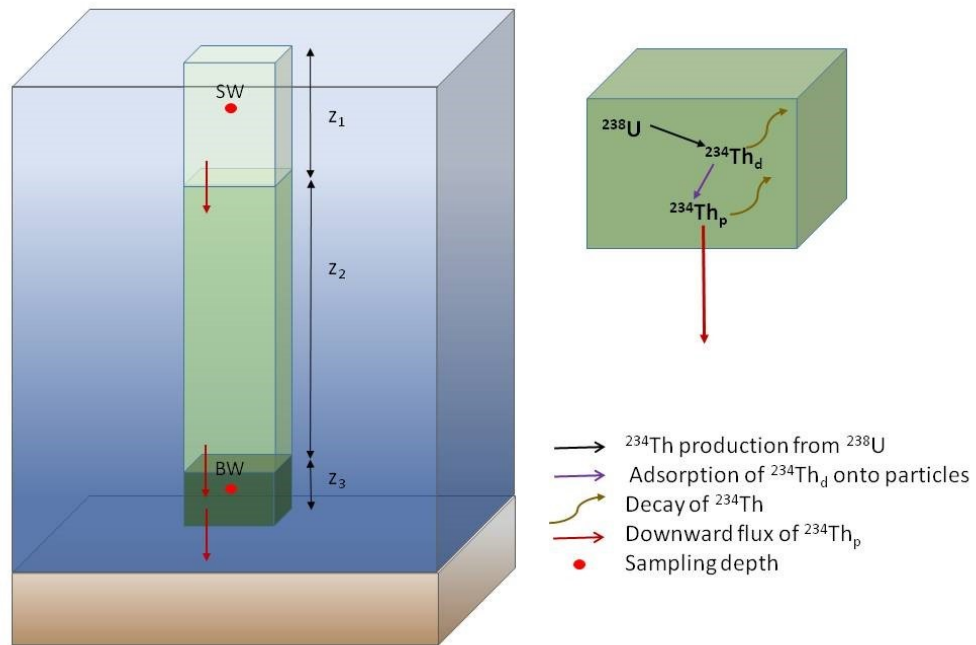


Figure 5.16: Scheme of the simple box model used for the calculation of ^{234}Th downward fluxes toward the sediment. The water column is divided into 3 boxes based on the density gradient of figure 5.7. Z_{i-3} indicates the layer thickness of the box. The red arrow represents the downward export fluxes. SW and BW represents the surface water and bottom water sampling depth. The green box illustrates factors that control the ^{234}Th distribution in each box.

Due to the relatively sparse sampling resolution in the water column (two sampling depth) (table 5.1), the applied box model consisted of 3 boxes. The boxes are defined according to the density depth profile in figure 5.7, where a mixed surface layer to 8 m was observed, followed by a strong density gradient down to ~ 1.5 mab. Therefore, the surface box (z_1) is defined from the surface (z_0) to 8 m below the surface (z_{8m}); the mid box (z_2) is

located between 8m water depth (z_{8m}) and 1.5 m above bottom ($z_{1.5mab}$) and the bottom water box (z_3) from 1.5 mab ($z_{1.5mab}$) to the seafloor (z_{max}). The surface water- and bottom water sampling depth (SW, BW) are included in the surface water box i.g. bottom water box. The mid box consists of the activity gradient of the SW and BW. In each box the ^{234}Th distribution is controlled by the production of $^{234}\text{Th}_d$ from the decay of ^{238}U ; the adsorption of $^{234}\text{Th}_d$ onto particles; the decay of $^{234}\text{Th}_p$ and $^{234}\text{Th}_d$ itself and the export of settling particles out of the box (figure 5.16, green box). Therefore, the cumulative export flux comprises the export flux of the overlying boxes. By multiplying the ^{234}Th fluxes in the water column with ratios of TPM to $^{234}\text{Th}_p$ the export of TPM from a given box of water can be calculated. The results of cumulative ^{234}Th and TPM fluxes at the three stations are shown in figure 5.17.

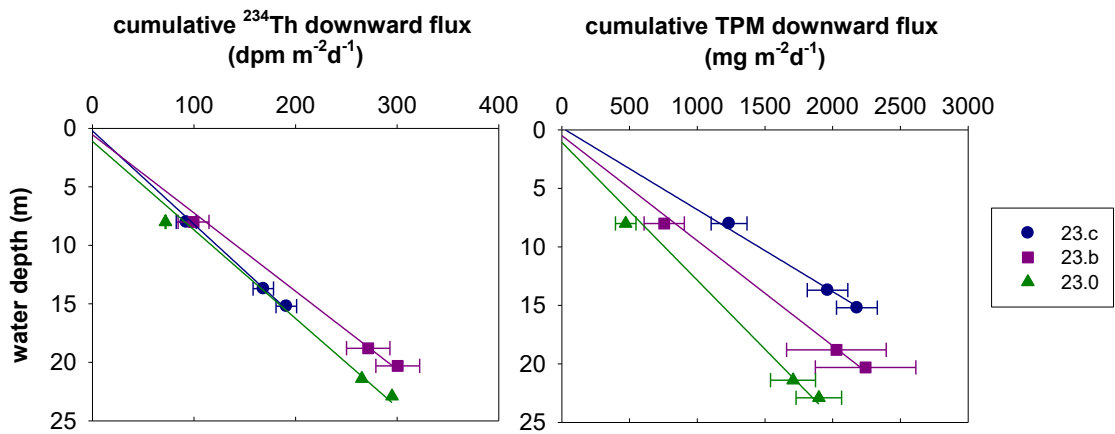


Figure 5.17: Cumulative ^{234}Th und total particulate matter (TPM) downward flux in the water column of three stations in the Mecklenburg Bay. The errors are based on the error propagation of SD errors of ^{234}Th activities and TPM concentration.

Both the ^{234}Th as well as the TPM fluxes increase almost linearly towards the sediment. The increase of cumulative ^{234}Th flux per meter depth is very similar at all stations and is highest at station 23.b ($16.3 \text{ dpm m}^{-2}\text{d}^{-1}$) followed by 23.0 ($15 \text{ dpm m}^{-2}\text{d}^{-1}$) and 23.c ($13.7 \text{ dpm m}^{-2}\text{d}^{-1}$). This indicates similar particle dynamics in the study area. The overall increasing export fluxes from the surface to the sediment can be explained by the increasing fraction of sediment particles to the TPM pool with increasing water depth. As already discussed in section 3.3.4 and 5.4.3 sediment particles show higher surface area which can lead to increasing ^{234}Th uptake potential. On the other hand, it is known that increasing sediment fractions in the water column result in higher settling velocities (e.g. Leipe et al., 2000) and the minerals act as ballast for POC rich particles (Armstrong et al., 2001; Gustafsson et al., 2006 and references therein). Both, the high surface area of the particles and the ballasting effect, can be responsible for increasing ^{234}Th fluxes towards the sediment.

The increasing cumulative TPM flux per meter decreases with increasing distance to the coast from 131.1 mg m⁻²d⁻¹ at station 23.c to 95.7 mg m⁻²d⁻¹ at station 23.o. This is related to the generally increasing TPM concentration from station 23.o to 23.c (table 5.4), probably due to the increasing influence of the shallow water areas.

The observed cumulative downward ²³⁴Th and TPM fluxes of this study are somewhat lower compared to estimated values of Forster et al. (2009) in the south-western Baltic Sea. This can be explained by the relatively high ²³⁴Th/²³⁴U disequilibria compared to the findings of Forster et al. (2009) as discussed in section 5.4.2.

The inventories of sedimentary ²³⁴Th_{ex} can be converted into the depositional flux by using the equation 5.13 in which z_{sed} represents the sediment depth (Th_{sed} = U_{sed}). The term (²³⁸U - ²³⁴Th_{tot}) is substituted by the inventory of ²³⁴Th_{ex}. The respective depositional fluxes of station 23.c, 23.b and 23.o are 69.2, 60.6 and 37.8 dpm m⁻²d⁻¹. This is ~3 - 9 times lower compared to the water column-derived cumulative ²³⁴Th fluxes near the seafloor of 190.9 ± 10.1 dpm m⁻²d⁻¹ at station 23.c, 295 ± n.d. dpm m⁻²d⁻¹ at station 23.o and 300.6 ± 21.5 dpm m⁻²d⁻¹ at station 23.b (figure 5.17). Forster et al. (2009) reported depositional fluxes in the Mecklenburg Bay based on measurements of Kersten et al. (2005) of 8340 and 11100 dpm m⁻²d⁻¹ which are ~120-300 times higher compared to the results presented in this study. Such strong differences are related to the generally significant lower ²³⁴Th_{ex} values in this study (0.02 - 0.73 dpm g⁻¹, figure 5.13 and 5.14) compared to Kersten et al. (2005) (0.13- 4.68 dpm g⁻¹). It can be assumed that methodical variations and natural variabilities are the major reasons for this discrepancy. Kersten et al. (2005) extracted ²³⁴Th in a concentrated HF/HClO₄/HNO₃ acid mixture. Probably the total dissolution of the sediment could result in higher extraction efficiency. As described in section 5.2.5, Siddeeg et al. (2014) found specific activities of ²³⁴Th extracted by leaching, relative to total dissolution, in a range of 30 - 75 %. In the presented case the extraction efficiency compared to Kersten et al. (2005) was just ~16 %. Therefore, a final answer why these strong discrepancies in the same area exist cannot be given at this stage.

The strong discrepancy between the water column-derived ²³⁴Th flux and the sediment-derived ²³⁴Th flux (water >> sediment) can also be explained by the strong mobility of the fluffy layer. Based on the results, it would mean that more ²³⁴Th reaches the seafloor as can be effectively found in the sediment in form of ²³⁴Th_{ex}. It is assumed that a large fraction of settled ²³⁴Th_p is related to recently sedimented material, which covered the sediment in form of the fluffy layer. As already discussed in section 5.4.1 and 5.4.4, this material can be resuspended easily. Therefore, it is assumed that the fluffy material is in permanent exchange with the bottom water column and does not remain a very long time

at the sediment surface. This would also explain the low sediment residence time (table 5.4). In summary, this indicates very dynamic exchange processes at the sediment-water interfaces, which is typical for highly dynamic coastal water systems.

It can be concluded that the discrepancy between the water column-derived ^{234}Th flux and the sediment-derived ^{234}Th flux is a result of both, methodical uncertainties during the leaching process and natural variability due to the presence of a fluffy layer which lead to a highly dynamic particle exchange at the sediment-water-interface.

5.4.6 Particle reworking in the sediment

The particle residence time in the sediment also characterises the length of time that sediment remains within the observed sediment depth. The residence time of the excess ^{234}Th inventory is highest at station 23.c followed by 23.o and 23.b (table 5.4). Together with the low sediment mixing coefficients (D_b) of $0.64 \text{ cm}^2 \text{ y}^{-1}$ at station 23.c (figure 5.14) it can be assumed that the particle reworking is reduced at this station compared to the other stations which leads to a higher residence time of particle-associated ^{234}Th . Based on sediment data of sandy sediment habitat of the south-western Baltic sea, Gogina et al. (2016) reported that the benthic community is dominated by Hydrobiidae, *Pygospio elegans* and *Cerastoderma glaucum*. This species are known to live on the sediment surface or within the 0 - 4 cm sediment depth (Gogina and Zettler, 2010; Urban-Malinga et al., 2014). This agrees with the found $^{234}\text{Th}_{\text{ex}}$ in the upper 3 cm of the sediment. According to the results of this study (figure 5.14 and table 5.4) it can be concluded that station 23.b and 23.o are highly dynamic in sediment reworking. The distinct subsurface maxima of excess ^{234}Th indicate intensive non local particle transport into deeper sediment layer which are typical for deep borrow polychaetes like *Scoloplos amiger* and bivalve like *Arctica islandica* (Gogina et al., 2010). In the deeper part of the Mecklenburg Bay Gogina et al. (2016) postulated a community in the sediment that is dominated by *Diastylis* sp., *Corbula gibba*, *Dipolydora quadrilobata*, *Arctica islandica*, *Aricidea suecica* and *Abra alba*. While e.g. *C. gibba* and *Diastylis* sp. are shallow burrowing species, *A. islandica* is a very deep borrowing species which is very abundant in the deeper parts of the Mecklenburg bay (Gogina and Zettler, 2010; Darr et al., 2013). *A. islandica* is known to be a mobile deposit feeder which feeds below the surface and passes material to deeper sediment layers by burrowing (Taylor, 1976). At station 23.b some shells of *A. islandica* is observed, therefore it can be assumed that this bivalve could be responsible for the strong particle reworking at this station.

SUMMARY AND CONCLUSION

The object of this study is to deduce factors controlling ^{234}Th adsorption and to describe the influence for the application of ^{234}Th as particle tracer. Both, laboratory experiments and field measurements were conducted to investigate ^{234}Th adsorption behaviour onto particles and colloids as well as on different sediment types. These findings were applied to interpret the ^{234}Th distribution at three stations in the Mecklenburg Bay, south-western Baltic Sea.

In laboratory experiments, the adsorption of ^{234}Th onto different natural particles with respect to particle surface and quality was investigated. Therefore, different organic coated particles such as *Rhodomonas* spp., *Surirella* spp. and *Synechococcus* spp.; and the mineral surface of the fine sediment fraction $<100\mu\text{m}$ were used. According to the particle concentration-based $\log K_d$ values, most ^{234}Th is associated to the inorganic mineral surface area, followed by the organic coated particles. However, this trend is reversed when the particle surface area of $\log K_A$ is considered, where the organic coated particles of *Rhodomonas* spp. and *Surirella* spp. demonstrate a higher ^{234}Th uptake potential. This finding supports the assumption of preferential ^{234}Th adsorption to organic particles. It can be speculated that differences in ^{234}Th adsorption between the organic coated particles result from the variations in surface composition, due to varying functional properties. It is concluded that ^{234}Th uptake potential strongly depends on both, the composition as well as the surface area of the particles. Therefore, variations in particle and carbon fluxes which resulted from the $^{234}\text{Th}/^{238}\text{U}$ disequilibria, are not only caused by the chemical composition due to more or less efficient aggregation or sinking behaviour, but also from the varying uptake potential of different surface area of the particles. For instance, this could be important for the investigation of particle dynamics near the seafloor or areas of strong terrestrial influence, where particles with a large ^{234}Th uptake potential are presented. At similar particle concentration, as in the surface water, this could lead to an increasing ^{234}Th uptake onto these particles which would generate a larger $^{234}\text{Th}/^{238}\text{U}$ disequilibrium. The calculation of fluxes based on these $^{234}\text{Th}/^{238}\text{U}$ disequilibria would virtually generate a higher ^{234}Th and particle load in bottom waters.

Overall, the presented results concerning the adsorption behaviour of ^{234}Th onto natural particles highlight the importance of the particle's surface area and quality in ^{234}Th scavenging processes. The strong positive correlation between $\log K_A$ and particulate $\text{C}/^{234}\text{Th}$ ratio indicate that there is a relationship between the chemical composition and the particle surface. The particle surface area seems to be more crucial in ^{234}Th adsorption

than the particle concentration. Nevertheless, depending on the scientific question being asked, different parameters become appreciated. For investigation of the role of different particle types in ^{234}Th scavenging, the $\log K_d$ and the percentage of particulate ^{234}Th is not sufficient.

However, it should be noted that the differences in adsorption to different types of particles were investigated only for single particles rather than the total spectrum of natural particles found in the ocean. For this reason, additional studies are required to evaluate a broader range of particle types, especially with respect to investigate the preferential adsorption of ^{234}Th where two or more different particle mixtures are presented. However, the separation of the particle types and the inter-particulate effect will be challenging.

In order to determine the influence of colloidal material in ^{234}Th scavenging, the ^{234}Th adsorption onto the fine sediment fraction in presence and absence of one commercial available polysaccharide type and the natural colloidal fraction was investigated. In presence of one polysaccharide type the adsorption onto the mineral surface is slightly increased. However, in presence of the natural colloidal fraction, a significant enhanced ^{234}Th adsorption onto the particles is observed. It is concluded that not only one fraction is responsible for the association of ^{234}Th onto particles. More likely the whole spectrum of colloidal material leads to an enhanced adsorption of ^{234}Th to mineral particles. The increased ^{234}Th adsorption onto the mineral surface is likely related to coating the particles with the natural colloidal material which could change the surface properties and reactivity. According to the presented results, it can be concluded that colloids likely act as an intermediate in ^{234}Th scavenging which can enhance ^{234}Th uptake potential of less reactive, inorganic surfaces. It is conceivable that differences in colloidal composition leads to varying ^{234}Th uptake potential. To determine the differences in ^{234}Th adsorption depending on colloidal composition additional, comparative experiments of varying colloidal material of different oceanic region (e.g. estuaries versus open ocean) are needed. Such investigations would be important for the interpretation and understanding of ^{234}Th based data on a molecular level.

To investigate the role of varying functional group composition in ^{234}Th adsorption, experiments with different polysaccharides, which represents a major fraction of the colloidal pool, were conducted. A strong correlation between the amount of sulphated functional groups and the ^{234}Th activity is observed. This indicates that sulphated groups are involved in ^{234}Th uptake on molecular level. However significant differences in $\log K_d$ between the polysaccharides types could not be observed, probably due to the reduced pH

during the experiments with deionised water. Therefore, it cannot be excluded that the results are affected by errors. A final conclusion of functional groups which are involved in ^{234}Th adsorption cannot be given at this stage. Additional experiments should clarify the role of varying fractions of the colloidal pool (e.g. amino acids and humic acids) and the influence of functional group composition in ^{234}Th uptake. According to the presented results, it is strongly recommended to consider the experimental conditions, especially the pH level.

At three stations in the Mecklenburg Bay, Baltic Sea, a strong increase of ^{234}Th and particle fluxes and decrease of the particle-associated residence times towards the sediment can be observed. This seems to be related to the increasing fraction of sediment and/or fluff material in the bottom water column. On the one hand this leads to an enhanced ballasting effect due to increasing sinking velocities of sediment material. On the other hand, it can be assumed that sediment particles show a larger surface area compared to pelagic particles as already described above. It can be concluded that both, the presence of sediment particles with enhanced sinking behaviour, but also the increased ^{234}Th uptake potential due to the larger surface areas could lead to the increased ^{234}Th and particle fluxes in the bottom water column of the study area.

In laboratory experiments the adsorption of ^{234}Th onto different sediment types and in varying hydrodynamic regimes were investigated. Significant differences in ^{234}Th adsorption between varying flow conditions could not be observed. This indicates that the hydrodynamic regime does not play a crucial role in ^{234}Th scavenging. In addition, the ^{234}Th uptake potential at different sediment types are very similar, most likely due to the overall pronounced fluffy layer on top of the sediment surface which was resuspended. The actual sediment surface does not seem to be resuspended during the experiments. Therefore, it is assumed that moderate flow conditions in the study area leads only to resuspension of the fluffy layer while the underlying sediment remains relatively unaffected. In addition, the calculated ^{234}Th fluxes down to the sediment are some orders of magnitude higher compared to the ^{234}Th depositional flux which is necessary to supply the ^{234}Th inventory in the sediment. Amongst analytical problems in determination of sedimentary ^{234}Th , the fluffy layer could also be responsible for the strong discrepancy. According to the experimental and field observation, it can be concluded that the presence of a fluffy layer enhanced the mobility of particles and it seems to be in permanent exchange with the overlying water column. Due to the high hydrodynamic condition at the sediment water interface in coastal water, this material does not remain

very long time at the sediment surface. Therefore, the fluff material seems to play a more important role in particle and ^{234}Th dynamic in the study area than previously expected.

The investigation of the ^{234}Th distributions in the study area in relation to the experimental findings described above provides information about the factors that control ^{234}Th scavenging and the applications of ^{234}Th as particle tracer. The results could help to understand ^{234}Th adsorption processes which would be useful for the use of ^{234}Th as tracer for particle dynamics.

REFERENCES

- Aarnos, H., Ylostalo, P. and Vahatalo, A.V. (2012) Seasonal phototransformation of dissolved organic matter to ammonium, dissolved inorganic carbon, and labile substrates supporting bacterial biomass across the Baltic Sea. *Journal of Geophysical Research-Biogeosciences* 117.
- Allredge, A.L. and Jackson, G.A. (1995) Preface: Aggregation in marine system. *Deep-Sea Research Part II* 42, 1-7.
- Aller, R.C. and Cochran, K.J. (1976) $^{234}\text{Th}/^{238}\text{U}$ disequilibrium in near-shore sediment: Particle reworking and diagenetic time scales. *Earth and Planetary Science Letters* 29, 37-50.
- Alvarado Quiroz, N.G., Hung, C.C. and Santschi, P.H. (2006) Binding of thorium(IV) to carboxylate, phosphate and sulfate functional groups from marine exopolymeric substances (EPS). *Marine Chemistry* 100, 337-353.
- Amon, R.M.W. and Benner, R. (1994) Rapid cycling of high-molecular-weight dissolved organic matter in the ocean. *Nature* 369, 549-552.
- Anderson, R.F. and Fleer, A.P. (1982) Determination of natural actinides and plutonium in marine particulate material. *Analytical Chemistry* 54, 1142-1147.
- Andersson, P.S., Wasserburg, G.J., Chen, J.H., Papanastassiou, D.A. and Ingri, J. (1995) ^{238}U - ^{234}U and ^{232}Th - ^{230}Th in the Baltic Sea and in river water. *Earth and Planetary Science Letters* 130, 217-234.
- Armstrong, R.A., Lee, C., Hedges, J.I., Honjo, S. and Wakeham, S.G. (2001) A new, mechanistic model for organic carbon fluxes in the ocean based on the quantitative association of POC with ballast minerals. *Deep Sea Research Part II: Topical Studies in Oceanography* 49, 219-236.
- Azetsu-Scott, K. and Niven, S.E.H. (2005) The role of transparent exopolymer particles (TEP) in the transport of ^{234}Th in coastal water during a spring bloom. *Continental Shelf Research* 25, 1133-1141.
- Bacon, M.P. and Anderson, R.F. (1982) Distribution of thorium isotopes between dissolved and particulate forms in the deep-sea. *Journal of Geophysical Research Oceans* 87, 2045-2056.
- Bacon, M.P. and van der Loeff, M.M.R. (1989) Removal of Th-234 by scavenging in the bottom nepheloid layer of the ocean. *Earth and Planetary Science Letters* 92, 157-164.
- Bale, A.J. and Kenny, A.J. (2005) Sediment analysis and seabed characterization. In: *Methods for the study of marine benthos*. Eleftheriou, A., McIntyre, A. Blackwell Publishing.
- Baskaran, M., Santschi, P.H., Benoit, G. and Honeyman, B.D. (1992) Scavenging of Thorium isotopes by colloids in seawater of the Gulf of Mexico. *Geochimica et Cosmochimica Acta* 56, 3375-3388.

References

- Baskaran, M., Swarzenski, P.W. and Porcelli, D. (2003) Role of colloidal material in the removal of ^{234}Th in the Canada basin of the Arctic Ocean. *Deep Sea Research Part I: Oceanographic Research Papers* 50, 1353-1373.
- Bauer, J.E., Cai, W.-J., Raymond, P.A., Bianchi, T.S., Hopkinson, C.S. and Regnier, P.A.G. (2013) The changing carbon cycle of the coastal ocean. *Nature* 504, 61-70.
- Bauer, J.E. and Carlson, C.A. (2002) Chapter 8 - Carbon Isotopic Composition of DOM A2 - Hansell, Dennis A, Biogeochemistry of Marine Dissolved Organic Matter. Academic Press, San Diego, pp. 405-453.
- Baumann, M.S., Moran, S.B., Kelly, R.P., Lomas, M.W. and Shull, D.H. (2013) ^{234}Th balance and implications for seasonal particle retention in the eastern Bering Sea. *Deep-Sea Research Part II: Topical Studies in Oceanography* 94, 7-21.
- Beaulieu, S.E. (2003) Resuspension of phytodetritus from the sea floor: A laboratory flume study. *Limnology and Oceanography* 43, 1235-1244.
- Bobertz, B., Harff, J. and Bohling, B. (2009) Parameterisation of clastic sediments including benthic structures. *Journal of Marine Systems* 75, 371-381.
- Bohling, B. (2005) Estimating the risk for erosion of surface sediments in the Mecklenburg Bight (south-western Baltic Sea). *Baltica* 19, 3-12.
- Boryto, A. and Skwarzec, B. (2014) Activity disequilibrium between ^{234}U and ^{238}U isotopes in natural environment. *Journal of Radioanalytical and Nuclear Chemistry* 300, 719-727.
- Brown, E. (2005) Nuclear Data Sheet 104, 427. National Nuclear Data Center, Brookhaven National Laboratory.
- Brunauer, S., Emmett, P.H. and Teller, E. (1938) Adsorption of gases in multimolecular layers. *Journal of the American Chemical Society* 60, 309-319.
- Buck, K.N., Selph, K.E. and Barbeau, K.A. (2010) Iron-binding ligand production and copper speciation in an incubation experiment of Antarctic Peninsula shelf waters from the Bransfield Strait, Southern Ocean. *Marine Chemistry* 122, 148-159.
- Buesseler, K.O., Andrews, J.A., Hartman, M.C., Belostock, R. and Chai, F. (1995) Regional estimates of the export flux of particulate organic carbon derived from thorium-234 during the JGOFS EqPac program. *Deep Sea Research Part II: Topical Studies in Oceanography* 42, 777-804.
- Buesseler, K.O., Bacon, M.P., Cochran, J.K. and Livingston, H.D. (1992) Carbon and nitrogen export during the JGOFS North-Atlantic Bloom Experiment estimated from ^{234}Th : ^{238}U disequilibria. *Deep-Sea Research Part A* 39, 1115-1137.
- Buesseler, K.O., Benitez-Nelson, C.R., Moran, S.B., Burd, A., Charette, M., Cochran, J.K., Coppola, L., Fisher, N.S., Fowler, S.W., Gardner, W.D., Guo, L.D., Gustafsson, O., Lamborg, C., Masque, P., Miquel, J.C., Passow, U., Santschi, P.H., Savoye, N., Stewart, G. and Trull, T. (2006) An assessment of particulate organic carbon to Thorium-234 ratios in the ocean and their impact on the application of ^{234}Th as a POC flux proxy. *Marine Chemistry* 100, 213-233.

- Charette, M.A. and Moran, S.B. (1999) Rates of particle scavenging and particulate organic carbon export estimated using ^{234}Th as a tracer in the subtropical and equatorial Atlantic Ocean. *Deep Sea Research Part II: Topical Studies in Oceanography* 46, 885-906.
- Chase, Z., Anderson, R.F., Fleisher, M.Q. and Kubik, P.W. (2002) The influence of particle composition and particle flux on scavenging of Th, Pa and Be in the ocean. *Earth and Planetary Science Letters* 204, 215-229.
- Chen, J.H., Edwards, R.L. and Wasserburg, G.J. (1986) ^{238}U , ^{234}U and ^{232}Th in Seawater. *Earth and Planetary Science Letters* 80, 241-251.
- Chuang, C.Y., Santschi, P.H., Ho, Y.F., Conte, M.H., Guo, L., Schumann, D., Ayranov, M. and Li, Y.H. (2013) Role of biopolymers as major carrier phases of Th, Pa, Pb, Po, and Be radionuclides in settling particles from the Atlantic Ocean. *Marine Chemistry* 157, 131-143.
- Chuang, C.Y., Santschi, P.H., Jiang, Y., Ho, Y.F., Quigg, A., Guo, L., Ayranov, M. and Schumann, D. (2014) Important role of biomolecules from diatoms in the scavenging of particle-reactive radionuclides of thorium, protactinium, lead, polonium, and beryllium in the ocean: A case study with *Phaeodactylum tricornutum*. *Limnology and Oceanography* 59, 1256-1266.
- Chuang, C.Y., Santschi, P.H., Wen, L.S., Guo, L., Xu, C., Zhang, S., Jiang, Y., Ho, Y.F., Schwehr, K.A., Quigg, A., Hung, C.C., Ayranov, M. and Schumann, D. (2015) Binding of Th, Pa, Pb, Po and Be radionuclides to marine colloidal macromolecular organic matter. *Marine Chemistry* 173, 320-329.
- Coale, K.H. and Bruland, K.W. (1985) ^{234}Th : ^{238}U disequilibria within the California Current. *Limnology and Oceanography* 30, 22-33.
- Cochran, J.K., Buesseler, K.O., Bacon, M.P. and Livingston, H.D. (1993) Thorium isotopes as indicators of particle dynamics in the upper ocean - results from the JGOFS North-Atlantic bloom experiment. *Deep-Sea Res. Part I-Oceanogr. Res. Pap.* 40, 1569-1595.
- Cochran, J.K. and Masqué, P. (2003) Short-lived U/Th series radionuclides in the ocean: Tracers for scavenging rates, export fluxes and particle dynamics. *Reviews in Mineralogy and Geochemistry* 52, 461-492.
- Cochran, J.K., Miquel, J.C., Armstrong, R., Fowler, S.W., Masqué, P., Gasser, B., Hirschberg, D., Szlosek, J., Rodriguez y Baena, A.M., Verdeny, E. and Stewart, G.M. (2009) Time-series measurements of ^{234}Th in water column and sediment trap samples from the northwestern Mediterranean Sea. *Deep-Sea Research Part II: Topical Studies in Oceanography* 56, 1487-1501.
- Cornell, R.M. (1992) Adsorption behaviour of cesium on marl. *Clay Minerals* 27, 363-371.
- Cornell, R.M. (1993) Adsorption of cesium on minerals: A review. *Journal of Radioanalytical and Nuclear Chemistry Articles* 171, 483-500.

References

- Darr, A., Gogina, M. and Zettler, M.L. (2013) Detecting hot-spots of bivalve biomass in the south-western Baltic Sea. *Journal of Marine Systems* 134, 69-80.
- De Brouwer, J.F.C., Wolfstein, K. and Stal, L.J. (2002) Physical characterization and diel dynamics of different fractions of extracellular polysaccharides in an axenic culture of a benthic diatom. *European Journal of Phycology* 37, 37-44.
- Decho, A.W. (1990) Microbial exopolymer secretions in ocean environments: their role(s) in food webs and marine processes. *Oceanography and Marine Biology: An Annual Review* 28, 73-153.
- Dietz, M. (2015) Der einfluss von Markophyten auf die Erodierbarkeit eines küstennahen Sedimentes. Master Thesis. Department of marine sciences, University of Rostock. 84.
- Eisma, D. (1986) Flocculation and de-flocculation of suspended matter in estuaries. *Netherlands Journal of Sea Research* 20, 183-199.
- Evangelidou, N., Florou, H. and Scoullou, M. (2011) POC and particulate ^{234}Th export fluxes estimated using $^{234}\text{Th}/^{238}\text{U}$ disequilibrium in an enclosed Eastern Mediterranean region (Saronikos Gulf and Elefsis Bay, Greece) in seasonal scale. *Geochimica et Cosmochimica Acta* 75, 5367-5388.
- Fisher, M.L., Allen, R., Luo, Y. and Curtiss III, R. (2013) Export of extracellular polysaccharides modulates adherence of the Cyanobacterium *Synechocystis*. *PLoS ONE* 8.
- Fleer, A.P. (1991) Updated determination of particulate and dissolved Thorium-234. In: *Marine Particles: Analysis and Characterization*. Hurd, D.C., Spencer, D.W. American Geophysical Union.
- Forster, S., Turnewitsch, R., Powilleit, M., Werk, S., Peine, F., Ziervogel, K. and Kersten, M. (2009) Thorium-234 derived information on particle residence times and sediment deposition in shallow waters of the south-western Baltic Sea. *Journal of Marine Systems* 75, 360-370.
- Gardea-Torresdey, J.L., Arenas, J.L., Francisco, N.M.C., Tiemann, K.J. and Webb, R. (1998) Ability of immobilized cyanobacteria to remove metal ions from solution and demonstration of the presence of metallothionein genes in various strains *Journal of Hazardous Substance Research* 1.
- Geibert, W. and Usbeck, R. (2004) Adsorption of thorium and protactinium onto different particle types: Experimental findings. *Geochimica et Cosmochimica Acta* 68, 1489-1501.
- Gerino, M., Aller, R.C., Lee, C., Cochran, J.K., Aller, J.Y., Green, M.A. and Hirschberg, D. (1998) Comparison of different tracers and methods used to quantify bioturbation during a spring bloom: ^{234}Th -Thorium, luminophores and chlorophyll-*a*. *Estuarine, Coastal and Shelf Science* 46, 531-547.
- Gogina, M., Glockzin, M. and Zettler, M.L. (2010) Distribution of benthic macrofaunal communities in the western Baltic Sea with regard to near-bottom environmental parameters. 1. Causal analysis. *Journal of Marine Systems* 79, 112-123.

- Gogina, M., Nygard, H., Blomqvist, M., Daunys, D., Josefson, A.B., Kotta, J., Maximov, A., Warzocha, J., Yermakov, V., Gräwe, U. and Zettler, M.L. (2016) The Baltic Sea scale inventory of benthic faunal communities. *ICES Journal of Marine Science* 73, 1196-1213.
- Gogina, M. and Zettler, M.L. (2010) Diversity and distribution of benthic macrofauna in the Baltic Sea: Data inventory and its use for species distribution modelling and prediction. *Journal of Sea Research* 64, 313-321.
- Gügi, B., Le Costaouec, T., Burel, C., Lerouge, P., Helbert, W. and Bardor, M. (2015) Diatom-specific oligosaccharide and polysaccharide structures help to unravel biosynthetic capabilities in diatoms. *Marine drugs* 13, 5993-6018.
- Guo, L., Chen, M. and Gueguen, C. (2002a) Control of Pa/Th ratio by particulate chemical composition in the ocean. *Geophysical Research Letters* 29, 22-21 - 22-24.
- Guo, L., Coleman Jr, C.H. and Santschi, P.H. (1994) The distribution of colloidal and dissolved organic carbon in the Gulf of Mexico. *Marine Chemistry* 45, 105-119.
- Guo, L., Santschi, P.H. and Baskaran, M. (1997) Interactions of thorium isotopes with colloidal organic matter in oceanic environments. *Colloids and Surfaces A: Physicochemical and Engineering Aspects* 120, 255-271.
- Guo, L.D., Hung, C.C., Santschi, P.H. and Walsh, I.D. (2002b) ^{234}Th scavenging and its relationship to acid polysaccharide abundance in the Gulf of Mexico. *Marine Chemistry* 78, 103-119.
- Gustafsson, Ö., Larsson, J., Andersson, P. and Ingri, J. (2006) The POC/ ^{234}Th ratio of settling particles isolated using split flow-thin cell fractionation (SPLITT). *Marine Chemistry* 100, 314-322.
- Hartnett, H.E., Keil, R.G., Hedges, J.I. and Devol, A.H. (1998) Influence of oxygen exposure time on organic carbon preservation in continental margin sediments. *Nature* 391, 572-575.
- Hayes, C.T., Anderson, R.F., Fleisher, M.Q., Vivancos, S.M., Lam, P.J., Ohnemus, D.C., Huang, K.-F., Robinson, L.F., Lu, Y., Cheng, H., Edwards, R.L. and Moran, S.B. (2015) Intensity of Th and Pa scavenging partitioned by particle chemistry in the North Atlantic Ocean. *Marine Chemistry* 170, 49-60.
- Hedges, J.I. and Keil, R.G. (1995) Sedimentary organic matter preservation: an assessment and speculative synthesis. *Marine Chemistry* 49, 81-115.
- Henderson, G.M., Heinze, C., Anderson, R.F. and Winguth, A.M.E. (1999) Global distribution of the ^{230}Th flux to ocean sediments constrained by GCM modelling. *Deep Sea Research Part I: Oceanographic Research Papers* 46, 1861-1893.
- Higgins, M.J., Crawford, S.A., Mulvaney, P. and Wetherbee, R. (2000) The topography of soft, adhesive diatom 'trails' as observed by atomic force microscopy. *Biofouling* 16, 133-139.

References

- Hillebrand, H., Dürselen, C.-D., Kirschtel, D., Pollinger, U. and Zohary, T. (1999) Biovolume calculation for pelagic and benthic microalgae. *Journal of Phycology* 35, 403-424.
- Hirose, K., Saito, T., Lee, S.H. and Gastaud, J. (2011) Vertical distributions of the strong organic ligand in the twilight zone of Southern Hemisphere Ocean particulate matter. *Progress in Oceanography* 89, 108-119.
- Hjulström, F. (1935) Studies of the morphological activity of rivers as illustrated by the River Fyris. Ph.D. Thesis. Geological Institute University of Uppsala. 306.
- Hoagland, K.D., Rosowski, J.R., Gretz, M.R. and Roemer, S.C. (1993) Diatom extracellular polymeric substances: Function, fine structure, chemistry, and physiology. *Journal of Phycology* 29, 537-565.
- Honeyman, B.D., Balistrieri, L.S. and Murray, J.W. (1988) Oceanic trace metal scavenging: the importance of particle concentration. *Deep Sea Research Part A. Oceanographic Research Papers* 35, 227-246.
- Honeyman, B.D. and Santschi, P.H. (1989) A Brownian-pumping model for oceanic trace metal scavenging: Evidence from Th isotopes. *Journal of Marine Research* 47, 951-992.
- Jähmlich, S., Lund-Hansen, L.C. and Leipe, T. (2002) Enhanced settling velocities and vertical transport of particulate matter by aggregation in the benthic boundary layer. *Geografisk Tidsskrift* 101, 37-49.
- Jensen, J.B., Bennike, O., Witkowski, A., Lemke, W. and Kuijpers, A. (1999) Early Holocene history of the southwestern Baltic Sea: The Ancylus Lake stage. *Boreas* 28, 437-453.
- Kaynar, Ü.H., Mehmet, A., Hiçsönmez, Ü. and Kaynar, S.Ç. (2015) Removal of thorium (IV) ions from aqueous solution by a novel nanoporous ZnO: Isotherms, kinetic and thermodynamic studies. *Journal of Environmental Radioactivity* 150, 145-151.
- Kersten, M., Leipe, T. and Tauber, F. (2005) Storm disturbance of sediment contaminants at a hot-spot in the Baltic sea assessed by ^{234}Th radionuclide tracer profiles. *Environmental Science and Technology* 39, 984-990.
- Kersten, M., Thomsen, S., Pribsch, W. and Garbe-Schönberg, C.-D. (1998) Scavenging and particle residence times determined from $^{234}\text{Th}/^{238}\text{U}$ disequilibria in the coastal waters of Mecklenburg Bay. *Applied Geochemistry* 13, 339-347.
- Kim, D., Choi, M.S., Oh, H.Y., Song, Y.H., Noh, J.H. and Kim, K.H. (2011) Seasonal export fluxes of particulate organic carbon from $^{234}\text{Th}/^{238}\text{U}$ disequilibrium measurements in the Ulleung Basin¹ (Tsushima Basin) of the East Sea¹ (Sea of Japan). *Journal of Oceanography* 67, 577-588.
- Köster, R. and Lemke, W. (1996) Morphologie und Bodenbedeckung. In: Meereskunde der Ostsee. Meereskunde der Ostsee. Springer.
- Kraemer, S.M., Duckworth, O.W., Harrington, J.M. and Schenkeveld, W.D.C. (2014) Metallophores and trace metal biogeochemistry. *Aquatic Geochemistry* 21, 159-195.

- Kretschmer, S., Geibert, W., Rutgers van der Loeff, M.M. and Mollenhauer, G. (2010) Grain size effects on $^{230}\text{Th}_{\text{xs}}$ inventories in opal-rich and carbonate-rich marine sediments. *Earth and Planetary Science Letters* 294, 131-142.
- Kretschmer, S., Geibert, W., Rutgers van der Loeff, M.M., Schnabel, C., Xu, S. and Mollenhauer, G. (2011) Fractionation of ^{230}Th , ^{231}Pa , and ^{10}Be induced by particle size and composition within an opal-rich sediment of the Atlantic Southern Ocean. *Geochimica et Cosmochimica Acta* 75, 6971-6987.
- Kuhrts, C., Fennel, W. and Seifert, T. (2004) Model studies of transport of sedimentary material in the western Baltic. *Journal of Marine Systems* 52, 167-190.
- Lalande, C., Moran, S.B., Wassmann, P., Grebmeier, J.M. and Cooper, L.W. (2008) ^{234}Th -derived particulate organic carbon fluxes in the northern Barents Sea with comparison to drifting sediment trap fluxes. *Journal of Marine Systems* 73, 103-113.
- Lampitt, R.S., Boorman, B., Brown, L., Lucas, M., Salter, I., Sanders, R., Saw, K., Seeyave, S., Thomalla, S.J. and Turnewitsch, R. (2008) Particle export from the euphotic zone: Estimates using a novel drifting sediment trap, ^{234}Th and new production. *Deep Sea Research Part I: Oceanographic Research Papers* 55, 1484-1502.
- Leipe, T., Kersten, M., Heise, S., Pohl, C., Witt, G., Liehr, G., Zettler, M. and Tauber, F. (2005) Ecotoxicity assessment of natural attenuation effects at a historical dumping site in the western Baltic Sea. *Marine Pollution Bulletin* 50, 446-459.
- Leipe, T., Loeffler, A., Emeis, K.C., Jaehmlich, S., Bahlo, R. and Ziervogel, K. (2000) Vertical patterns of suspended matter characteristics along a coastal-basin transect in the western Baltic Sea. *Estuarine, Coastal and Shelf Science* 51, 789-804.
- Lin, P., Chen, M. and Guo, L. (2015) Effect of natural organic matter on the adsorption and fractionation of thorium and protactinium on nanoparticles in seawater. *Marine Chemistry* 173, 291-301.
- Lin, P., Guo, L. and Chen, M. (2014) Adsorption and fractionation of thorium and protactinium on nanoparticles in seawater. *Marine Chemistry* 162, 50-59.
- Lund-Hansen, L.C., Laima, M., Mouritsen, K., Lam, N.N. and Hai, D.N. (2002) Effects of benthic diatoms, fluff layer, and sediment conditions on critical shear stress in a non-tidal coastal environment. *Journal of the Marine Biological Association of the United Kingdom* 82, 929-936.
- Lundkvist, M., Gangelhof, U., Lunding, J. and Flindt, M.R. (2007) Production and fate of extracellular polymeric substances produced by benthic diatoms and bacteria: A laboratory study. *Estuarine, Coastal and Shelf Science* 75, 337-346.
- Ma, H., Zeng, Z., He, J., Han, Z., Lin, W., Chen, L., Cheng, J. and Zeng, S. (2014) ^{234}Th -derived particulate organic carbon export in the Prydz Bay, Antarctica. *Journal of Radioanalytical and Nuclear Chemistry* 299, 621-630.

- Mari, X., Migon, C. and Nicolas, E. (2009) Reactivity of transparent exopolymeric particles: A key parameter of trace metal cycling in the lagoon of Nouméa, New Caledonia. *Marine Pollution Bulletin* 58, 1874-1879.
- Martin, M.J. (2007) Nuclear Data Sheets 108,1583. National Nuclear Data Center, Brookhaven National Laboratory.
- Miller, M.C., McCave, I.N. and Komar, P.D. (1977) Threshold of sediment motion under unidirectional currents. *Sedimentology* 24, 507-527.
- Moran, S.B. and Buesseler, K.O. (1992a) Short residence time of colloids in the upper ocean estimated from ^{238}U - ^{234}Th disequilibria. *Nature* 359, 221-223.
- Moran, S.B. and Buesseler, K.O. (1992b) Short residence time of colloids in the upper ocean estimated from ^{238}U - ^{234}Th disequilibria. *Nature* 359, 221-223.
- Murray, J.W., Young, J., Newton, J., Dunne, J., Chapin, T., Paul, B. and McCarthy, J.J. (1996) Export flux of particulate organic carbon from the central equatorial Pacific determined using a combined drifting trap - ^{234}Th approach. *Deep Sea Research Part II: Topical Studies in Oceanography* 43, 1095-1132.
- Myklestad, S.M., Skanoy, E. and Hestmann, S. (1997) A sensitive and rapid method for analysis of dissolved mono- and polysaccharides in seawater. *Marine Chemistry* 56, 279-286.
- Neilands, J.B. (1995) Siderophores: Structure and Function of Microbial Iron Transport Compounds *The Journal of Biological Chemistry* 270, 26723-26726.
- Niedermeyer, R.-O., Lampe, R., Janke, W., Schwarzer, K., Duphorn, K., Kliewe, H. and Werner, F. (2011) Die deutsche Ostseeküste. Sammling geologischer Führer. , Borntraeger.
- Nour, S., Burnett, W.C. and Horwitz, E.P. (2002) ^{234}Th analysis of marine sediments via extraction chromatography and liquid scintillation counting. *Applied Radiation and Isotopes* 57, 235-241.
- Obst, M., Dynes, J.J., Lawrence, J.R., Swerhone, G.D.W., Benzerara, K., Karunakaran, C., Kaznatcheev, K., Tyliszczak, T. and Hitchcock, A.P. (2009) Precipitation of amorphous CaCO_3 (aragonite-like) by cyanobacteria: A STXM study of the influence of EPS on the nucleation process. *Geochimica et Cosmochimica Acta* 73, 4180-4198.
- Ogawa, H. and Tanoue, E. (2003) Dissolved organic matter in oceanic waters. *Journal of Oceanography* 59, 129-147.
- Owens, S.A., Pike, S. and Buesseler, K.O. (2015) Thorium-234 as a tracer of particle dynamics and upper ocean export in the Atlantic Ocean. *Deep-Sea Research Part II: Topical Studies in Oceanography* 116, 42-59.
- Ozturk, S., Aslim, B., Suludere, Z. and Tan, S. (2014) Metal removal of cyanobacterial exopolysaccharides by uronic acid content and monosaccharide composition. *Carbohydrate Polymers* 101, 265-271.

References

- Passow, U. (2002a) Production of transparent exopolymer particles (TEP) by phyto- and bacterioplankton. *Marine Ecology Progress Series* 236, 1-12.
- Passow, U. (2002b) Transparent exopolymer particles (TEP) in aquatic environments. *Progress in Oceanography* 55, 287-333.
- Passow, U., Dunne, J., Murray, J.W., Balistrieri, L. and Alldredge, A.L. (2006) Organic carbon to ^{234}Th ratios of marine organic matter. *Marine Chemistry* 100, 323-336.
- Peine, F., Turnewitsch, R., Mohn, C., Reichelt, T., Springer, B. and Kaufmann, M. (2009) The importance of tides for sediment dynamics in the deep sea-Evidence from the particulate-matter tracer ^{234}Th in deep-sea environments with different tidal forcing. *Deep-Sea Res. Part I-Oceanogr. Res. Pap.* 56, 1182-1202.
- Pereira, S., Micheletti, E., Zille, A., Santos, A., Moradas-Ferreira, P., Tamagnini, P. and De Philippis, R. (2011) Using extracellular polymeric substances (EPS)-producing cyanobacteria for the bioremediation of heavy metals: Do cations compete for the EPS functional groups and also accumulate inside the cell? *Microbiology* 157, 451-458.
- Pierre, G., Zhao, J.M., Orvain, F., Dupuy, C., Klein, G.L., Graber, M. and Maugard, T. (2014) Seasonal dynamics of extracellular polymeric substances (EPS) in surface sediments of a diatom-dominated intertidal mudflat (Marennes-Oléron, France). *Journal of Sea Research* 92, 26-35.
- Pope, S.B. (2000) Turbulent Flows. Cambridge University Press, Cornell University, New York.
- Quigley, M.S., Santschi, P.H., Guo, L. and Honeyman, B.D. (2001) Sorption irreversibility and coagulation behavior of ^{234}Th with marine organic matter. *Marine Chemistry* 76, 27-45.
- Quigley, M.S., Santschi, P.H., Hung, C.C., Guo, L.D. and Honeyman, B.D. (2002) Importance of acid polysaccharides for ^{234}Th complexation to marine organic matter. *Limnology and Oceanography* 47, 367-377.
- Ritzrau, W., Graf, G., Scheltz, A. and Queisser, W. (2001) Benthic-pelagic coupling and carbon dynamics in the Northern North Atlantic. In: The Northern North Atlantic. Schäfer, E.P. Springer Verlag Berlin Heidelberg.
- Roberts, K.A., Xu, C., Hung, C.C., Conte, M.H. and Santschi, P.H. (2009) Scavenging and fractionation of thorium vs. protactinium in the ocean, as determined from particle-water partitioning experiments with sediment trap material from the Gulf of Mexico and Sargasso Sea. *Earth and Planetary Science Letters* 286, 131-138.
- Santschi, P.H. (2005) Marine Colloids, Water Encyclopedia. John Wiley & Sons, Inc.
- Santschi, P.H., Hung, C.-C., Schultz, G. and Alvarado-Quiroz, N. (2003) Control of acid polysaccharide production and ^{234}Th and POC export fluxes by marine organisms. *Geophysical Research Letters* 30, 16-11/16-12.

- Santschi, P.H., Murray, J.W., Baskaran, M., Benitez-Nelson, C.R., Guo, L.D., Hung, C.C., Lamborg, C., Moran, S.B., Passow, U. and Roy-Barman, M. (2006) Thorium speciation in seawater. *Marine Chemistry* 100, 250-268.
- Shields, A. (1936) Anwendung der Aehnlichkeitsmechanik und der Turbulenzforschung auf die Geschiebebewegung. Ph.D. Thesis. Preussischen Versuchsanstalt für Wasserbau, Technical University Berlin.
- Siddeeg, S.M., Bryan, N.D. and Livens, F.R. (2014) Dispersion of U-series natural radionuclides in stream sediments from Edale, UK. *Environmental Sciences: Processes and Impacts* 16, 991-1000.
- Skwarzec, B., Boryło, A. and Strumińska, D.I. (2004) Activity disequilibrium between ^{234}U and ^{238}U isotopes in southern Baltic. *Water, Air, and Soil Pollution* 159, 165-173.
- Soetaert, K., Herman, P.M.J., Middelburg, J.J., Heip, C., deStigter, H.S., van Weering, T.C.E., Epping, E. and Helder, W. (1996) Modeling ^{210}Pb -derived mixing activity in ocean margin sediments: Diffusive versus nonlocal mixing. *Journal of Marine Research* 54, 1207-1227.
- Soulsby, R.L. and Whitehouse, R.J.S. (1997) Threshold of Sediment Motion in Coastal Environments Pacific Coasts and Ports '97: Proceedings of the 13th Australasian coastal and ocean engineering conference and the 6th Australasian port and harbour conference, University of Canterbury, Christchurch, New Zealand.
- Stolzenbach, K.D., Newman, K.A. and Wong, C.S. (1992) Aggregation of fine particles at the sediment-water interface. *Journal of Geophysical Research Oceans* 97, 17889-17898.
- Tan, X., Wang, X., Chen, C. and Sun, A. (2007) Effect of soil humic and fulvic acids, pH and ionic strength on Th(IV) sorption to TiO₂ nanoparticles. *Applied Radiation and Isotopes* 65, 375-381.
- Tauber, F. and Lemke, W. (1995) Map of sediment distribution in the Western Baltic Sea (1: 100,000), Sheet flaster - møn. *Deutsche Hydrografische Zeitschrift* 47, 171-178.
- Taylor, A.C. (1976) Burrowing behaviour and anaerobiosis in the bivalve *Arctica islandica* (L.). *Journal of the Marine Biological Association of the United Kingdom* 56, 95-109.
- Thomsen, L. and Gust, G. (2000) Sediment erosion thresholds and characteristics of resuspended aggregates on the western European continental margin. *Deep Sea Research Part I: Oceanographic Research Papers* 47, 1881-1897.
- Tourney, J. and Ngwenya, B.T. (2014) The role of bacterial extracellular polymeric substances in geomicrobiology. *Chemical Geology* 386, 115-132.
- Tsoufanidis, N. and Landsberger, S. (1995) Measurement and Detection of Radiation. *CRC Press, Taylor & Francis Group*.
- Turnewitsch, R. (1999) Particle transport in the near-bottom water column and surface of the abyssal Arabian Sea. Ph.D Thesis. Faculty of mathematics and natural sciences, Christian-Albrechts-University, Kiel. 179.

- Turnewitsch, R. and Graf, G. (2003) Variability of particulate seawater properties related to bottom mixed layer-associated internal waves in shallow water on a time scale of hours. *Limnology and Oceanography* 48, 1254-1264.
- Turnewitsch, R., Reyss, J.L., Nycander, J., Waniek, J.J. and Lampitt, R.S. (2008) Internal tides and sediment dynamics in the deep sea-Evidence from radioactive $^{234}\text{Th}/^{238}\text{U}$ disequilibria. *Deep-Sea Res. Part I-Oceanogr. Res. Pap.* 55, 1727-1747.
- Turnewitsch, R. and Springer, B.M. (2001) Do bottom mixed layers influence ^{234}Th dynamics in the abyssal near-bottom water column? *Deep-Sea Res. Part I-Oceanogr. Res. Pap.* 48, 1279-1307.
- Urban-Malinga, B., Drgas, A., Gromisz, S.a. and Barnes, N. (2014) Species-specific effect of macrobenthic assemblages on meiobenthos and nematode community structure in shallow sandy sediments. *Marine Biology* 161, 195-212.
- van der Loeff, R.M.M. and Moore, W.S. (1999) The analysis of natural radionuclides in seawater. In: Grasshoff, Ehrhardt and Kremling, *Methods of Seawater Analysis*. Wiley-VCH, Weinheim, 365-397.
- Verardo, D.J., Froelich, P.N. and McIntyre, A. (1990) Determination of organic carbon and nitrogen in marine sediments using the Carlo-Erba NA-1500 analyzer. *Deep-Sea Research Part A* 37, 157-165.
- Volk, T. and Hoffert, M.I. (1985) Ocean carbon pumps - Analysis of relative strengths and efficiencies in ocean-driven atmospheric CO_2 changes. *Geophysical Monographs* 32, 99-110.
- Wang, Q., Hamilton, P.B. and Kang, F. (2014) Observations on attachment strategies of periphytic diatoms in changing lotic systems (Ottawa, Canada). *Nova Hedwigia* 99, 239-253.
- Waples, J.T., Orlandini, K.A., Weckerly, K.M., Edgington, D.N. and Val Klump, J. (2003) Measuring low concentrations of ^{234}Th in water and sediment. *Marine Chemistry* 80, 265-281.
- Wei, C.-L. and Murray, J.W. (1992) Temporal variations of ^{234}Th activity in the water column of Dabob Bay: particle scavenging. *Limnology and Oceanography* 37, 296-314.
- Wentworth, C.K. (1922) A scale of grade and class terms for clastic sediments. *The Journal of Geology* 30, 377-392.
- Werk, S. (2003) Laborversuche zum Adsorptionsverhalten von $^{234}\text{Thorium}$ an natürlichen Partikeln. Diploma Thesis. Department of aquatic ecology, University of Rostock. 87.
- Widdows, J., Brinsley, M.D., Bowley, N. and Barrett, C. (1998) A benthic annular flume for in situ measurement of suspension feeding/biodeposition rates and erosion potential of intertidal cohesive sediments. *Estuarine, Coastal and Shelf Science* 46, 27-38.
- Xu, C., Santschi, P.H., Hung, C.C., Zhang, S., Schwehr, K.A., Roberts, K.A., Guo, L., Gong, G.C., Quigg, A., Long, R.A., Pinckney, J.L., Duan, S., Amon, R. and Wei, C.L. (2011)

- Controls of ^{234}Th removal from the oligotrophic ocean by polyuronic acids and modification by microbial activity. *Marine Chemistry* 123, 111-126.
- Xu, C., Santschi, P.H., Schwehr, K.A. and Hung, C.C. (2009) Optimized isolation procedure for obtaining strongly actinide binding exopolymeric substances (EPS) from two bacteria (*Sagittula stellata* and *Pseudomonas fluorescens* Biovar II). *Bioresource Technology* 100, 6010-6021.
- Xu, J., Zhou, L., Jia, Y., Liu, Z. and Adesina, A.A. (2014) Adsorption of thorium (IV) ions from aqueous solution by magnetic chitosan resins modified with triethylenetetramine. *Journal of Radioanalytical and Nuclear Chemistry*.
- Xu, Q.-H., Pan, D.-Q. and Wu, W.-S. (2015) Effects of pH, ionic strength, humic substances and temperature on Th(IV) sorption onto ZSM-5. *Journal of Radioanalytical and Nuclear Chemistry* 305, 535-541.
- Yilmaz, E.S., Aslim, B. and Cansunar, E. (2012) Potential of nickel(II) removal by *Synechocystis* sp. Isolates. *Fresenius Environmental Bulletin* 21, 853-859.
- Yin, J.P., Wang, Y.S., Xu, J.R. and Sun, S. (2006) Advances of studies on marine carbon cycle. *Acta Ecologica Sinica* 26, 566-575.
- Zhang, L., Chen, M., Yang, W., Xing, N., Li, Y., Qiu, Y. and Huang, Y. (2004) Size-fractionated thorium isotopes (^{228}Th , ^{230}Th , ^{232}Th) in surface waters in the Jiulong River estuary, China. *Journal of Environmental Radioactivity* 78, 199-216.
- Zhang, S., Xu, C. and Santschi, P.H. (2008) Chemical composition and ^{234}Th (IV) binding of extracellular polymeric substances (EPS) produced by the marine diatom *Amphora* sp. *Marine Chemistry* 112, 81-92.
- Ziervogel, K. and Arnosti, C. (2007) Polysaccharide hydrolysis in aggregates and free enzyme activity in aggregate-free seawater from the north-eastern Gulf of Mexico. *Environmental Microbiology*.
- Ziervogel, K. and Bohling, B. (2003) Sedimentological parameters and erosion behaviour of submarine coastal sediments in the south-western Baltic Sea. *Geo-Marine Letters* 23, 43-52.

OTHER REFERENCES:

World nuclear association

Naturally-Occurring Radioactive Materials (NORM)

[Online in world wide web]: URL: <http://www.world-nuclear.org/information-library/safety-and-security/radiation-and-health/naturally-occurring-radioactive-materials-norm.aspx> [from: 24.05.2016]

DANKSAGUNG

Ich bedanke mich herzlich bei Prof. Dr. Gerhard Graf für die Möglichkeit gemeinsam das Projekt beantragt und dran gearbeitet zu haben, für das entgegengebrachte Vertrauen und die gute Betreuung.

Ganz besonderen Dank gilt Robert Turnewitsch für die die zahlreichen Hilfsstellungen und Lösungsvorschläge ohne die ich oft nicht weitergekommen wäre.

Mein Dank gilt Carol Arnosti, Sherif Ghobrial, Kai Ziervogel und der gesamten Arbeitsgruppe für die Bereitstellung der Methoden, den zahlreichen Tipps zu den Experimenten und natürlich für die tolle Zeit in Chapel Hill.

Ich bedanke mich bei Michiel R. van der Loeff (AWI) für die Hilfestellung bei der Etablierung der leaching Methode und die zahlreichen Fragen; bei Rainer Bahlo (IOW) für die Elementaranalyse; bei Christian Burmeister (IOW) für die Vorbereitung und Nutzung der Duchflusszentrifuge und bei Dr. Leopold Sauheitl und seine Kollegen (Uni Hannover) für die Messung der Partikeloberfläche von Mergel. Außerdem danke ich Jana Wölfel und Martin Albrecht für die Bereitstellung der Algenkulturen, die Tipps zur Pflege und die Nutzung und Hilfestellung am Mikroskop.

Außerdem danke ich der Crew der ‚Goor II‘ und ‚Praunus‘ für den reibungslosen Ablauf und die erfolgreiche Probenahme, sowie meinen wissenschaftlichen Kollegen Martin Powilleit, Florian Peine und Franziska Bitschofsky die mich bei den Probennahmen unterstützt haben.

An die gesamte Arbeitsgruppe der Meeresbiologie Uni Rostock geht mein herzlichster Dank für das sehr angenehme Arbeitsklima, die vielen Anregungen und Hilfestellungen, sowie die Mensagänge und zahlreichen Pausen zwischendurch. An dieser Stelle danke ich ganz besonders Frau E. Meier und Holger Pielenz für die Hilfestellungen und Unterstützung sowohl beim Messen der Proben als auch bei technischen Fragen. Judith Rahel Renz, Stefan Forster, Kerstin Perner, Franzi Glück, Moritz Kloose und Judith Georgii gilt mein Dank vor allem für die Korrekturarbeiten und Tipps in der letzten Phase.

Ganz besonders danke ich meiner Familie, Freunden und Stefan für die mentale Unterstützung, Fürsorge, Liebe, Halt und den Optimismus und Ansporn. Ihr seid das Wichtigste in meinem Leben.

Ich danke der DFG für die finanzielle Unterstützung des Projektes.

Appendix

APPENDIX

Table App. I: Particulate, dissolved, total and initial total ²³⁴Th activity as well as the particulate organic carbon content (POC) of the experiments of section 3. Errors of the ²³⁴Th activity indicate the 95 % confidence level and the a- labels errors represents the SD.

		²³⁴ Th (dpm l ⁻¹)				POC (mg l ⁻¹)
		particulate	dissolved	total	initial total	
<i>Rhodomonas</i> spp.	10 min			9.36 ± 0.75	15.47	1.00 ± 0.04 ^a
	3 h	2.39 ± 0.25	4.90 ± 2.02			
<i>Suriralla</i> spp.	10 min			10.11 ± 2.19	17.00	1.01 ± 0.12 ^a
	3 h	2.75 ± 0.21	7.07 ± 1.61			
<i>Synechococcus</i> spp.	10 min			10.26 ± 1.06	15.45	0.84 ± 0.07 ^a
	3 h	4.24 ± 0.68	4.68 ± 0.17			
fine sediment fraction	10 min			16.11 ± 0.59	15.52	0.25 ± 0.14 ^a
	3 h	8.42 ± 1.57	3.02 ± 0.44			
control run	10 min			16.00 ± 1.26	15.43	
	30 min			14.36 ± 0.76		
	1 h			13.98 ± 0.72		
	2 h			12.32 ± 1.56		
	3 h			11.62 ± 0.04		

Appendix

Table App. II: Total initial, dissolved and colloidal ²³⁴Th activity of the experiment A of section 4 corrected for the 49 % ²³⁴Th loss onto container walls. The errors indicate the SD of n = 3, ^a n = 2.

	²³⁴ Th (dpm l ⁻¹)		
	initial total	dissolved	colloidal
Fuoidan	19.10 ± 0.00	14.25 ± 2.71	4.86 ± 2.71
Chondroitin	17.15 ± 2.03	12.19 ± 3.43	4.96 ± 1.39
Pullulan	17.91 ± 1.35 ^a	10.62 ± 0.18 ^a	7.30 ± 1.53 ^a

Table App. III: Particulate, colloidal and dissolved ²³⁴Th activity of the experiment B of section 4 corrected for the 49 % ²³⁴Th loss onto container walls. The errors indicate the SD of n = 3, ^a n = 2.

	²³⁴ Th (dpm l ⁻¹)		
	particulate	colloidal	dissolved
mineral particles	0.11 ± n.d.		10.08 ± 0.48
Fuoidan		9.08 ± 0.84 ^a	1.66 ± 0.84 ^a
Fuoidan + mineral particles	0.19 ± n.d.	4.69 ± 0.85 ^a	5.86 ± 0.85 ^a

Table App. IV: Particulate and dissolved ²³⁴Th activity as well as the added particle concentration of the fine sediment particle of the experiment C of section 4. Activities in deionized water are corrected for the 49 % ²³⁴Th loss onto container walls. The errors indicate the SD of n = 3.

	²³⁴ Th (dpm l ⁻¹)		added particle concentration (mg l ⁻¹)
	particulate	dissolved	
seawater	6.24 ± 1.39	9.34 ± 2.12	7.28 ± 0.21
deionised water	0.55 ± 0.29	18.02 ± 0.90	7.55 ± 0.21

Table App. V: Particulate and dissolved ²³⁴Th activity as well as the particle concentration before starting the experiments (t₀) of section 5.3.3. The errors indicate the SD of n = 3.

		²³⁴ Th (dpm l ⁻¹)		particle concentration (mg l ⁻¹)
		particulate	dissolved	
23.c	initial	5.76	6.44	1.55 ± 0.29
	erosion	6.92	5.69	1.59 ± 0.16
23.b	initial	10.21	3.76	1.59 ± 0.30
	erosion	14.38	1.13	1.64 ± 0.25
23.0	initial	n.d.	n.d.	1.85 ± 0.27
	erosion	6.27	3.74	1.46 ± 0.12

Appendix

Table App. VI: Particulate and dissolved ^{234}Th activity as well as the particle concentration of the resuspension phase of the experiment of section 5.3.3. The errors indicate the SD of $n = 3$.

		^{234}Th (dpm l ⁻¹)		particle concentration (mg l ⁻¹)
		particulate	dissolved	
23.c	initial	7.58 ± n.d.	5.83 ± n.d.	3.26 ± 1.54
	erosion	9.13 ± n.d.	5.75 ± n.d.	2.02 ± 0.07
23.b	initial	10.76 ± n.d.	4.42 ± n.d.	4.11 ± 0.45
	erosion	13.39 ± n.d.	2.13 ± n.d.	4.33 ± 0.11
23. o	initial	6.23 ± 0.44	1.74 ± 0.08	7.87 ± 0.34
	erosion	6.06 ± n.d.	4.01 ± n.d.	8.51 ± 0.56

Table App. VII: Particulate carbon content of the water samples (SW – surface water, BW – bottom water) of the three stations in the Mecklenburg Bay, Baltic Sea. Errors indicate the SD of $n = 3$.

		particulate carbon (mg l ⁻¹)
23.c	SW	0.33 ± 0.02
	BW	0.25 ± 0.01
23.b	SW	0.23 ± 0.01
	BW	0.12 ± 0.05
23. o	SW	0.26 ± 0.03
	BW	0.17 ± 0.02

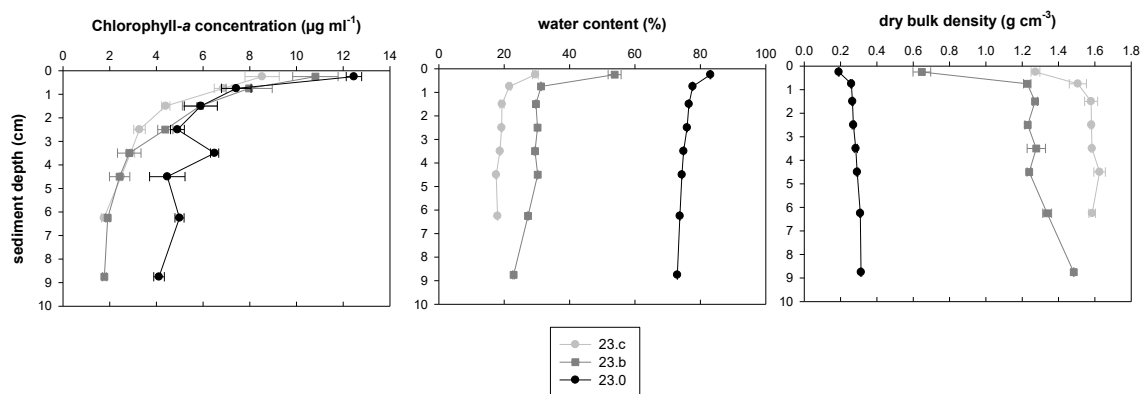


Figure App. I: The chlorophyll-*a* concentration, water content and dry bulk density in the sediment of the three stations in the Mecklenburg Bay, Baltic Sea. Errors indicate the SD of $n = 3$.

SELBSTSTÄNDIGKEITSERKLÄRUNG

Doktorandinnen/Doktoranden-Erklärung gemäß § 4 Absatz 1 Buchstaben g und h der Promotionsordnung der Mathematisch-Naturwissenschaftlichen Fakultät der Universität Rostock

Name: Schuster, Anne

Ich habe eine Dissertation zum Thema 'Factors controlling ^{234}Th scavenging and the application of ^{234}Th as particle Tracer' an der Mathematisch-Naturwissenschaftlichen Fakultät der Universität Rostock angefertigt. Dabei wurde ich von Herrn Prof. Dr. Gerhard Graf betreut.

Ich gebe folgende Erklärung ab:

1. Die Gelegenheit zum vorliegenden Promotionsvorhaben ist mir nicht kommerziell vermittelt worden. Insbesondere habe ich keine Organisation eingeschaltet, die gegen Entgelt Betreuerinnen/Betreuer für die Anfertigung von Dissertationen sucht oder die mir obliegenden Pflichten hinsichtlich der Prüfungsleistungen für mich ganz oder teilweise erledigt.
2. Ich versichere hiermit an Eides statt, dass ich die vorliegende Arbeit selbstständig angefertigt und ohne fremde Hilfe verfasst habe. Dazu habe ich keine außer den von mir angegebenen Hilfsmitteln und Quellen verwendet und die den benutzten Werken inhaltlich und wörtlich entnommenen Stellen habe ich als solche kenntlich gemacht.

Rostock, den 31.08.2016

Anne Schuster
